ISSN 2221-6413 (Print), ISSN 2223-2559 (Online)
Coden: PJSIB5 60(1) 1-58 (2017)

Pakistan Journal of Scientific and Industrial Research

Series A: Physical Sciences

Vol. 60, No.1, January-February, 2017

(for on-line access please visit web-site http://www.pjsir.org)

Published by
Scientific Information Centre
Pakistan Council of Scientific and Industrial Research
Karachi, Pakistan

AIMS & SCOPE

Pakistan Journal of Scientific and Industrial Research (PJSIR) was started in 1958 to disseminate research results based on utilization of locally available raw materials leading to production of goods to cater to the national requirements and to promote S&T in the country. Over the past 59 years, the journal conveys high quality original research results in both basic and applied research in Pakistan. A great number of major achievements in Pakistan were first disseminated to the outside world through PJSIR.

It is a peer reviewed journal and published in both print and electronic form. Original research articles, review articles and short communications from varied key scientific disciplines are accepted however, papers of Pure Mathematics, Computer Sciences, Engineering and Medical Sciences are not entertained.

From 54th Volume in 2011, it has been bifurcated into Series A: Physical Sciences & Series B: Biological Sciences. Each series appears three times in a year as follows:

Physical Sciences in January-February, May-June and September-October issues. It includes research related to Natural Sciences, Organic Chemistry, Inorganic Chemistry, Industrial Chemistry, Physical Chemistry, Environmental Sciences, Geology, Physics, Polymer Sciences and Technology.

Biological Sciences in March-April, July-August and November-December issues. Papers included in this series are from Agriculture, Agronomy, Botany, Biochemistry, Biotechnology, Food Sciences, Genetic Engineering, Pharmaceutical Sciences, Microbiology, Marine Sciences, Soil Sciences, Tissue Culture, Zoology and Technology.

Due to many global issues, we are encouraging contributions from scientists and researchers from all across the globe with the sole purpose of serving scientific community worldwide on the whole and particularly for our region and third world countries.

Pakistan Journal of Scientific and Industrial Research
Series A: Physical Sciences

Pakistan Journal of Scientific and Industrial Research started in 1958, has been bifurcated in 2011 into:

Series A: Physical Sciences [**ISSN 2221-6413 (Print); ISSN 2223-2559 (online)]** (appearing as issues of January-February, May-June and September-October) and
Series B: Biological Sciences [**ISSN 2221-6421 (Print); ISSN 2223-2567 (online)]** (appearing as issues of March-April, July-August and November-December).
Each Series will appear three times in a year.

This Journal is indexed/abstracted in Biological Abstracts and Biological Abstracts Reports, Chemical Abstracts, Geo Abstracts, CAB International, BioSciences Information Service, Zoological Record, BIOSIS, NISC, NSDP, Current Contents, CCAB, Rapra Polymer Database, Reviews and Meetings and their CD-ROM counterparts etc.

Subscription rates (including handling and Air Mail postage): ***Local:*** Rs. 2500 per volume, single issue Rs. 425; ***Foreign:*** US$ 450 per volume, single issue US$ 75.

Electronic format of this journal is available with: Bell & Howell Information and Learning, 300, North Zeeb Road, P.O. 1346, Ann Arbor, Michigan 48106, U.S.A; Fax.No.313-677-0108; http://www.proquest.com

Photocopies of back issues can be obtained through submission of complete reference to the Executive Editor against the payment of Rs. 25 per page per copy (by Registered Mail) and Rs. 115 per copy (by Courier Service), within Pakistan; US$ 10 per page per copy (by Registered Mail) and US$25 per page per copy (by Courier Service), for all other countries.

Printed and Published by: PCSIR Scientific Information Centre, PCSIR Laboratories Campus, Shahrah-e-Dr. Salimuzzaman Siddiqui, Karachi-75280, Pakistan.

Editorial Address

Executive Editor
Pakistan Journal of Scientific and Industrial Research, PCSIR Scientific Information Centre
PCSIR Laboratories Campus, Shahrah-e-Dr. Salimuzzaman Siddiqui, Karachi-75280, Pakistan
Tel: 92-21-99261914-99261916, 99261949, 99261917; Fax: 92-21-99261913; Web: http://www.pjsir.org, E-mail: info@pjsir.org

Pakistan Journal of Scientific and Industrial Research
Series A: Physical Sciences
Vol. 60, No.1, January-February, 2017

Contents

Turmeric Powder as a Natural Heavy Metal Chelating Agent: Surface Characterisation
Amtul Qayoom, Syed Arif Kazmi and Saeeda Nadir Ali 1

Beneficiation Study on Barite Ore of Duddar Area, District Lasbela, Balochistan Province, Pakistan
Muhammad Arif Bhatti, Kamran Raza Kazmi, Rashid Mehmood, Abdul Ahad, Anila Tabbassum and Adnan Akram 9

Experimental Investigation of Performance Characteristics of Compression Ignition Engine Fuelled with Punnai Oil Methyl Ester Blended Diesel
Mathan Raj Vijayaragavan, Ganapathy Subramanian, Lalgudi Ramachandran, Manikandaraja Gurusamy, Rahul Kumar Tiwari and Sanat Kumar 22

Qualitative Analysis of Siro-spun and Two Fold Yarns Tensile Properties under the Influence of Twist Factor
Muhammad Qamar Tusief, Nasir Mahmood, Nabeel Amin and Akmal Saeed 29

Appraisal of Drinking Water Quality in Lahore Residence, Pakistan
Khalid Mahmood and Muhammad Asim 34

Sulphide Removal from Sewage Wastewater by Oxidation Technique
Muhammad Tahir Butt, Naz Imtiaz, Naeem Abbas and Rauf Ahmad Khan 42

The Study of PM_{10} Concentration and Trace Metal Content in Different Areas of Karachi, Pakistan
Durdana Rais Hashmi, Akhtar Shareef and Farooq Ahmed Khan 50

Pak. j. sci. ind. res. Ser. A: phys. sci. 2017 **60**(1) 1-8

Turmeric Powder as a Natural Heavy Metal Chelating Agent: Surface Characterisation

Amtul Qayoom[a]*, Syed Arif Kazmi[b] and Saeeda Nadir Ali[a]
[a]Department of Chemistry, NED University of Engineering and Technology, Karachi-75270, Pakistan
[b]H.E.J. Research Institute of Chemistry, International Center for Chemical and Biological Sciences (ICCBS), University of Karachi, Karachi- 75270, Pakistan

(received March 21, 2016; revised September 10, 2016; accepted September 19, 2016)

Abstract. The present study was conducted to investigate surface properties of turmeric in order to evaluate its detoxification potential and ability to sequester toxic metals ions. Scanning Electron Microscopy (SEM), Energy Dispersion Spectroscopy (EDS), Infra-Red (IR) spectroscopy and potentiometric titrations were employed for characterisation of the surface of turmeric powder. Spectroscopic studies revealed that the surface of turmeric powder was porous mainly composed of polymeric -OH , -NH , $-CH_2$, -COO and -OH groups of polysaccharides. From potentiometric titrations and modelling of batch titration data, it was found that surface of the turmeric contains at least four binding sites with pKa values 3.56 (pK_1), 4.83 (pK_2), 7.68 (pK_3) and 10.4 (pK_4). Turmeric powder contains highest concentration of amino and hydroxyl groups for the pK_4 values i.e., 0.55 mmol/ g. The total binding sites concentration for turmeric powder was 1.2 mmol/ g.

Keywords: turmeric, chelation, surface characterisation, potentiometric titration

Introduction

Rapid increase in industrialisation, population growth and urbanisation has largely contributed to abundance of heavy metals in drinking water, air and soil. In many developing countries, agricultural land is often irrigated with raw sewage (Farrag *et al.,* 2016; Meng *et al.,* 2016; Yousaf *et al.,* 2016) . Industrial and domestic sewage is also disposed of into fresh water systems to be used to irrigate agricultural land. In Pakistan, untreated sewage and industrial water is commonly used for the cultivation of vegetables around the urban areas of Pakistan (Shakir *et al.,* 2017; Khan *et al.,* 2016; Uzma *et al.,* 2016). Thus, food is one of the key sources of toxic metals intake by human beings.

The practice of using certain plants or their parts as natural chelates for detoxification of living organisms is quite topical. Scientists from USA, India, Pakistan, China, France and others explored the properties of local food and plants for detoxification. Such are the cumin, turmeric, garlic, tea and others (Chang *et al.,* 2012; El-Ashmawy *et al.,* 2006; Wong and Kitts, 2006 by Komy, 2004). There are several herbs that are considered useful in the elimination of heavy metals. Inclusion of high sulphur foods such as asparagus, onions, garlic, legumes and eggs in diet assist the body in preventing uptake and retention of many toxic metals. Apples pectin binds most toxic metals and removes them from the body (Kartel *et al.,* 1999).

Plant derived materials consisting largely of polysaccharides, proteins and lipids have a broad range of functional groups, which can sequester metal ions e.g., hydroxyl, carboxylate, amino and sulphate groups etc. (Lesmana *et al.,* 2009; Choi and Yun, 2006). Besides these functional groups, polysaccharides also exhibit ion exchange affinities (Nasernejad *et al.,* 2005; Zouboulis *et al.,* 1999; Sag and Veglio *et al.,* 1997; Kutsal, 1996). Diversity of functional groups on their surface makes them act as natural chelates and their binding properties may be associated with their chemical heterogeneity.

Turmeric is widely used as a spice, colouring agent, preservative, cosmetic and as medicinal herb in traditional medicine systems (Unani, Ayurveda, Sidha and Tibetan) as studied by Remadevi and Ravindran (2007) and Eigner and Scholz (1999). The primary colouring pigment of turmeric i.e., curcumin is used as a food colour in spices, cheese, mustard, potato flakes, cereals, pickles, soups, yogurt, ice creams, etc., in Asiatic and Western cuisines . Studies have indicated that turmeric is non-toxic to humans even upon taking 8000 mg/ day taken continuously (Cheng *et at.,* 2001).

*Author for correspondence; E-mail: amtulq@gmail.com

Because of the presence of curcuminoids, proteins and carbohydrates, turmeric powder provides a variety of binding sites for metal ions and acts as a natural chelate (Qayoom and Kazmi, 2012; Qayoom Amtul *et al.,* 2009). The attraction depends on the surface constitution, type and number of ligand groups and their affinity for particular metals. The physical and chemical characteristic of turmeric is important to interpret interaction between turmeric surface and metal ions. Recently various studies have been conducted to investigate isolation and characterisation of turmeric constituents and their therapeutic potential and its role as detoxifying agent but no studies have been conducted to explore relationship between surface properties of turmeric and its detoxifying abilities (El-Barbary, 2016; Harsha *et al.,* 2016; Sun *et al.,* 2016) . Present research work was aimed to investigate surface properties of turmeric powder in order to evaluate its potential as a natural chelate for Cu(II) and Cd(II) from their aqueous solutions. SEM-EDS and IR analysis were carried out to study changes in morphology and identification of functional groups involved in Cu(II) and Cd(II) binding onto turmeric powder surface. Potentiometric titration data of turmeric suspensions was modelled using modelling programme ProtoFit to determine surface dissociation constants and metal binding site concentration.

Materials and Methods

Adsorbate stock solutions of copper(II) and cadmium(II) were prepared by dissolving 0.617 g $Cd(NO_3)_2 \cdot 4H_2O$ and 0.50 g $CuSO_4.5H_2O$ per liter of deionised water. Dilute solutions of different working concentrations of Cu(II) and Cd(II) were prepared from their stock solutions. Adsorption experiments were conducted as follows: Accurately weighed turmeric powder (0.500 ± 0.001g) was added to the 50.0 mL metal solution to obtain suspension. The suspension was adjusted to pH 6 for Cu(II) and pH 7 for Cd(II) by adding required volume of 0.1M HNO_3 and NaOH solutions. Both suspensions were stirred at a constant speed at temperatures 310 K for 60 min. The contents were then suction filtered through filter paper, Whatman no. 1 and air dried overnight at room temperature.

SEM-EDS Studies. The morphology of the turmeric powder before and after Cu(II) and Cd(II) binding was investigated by using Scanning Electron Microscope (JSM5910, JEOL, Japan) EDS detector (INCA200/ Oxford Instruments, UK). EDS analysis was employed to confirm the identification of metal ions present on sample surface.

IR studies. Turmeric powder samples prior and after treating with Cu(II) and Cd(II) solution were dried overnight at room temperature to avoid any moisture retained which could interfere with analysis of hydroxyl groups on the surface. The samples were ground and mixed well with KBr and then compressed in the disc. The discs were scanned through a wavelength range from 500 to 4000cm^{-1} into transmission mode using IR spectrometer (Bruker Vector 22 19300). IR spectra of control, Cu(II) and Cd(II) treated turmeric powder were recorded.

Potentiometric studies. Turmeric powder suspension was prepared having solid-to-liquid ratio of 10 g/ L in inert electrolyte concentrations of 0.1 M $NaNO_3$. The suspension was stirred for one hour to reach the equilibrium. The potentiometric titration was conducted by adding a known concentration of HCl to turmeric powder suspension to decrease the initial pH and then titrating with standardized solutions of NaOH. The pH of the suspension solution was recorded after each titrant addition by pH-meter calibrated with pH 4 and pH 7 buffers. Each sample was also conducted in blank. Triplicate measurements were made to ensure the reproducibility.

Experimental data obtained from potentiometric titration of turmeric powder suspension were normalized as surface charge (QH, mmol/ g) concentration versus suspension pH.

Q_H values were calculated according to the following charge balance equation (Pagnanelli *et al.,* 2005).

$$Q_H = \Sigma_{j=1}^{n} [s_j^-] = \frac{(C_B - C_A + [H^+] - [OH^-])V}{m} \qquad (1)$$

where:

S_j(mmol/g) = concentration of dissociated form of generic S_j sites in turmeric; C_B (mmol/L) and CA (mmol/L) = the base and acid concentrations, respectively after each addition; V (L) = the total suspension volume after each addition of titrant; H^+ (mmol/L) = protons concentration in the solution obtained by potentiometric measurements; OH^- (mmol/L) is estimated by taking into account water dissociation constant and m (g) = amount of turmeric powder. ProtoFit is modelling software designed to calculate surface protonation constants and concentration of binding sites from titration data.

Computational methods. Logger Pro 3.8.2 software was used to record the titration data on Pentium IV computer. This data allowed the qualitative and quantitative determination of acidic sites of turmeric surface. The modeling program ProtoFit version 2.0 was employed to fit the titration data to theoretical non-electrostatic proton binding model curve. Potentiometric titration data was used to estimate types of functional groups responsible for the observed buffering capacities, their associated proton binding constants as well as their concentrations on turmeric surface.

Surface protonation model (Background). A given surface may contain a number of functional groups, each with its own site concentration. These binding sites present on surfaces are capable of accepting or releasing proton from/to the solution. These binding sites could be acidic, basic or amphoteric depending upon protonation/deprotonation reactions taking place. Acidic sites are those that change from neutral to negatively charged with increasing pH and basic sites take on positive charge with decreasing pH and are neutral at higher pH conditions (Pan *et al.,* 2007)

$$\equiv SH^{o} \rightleftarrows \equiv S^{-} + H^{+} \quad (2)$$

$$\equiv SH_2^{+} \rightleftarrows \equiv SH^{o} + H^{+} \quad (3)$$

where:

≡ S represents binding site present on the surface; in Eq. (2) ≡ SH^{o} exhibits acidic behaviour, releasing a proton and in Eq. (3) ≡ SH^{o} acts as a basic site and absorbs proton. If a surface is capable of exhibiting both behaviours, it is amphoteric. The equilibrium mass action for Eq. (2) and (3) are:

$$\frac{\{\equiv S^{-}\}a_{H^+}}{\{\equiv SH^{o}\}} = K_1 \exp\frac{(F\Psi)}{RT} \quad (4)$$

$$\frac{\{\equiv SH^{o}\}a_{H^+}}{\{\equiv SH_2^{+}\}} = K_2 \exp\frac{(F\Psi)}{RT} \quad (5)$$

constrained by mass balance expression

$$\{\equiv SH\}_{total} = \{\equiv SH^{o}\} + \{\equiv S^{-}\} + \{\equiv SH_2^{+}\} \quad (6)$$

where:

{ } denotes the concentrations in mol/L of solution, a_{H^+} refers to the thermodynamic activity of H^+, F represents Faraday's constant, K_1 and K_2 are equilibrium constants, and T is absolute temperature (Van Cappellen *et al.,* 1993). The surface potential, Ψ is a function of surface charge, σ. The aim of surface protonation constants determination is to determine values of K_1 and/or K_2 and $\{\equiv SH\}_{total}$ for each discrete surface site as required by the given model.

Determination of the buffer value. Following proton mass balance equation is the basis for the ProtoFit approach for a system with zero solution alkalinity. (Turner and Fein, 2006).

$$\Delta n_{H^+,\,total,i} = \Delta n_{H^+,\,water,i} + \Delta n_{H^+,ads,i} \quad (7)$$

where:

Δn_{H^+} is the mole of protons added to the system as a whole (total), water and turmeric surface from the start to step. Surface proton buffering function (Q^{*}_{ads}) is the measure of pH dependency of the ability of surface to buffer solution pH and can be calculated using $\Delta n_{H^+\,total,\,i}$ as follows:

$$Q_{ads} = \frac{\Delta n_{H^+,ads,i}}{S} \quad (8)$$

where:

S is the mass of turmeric powder.

$$Q^{*}_{ads} = \frac{dQ_{ads}}{dpH} \quad (9)$$

In order to optimize model constants ProtoFit minimizes weighed sum of square difference i.e., SS* between (Q^{*}_{ads})and (F^{*}_{ads}) (model proton buffering function). The optimization continues to adjust the model constants until the value of SS* reaches at a minimum.

Results and Discussion

SEM-EDS. Scanning electron micrographs of unloaded, Cu(II) loaded and Cd(II) loaded turmeric powder are shown in Fig. 1. It can be observed that turmeric powder has significant numbers of pores, where metal ions can be trapped and adsorbed. A distinct change in surface morphology of turmeric powder was observed after binding of copper and cadmium. The peaks of carbon, nitrogen and oxygen were recorded in EDS spectra showing the presence of these elements in the turmeric powder as main constituents. EDS spectra of copper (II) and cadmium (II) adsorbed turmeric showed the peaks of copper and cadmium in addition to those recorded in the turmeric powder.

IR Studies. IR study was carried out to determine functional groups involved in Cu(II) and Cd(II) binding onto turmeric powder surface. The IR spectra of control, Cu(II) and Cd(II) treated turmeric are shown in Fig. 2-4, respectively and salient peaks of control and metal loaded turmeric powder samples are compared in Table 1.

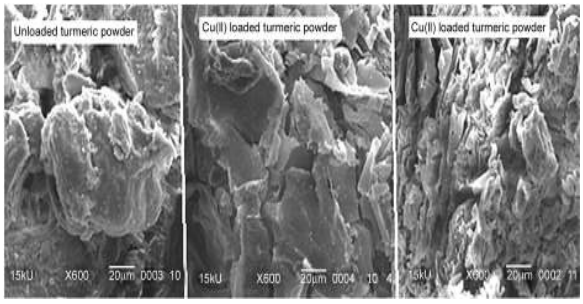

Fig 1. Scanning electron micrographs of unloaded, Cu(II) and Cd(II) loaded turmeric powder.

IR spectra showed that surface of turmeric powder is primarily comprised of polymeric OH, NH, CH_2 and COO groups, and OH groups. Hydroxyl groups originate basically from polysaccharides; carboxyl groups can be associated with proteins whereas amino groups are mostly present in proteins. All these groups have been known for their affinity for heavy metal chelation (Anayurt *et al.,* 2009; Al-Degs *et al.,* 2006).

The IR spectra of metal treated turmeric powder showed slight changes in the absorption peak frequencies. The absorbance of most of the peaks in Cu(II) and Cd(II) treated turmeric powder is slightly shifted to higher frequencies. This shift in the absorbance indicated that surface of the turmeric powder was capable of interacting

Table 1. Comparison of Infrared band in the region of 3500-500 cm^{-1}

Functional groups	unloaded turmeric powder	Cd-loaded turmeric powder	Cu-loaded turmeric powder
		cm^{-1}	
O-H and N-H stretching	3408	3424	3419
-CH stretching	2924.6	2925.6	2924.5
>C=N-, >C=C-, C=O stretch to N–H bending (cis form), $–CH_2$ scissoring or $–CH_3$ anti symmetrical bending vibration and O–H deformation	1631.2	1631.3	1634.5
	1429.5	1432	1427
$C(=O)O^{--}$ symmetric stretching	1375.7	1380.7	1383.2
The (C=O)-O^-stretching vibration, –OH in-plane deformation	1262.3	1274.4	1271.4
Stretching vibration of C-O-C	1160.2	1162.1	1162.1
Stretching vibration of OH	1031.5	1032.7	1031.0

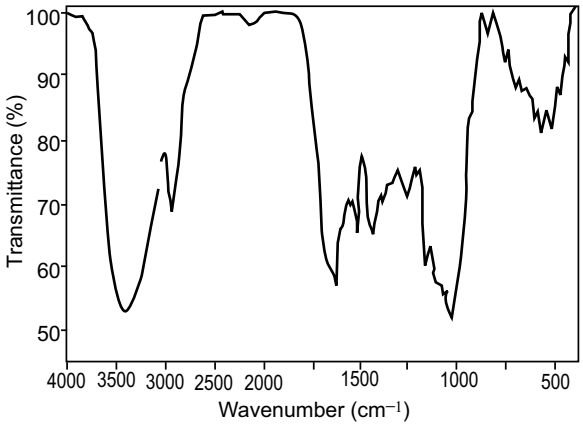

Fig. 2. IR spectra of unloaded turmeric powder.

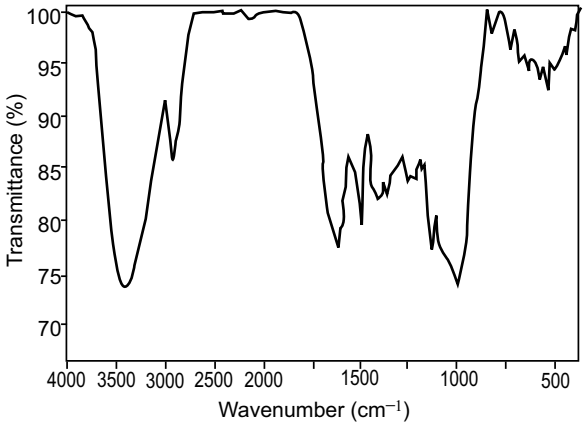

Fig. 3. IR Spectra of Cu(II) loaded turmeric powder.

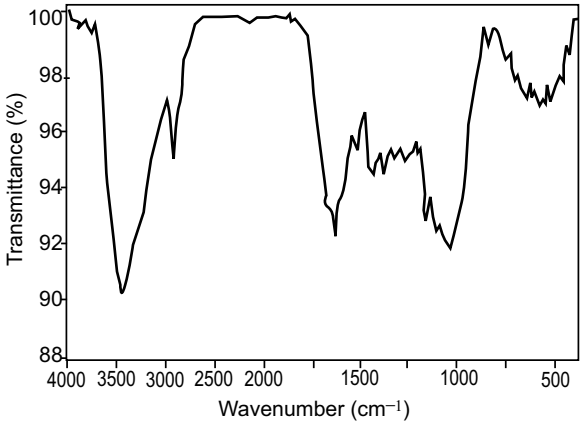

Fig. 4 IR Spectra of Cd(II) loaded turmeric powder

and binding metal ions. Changes in the spectra of loaded turmeric powder are attributed to the interaction of Cu(II) and Cd(II) with the hydroxyl, carboxyl and amino groups on the turmeric surface. The broadness of the O-H and N-H stretching band decreased in spectra of Cu(II) and Cd(II) loaded turmeric powder. This may be due to decrease in H-O-H interaction. No change was observed in the frequency of C–H group after treating with Cu(II) and Cd(II) ions. This showed that C–H group is not involved in the binding of Cu(II) and Cd(II) ions.

Potentiometric titration. A typical titration curve exhibiting that turmeric powder provides considerable buffering capacity over a wide pH range is presented in Fig. 5. This observed buffering is due to the protonation and deprotonation of functional groups present on the surface of the turmeric powder.

Point of Zero Charge (PZC) is defined as the pH value at which surface charge becomes equal to zero i.e., electrically neutral surface.

$$\sqrt{H^+} - \sqrt{OH^-} = 0 \qquad (11)$$

The value of PZC obtained from the x-intercept of Q_H versus pH plot (Fig. 6) was found to be 8.1. Thus at pH>8.1 turmeric powder surface became increasingly negatively charged and at pH below 8.1, the surface became increasingly positive charged. The existence of PZC indicated that the turmeric suspension developed a net positive charge at low pH values, indicating the presence of at least one positively ionizing, plausibly amino group. Those surfaces which only contain negatively ionizing groups such as carboxyl, hydroxyl and phosphoryl groups could not develop a net positive charge at low pH. Active sites in the acidic pH range are usually carboxyl groups whereas active sites in the basic pH range are chiefly amine and phenolic groups.

Modeling results. The results obtained after ProtoFit optimizations are summarized in Table 2. Weighed

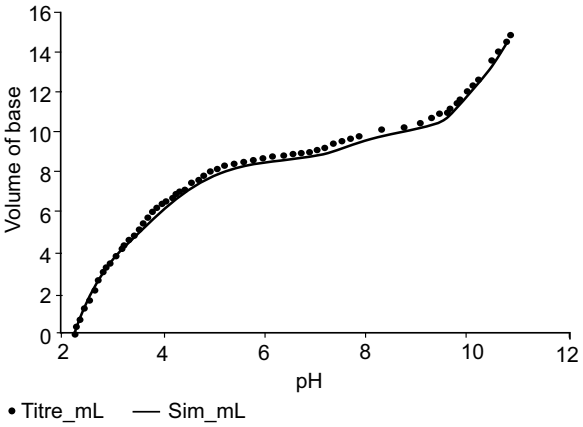

Fig. 5. Raw titration data compared with model simulation for 1g/100 mL suspension of turmeric powder in inert electrolyte concentrations of 0.1M $NaNO_3$.

sum of squares value, *SS** (smaller values reflect better fits), represents the goodness of the fit. ProtoFit continues to adjust the values of model constants until the value of *SS** reaches at a minimum. The best fit was achieved by using a non-electrostatic four acidic sites model in ProtoFit (Fig. 7). Hence, four different acidity constants

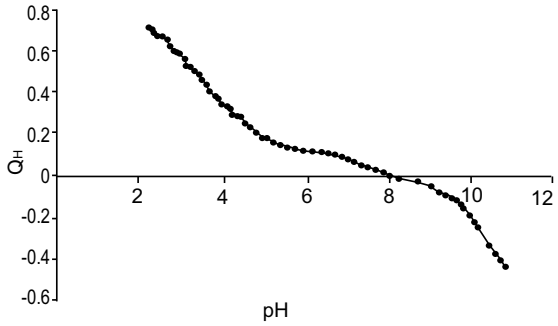

Fig. 6. Surface charge (Q_H, mmol/ g) versus pH of 1g/100 mL turmeric powder suspension in inert electrolyte concentrations of 0.1M $NaNO_3$.

Table. 2. Acidity constants and binding site concentrations (mmol/g) calculated by Protofit using the four site non-electrostatic model

pK_1	C_1	pK_2	C_2	pK_3	C_3	pK_4	C_4	C_{total}	S S *
3.56	0.35	4.83	0.16	7.68	0.15	10.4	0.55	1.2	7.23
29.16%		13.33%		12.5%		45.88%			
Strong carboxyl groups		Weak carboxyl groups		Very weak phenolic groups		Amines /hydroxyl			

were obtained: 3.56 (pK_1), 4.83 (pK_2), 7.68 (pK_3) and 10.4 (pK_4). pK_1 can be associated to strong carboxyl group attached to aromatic structures. pK_2 can be due to weak carboxyl group associated with aliphatic chains. pK_3 can be attributed to very weak phenolic groups and pK_4 can be ascribed to amino and/or hydroxyl group, respectively (Merdy *et al.,* 2009; Reddad *et al.,* 2002). Turmeric powder has highest concentration of amino and hydroxyl groups for the estimated pK_4 values i.e., 0.55 mmol/ g. The main parameter concerns the total

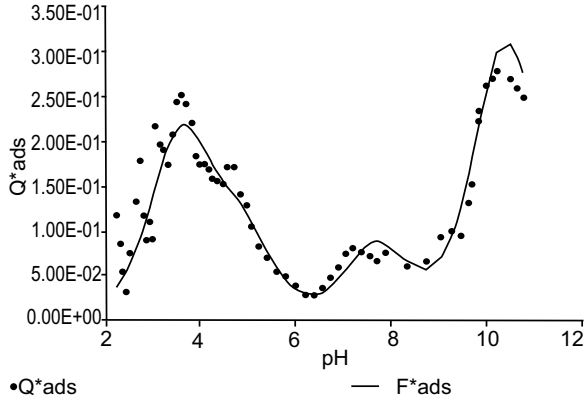

Fig. 7. Q^*_{ads} function compared with model predictions for 1g/100 mL suspension of turmeric powder in inert electrolyte concentrations of 0.1M $NaNO_3$.

binding site concentration (or buffering capacity). The total site concentration for turmeric powder was 1.2 mmol/ g.

It was found that the chelation of Cu(II) and Cd(II) strongly depends upon pH of the solution and surface speciation of the turmeric powder. At low pH values, functional groups present on the turmeric surface are fully protonated and metal ion chelation is negligible. On increasing pH, the functional groups gradually deprotonate, forming negatively charged metal binding sites which result in increasing Cu(II) and Cd(II) chelation.

Conclusion

In the present study, surface properties of turmeric powder were examined by spectroscopic techniques and potentiometric titrations. Spectroscopic studies revealed that the surface of turmeric powder was porous mainly composed of polymeric -OH, -NH, $-CH_2$, -COO and -OH groups of polysaccharides. It was found that surface of the turmeric contains at least four binding sites i.e., strong carboxyl group attached to aromatic structures, weak carboxyl group associated with aliphatic chains, very weak phenolic groups and amino and/or hydroxyl group, respectively. Turmeric powder contains highest concentration of amino and hydroxyl groups. Presence of these binding sites on turmeric surface makes it appropriate chelating agent for ingested toxic metals.

References

Al-Degs, Y. S., El-Barghouthi, M. I., Issa, A. A., Khraisheh, M. A., Walker, G. M. 2006. Sorption of Zn(II), Pb(II), and Co(II) using natural sorbents: equilibrium and kinetic studies. *Water Research,* **40:** 2645-2658.

Anayurt, R.A., Sari, A., Tuzen, M. 2009. Equilibrium, thermodynamic and kinetic studies on biosorption of Pb(II) and Cd(II) from aqueous solution by macrofungus (*Lactarius scrobiculatus*) biomass. *Chemical Engineering Journal,* **151:** 255-261.

Chang, M. S., Park, M. J., Jeong, M. C., Kim, D. M., Kim, G. H. 2012. Antioxidative activities and antibrowning effects of green tea extracts and propolis. *Korean Journal of Food and Cookery Science,* **28:** 319-326.

Cheng, A.L., Hsu, C.H., Lin, J.K., Hsu, M.M., Ho, Y.F., Shen, T.S., Ko, J.Y., Lin, J.T., Lin, B.R., Ming-Shiang, W., Yu, H.S., Jee, S. H., Chen, G. S., Chen, T.M., Chen, C. A., Lai, M.K., Pu, Y.S., Pan, M.H., Wang, Y.J., Tsai, C.C., Hsieh, C.Y. 2001. Phase I clinical trial of curcumin, a chemopreventive agent, in patients with high-risk or pre-malignant lesions. *Anticancer Research,* **21:** 2895-2900.

Choi, S.B., Yun, Y.-S. 2006. Biosorption of cadmium by various types of dried sludge: an equilibrium study and investigation of mechanisms. *Journal of Hazardous Materials,* **138:** 378-383.

Eigner, D., Scholz, D. 1999. *Ferula asafoetida* and *Curcuma longa* in traditional medical treatment and diet in Nepal. *Journal of Ethnopharmacology,* **67:** 1-6.

El-Ashmawy, I.M., Ashry, K. M., El-Nahas, A. F., Salama, O. M. 2006. Protection by turmeric and myrrh against liver oxidative damage and genotoxicity induced by lead acetate in mice. *Basic Clinical Pharmacology & Toxicology,* **98:** 32-37.

El-Barbary, M.I. 2016. Detoxification and antioxidant

effects of garlic and curcumin in *Oreochromis niloticus* injected with aflatoxin B_1 with reference to gene expression of glutathione peroxidase (GPx) by RT-PCR. *Fish Physiology and Biochemistry,* **42:** 617-629.

Farrag, K., El Bastamy, E.S., Ramadan, A. 2016. Health risk assessment of heavy metals in irrigated agricultural crops, El-Saff wastewater canal, Egypt. *CLEAN - Soil, Air, Water,* **44:** 1-10.

Harsha, M.R., Chandra Prakash, S. V., Dharmesh, S.M. 2016. Modified pectic polysaccharide from turmeric (*Curcuma longa*): A potent dietary component against gastric ulcer. *Carbohydrate Polymers,* **138:** 143-155.

Kartel, M.T., Kupchik, L.A., Veisov, B.K. 1999. Evaluation of pectin binding of heavy metal ions in aqueous solutions. *Chemosphere,* **38:** 2591-2596.

Khan, Z.I., Ahmad, K., Ashraf, M., Parveen, R., Bibi, Z., Mustafa, I., Noorka, I.R., Tahir, H.M., Akram, N.A., Ullah, M.F., Yaqoob, R. 2016. Risk assessment of heavy metal and metalloid toxicity through a contaminated vegetable (*Cucurbita maxima*) from wastewater irrigated area: A case study for a site-specific risk assessment in Jhang, Pakistan. *Human and Ecological Risk Assessment: An International Journal,* **22:** 86-98.

Komy, Z.R. 2004. Determination of acidic sites and binding toxic metal ions on cumin surface using nonideal competitive adsorption model. *Journal of Colloid and Interface Science,* **270:** 281-287.

Lesmana, S. O., Febriana, N., Soetaredjo, F. E., Sunarso, J., Ismadji, S. 2009. Studies on potential applications of biomass for the separation of heavy metals from water and wastewater. *Biochemical Engineering Journal,* **44:** 19-41.

Meng, W., Wang, Z., Hu, B., Wang, Z., Li, H., Goodman, R.C. 2016. Heavy metals in soil and plants after long-term sewage irrigation at Tianjin China: A case study assessment. *Agricultural Water Management,* **171:** 153-161.

Merdy, P., Gharbi, L.T., Lucas, Y. 2009. Pb, Cu and Cr interactions with soil: Sorption experiments and modelling. *Colloids and Surfaces A: Physicochemical and Engineering Aspects,* **347:** 192-199.

Nasernejad, B., Zadeh, T. E., Pour, B. B., Bygi, M. E., Zamani, A. 2005. Camparison for biosorption modeling of heavy metals (Cr(III), Cu(II), Zn (II)) adsorption from wastewater by carrot residues. *Process Biochemistry,* **40:** 1319-1322.

Pagnanelli, F., Mainelli, S., De Angelis, S., Toro, L. 2005. Biosorption of protons and heavy metals onto olive pomace: Modelling of competition effects. *Water Research,* **39:**1639-1651.

Pan, J., Liu, R., Tang, H. 2007. Surface reaction of *Bacillus cereus* biomass and its biosorption for lead and copper ions. *Journal of Environmental Sciences* (China), **19:** 403-408.

Premavali, S. 2007. Turmeric as a spice and colorant. In: *Turmeric: The Genus Curcuma.* P. N. Ravindran, K. N. Babu, and K. Sivaraman (eds.), pp. 437-450, 1st edition, CRC Press, USA.

Qayoom, A., Kazmi, S.A. 2012. Effect of temperature on equilibrium and thermodynamic parameters of Cu(II) adsorption onto turmeric powder. *Journal of Chemical Society of Pakistan,* **34:** 1084-1090.

Qayoom, A., Kazmi, S.A., Naushaba, R. 2009. Removal of Cu(II) ions from aqueous solutions by turmeric powder. *Journal of Chemical Society of Pakistan,* **31:** 876-881.

Reddad, Z., Gerente, C., Andres, Y., Le Cloirec, P. 2002. Modeling of single and competitive metal adsorption onto a natural polysaccharide. *Environmental Science & Technology,* **36:** 2242-2248.

Remadevi, R., Ravindran, P. N. 2007. Turmeric in traditional medicine, In: Turmeric: *The Genus Curcuma.* P. N. Ravindran, K. N. Babu and K. Sivaraman (eds.), pp. 409-436, 1st edition, CRC Press, USA.

Sag, Y., Kutsal, T. 1996. The selective biosorption of chromium(VI) and copper(II) ions from binary metal mixtures by *R. arrhizus*. *Process Biochemistry,* **31:** 561-572.

Shakir, S.K., Azizullah, A., Murad, W., Daud, M.K., Nabeela, F., Rahman, H., ur Rehman, S., Häder, D.P. 2017. Toxic metal pollution in Pakistan and its possible risks to public health. *Reviews of Environmental Contamination and Toxicology,* **242:** 1-60

Sun, W., Wang, S., Zhao, W., Wu, C., Guo, S., Hongwei, G., Hongxun, T., Lu, J.J., Wang, Y., Chen, X.P. 2016. Chemical constituents and biological research on plants in the genus Curcuma. *Critical Reviews in Food Science and Nutrition,* DOI: 10 1080/ 10408398. 2016 1176554

Turner, B.F., Fien, J.B. 2006. ProtoFit: A program for determining surface promotion constants from titration data. *Computers and Geosciences,* **32:** 1344-1356.

Uzma, S., Azizullah, A., Bibi, R., Nabeela, F., Muhammad, U., Ali, I., Rehman, Z.U., Häder, D.P.

2016. Effects of industrial wastewater on growth and biomass production in commonly grown vegetables. *Environmental Monitoring and Assessment,* **188:** 1-13.

Van Cappellen, P., Charlet, L., Stumm, W., Wersin, P. 1993. A surface complexation model of the carbonate mineral-aqueous solution interface. *Geochimica et Cosmochimica Acta,* **57:** 3505-3518.

Veglio, F., Beolchini, F., Gasbarro, A. 1997. Biosorption of toxic metals: an equilibrium study using free cells of *Arthrobacter* sp. *Process Biochemistry,* **32:** 99-105.

Wong, P.Y.Y., Kitts, D.D. 2006. Studies on the dual antioxidant and antibacterial properties of parsley (*Petroselinum crispum*) and cilantro (*Coriandrum sativum*) extracts. *Food Chemistry,* **97:**505-515.

Yousaf, B., Amina, Liu, G., Wang, R., Imtiaz, M., Rizwan, M.S., Zia-ur-Rehman, M., Qadir, A., Si, Y. 2016. The importance of evaluating metal exposure and predicting human health risks in urban–periurban environments influenced by emerging industry. *Chemosphere,* **150:** 79-89.

Zouboulis, A. I., Rousou, E. G., Matis, K. A., Hancock, I. C. 1999. Removal of toxic metals from aqueous mixtures. Part 1: Biosorption. *Journal of Chemical Technology & Biotechnology,* **74:** 429-436.

Pak. j. sci. ind. res. Ser. A: phys. sci. 2017 **60**(1) 9-22

Beneficiation Study on Barite Ore of Duddar Area, District Lasbela, Balochistan Province, Pakistan

Muhammad Arif Bhatti[a]*, Kamran Raza Kazmi[a], Rashid Mehmood[a], Abdul Ahad[b], Anila Tabbassum[c] and Adnan Akram[a]

[a]PCSIR Laboratories Complex, Ferozepur Road, Lahore-54600, Pakistan
[b]Department of Physics, University of Lahore, Raiwind Road, Lahore, Pakistan
[c]Institute of Chemistry, University of the Punjab, Lahore-54000, Pakistan

(received April 14, 2015; revised December 7, 2015; accepted January 12, 2016)

Abstract. This study highlights the results of processing an indigenous low to medium grade barite ore of Duddar area, district Lasbela, Balochistan, Pakistan. The ore was characterized by x-ray diffraction technique. The gravity concentration and forth flotation technologies were employed to beneficiate the ore in order to achieve commercial grade barite concentrate with economical recovery. The results showed that flotation was the better method than gravity concentration to concentrate the barite mineral. A process flow sheet was designed in the light of these experiments. The flotation tests revealed that barite concentrate assaying 95.85% $BaSO_4$ could be obtained with recovery of 82.06% from an ore containing 76.04% $BaSO_4$. The flotation concentrate was leached to get rid of objectionable impurities. The final leached barite concentrate possesses 98.86% $BaSO_4$ content and conforms to the specifications of industrial grade barite concentrate.

Keywords: Duddar area, barite, beneficiation, tabling, flotation, leaching, recovery

Introduction

Barite ($BaSO_4$) also known as heavy spar is an exceptional nonmetallic mineral with an incredible high specific gravity of 4.5 which makes it suitable for a wide range of industrial applications. Barite is mainly used as weighting agent in oil-well and natural gas drilling mud to increase mud density up to 2.5 g/cm^3. It is estimated that more than 80% of the barite produced in the world is used only for drilling purpose (Scott *et al*., 2010). Barite is chemically inert and insoluble hence finds its use as additive in the manufacture of rubber, paints, enamels, plastics, paper goods, wallpapers, asbestos goods, leaded glass and ceramics. Moreover, it is used in radiology for x-rays of the intestines and to make high-density concrete resistant to nuclear radiation. A more recent application of barite is in the formulation of brake shoe linings, noise reduction in engine compartments and spark-plug alloys (Singh *et al*., 2007; Mills, 2006).

Barite is the principal mineral of barium. It is usually milky white but may have shade of other colours such as tinted yellow, brown, grey, red green and blue depending on the impurities trapped during the formation of crystals. It forms thin to thick tabular crystals. It usually occurs in sedimentary rocks especially disseminated in limestone, dolostone and sandstone as veins, lenses, fillings, concretions and replacements. It is also a common mineral in hydrothermal veins where it is a gangue mineral associated with various sulphide minerals of lead, zinc, silver, copper, iron, antimony, cobalt and nickel. In a few locations, barite is deposited as a sinter in hot springs. Barite commonly occurs with accessory minerals such as calcite, dolomite, siderite, aragonite, fluorite, gypsum, anhydrite, chert, quartz, apatite and metal sulphides (Naseem *et al*., 2011; Blackburn, 1988).

The total world's reserves of barite in all categories are about 2 billion tonnes, but only about 740 million tonnes resources are identified. China, India, USA, Morocco, Mexico, Kazakhstan, Iran and Turkey are the leading producers of barite (Table 1A). China alone shares more than 50% of the world's barite production. Pakistan exports limited quantity of high grade ore (Table 1B) ranging from 42 to 118 thousand metric tonnes (Mcrae, 2015; Miller, 2011). Pakistan possesses sizeable deposits of barite ore widely distributed in Balochistan and Khyber Pukhtunkhwa Provinces. Significant deposits are located at Monar Talar, Gunga, Surmai, Sekran, Malkhor and Ranj Laki (district Kuzdar), Duddar, Bankhri, Kundi-Dharn, Dham Jhal, Mithi-Arrara, Kanrachzi, Hunurki, (district Lasbela) in Balochistan and at Kohala, (district Abbotabad), Kacchi, Faqir Mohammad, Tipra (district Haripur), Besham (District Kohistan), Gera Banda

*Author for correspondence; E-mail: arifbhattipcsir@yahoo.com

(district Swat) in Khyber Pukhtunkhwa. These are medium to high grade ore deposits having $BaSO_4$ content ranging from 20 to 92%. The estimated reserves of barite in Pakistan are more than 30 million tonnes (Zaigham and Mallick, 2000; Ahsan and Quraishi, 1997; Ahmad and Siddiqi, 1992).

Among these, Duddar barite ore deposit is important which is located on the eastern flank of the Mor Mountain Range at latitude of 26°05'N and longitude of 66°50'E. The Duddar mineralization occurs in two separate exposures known as Duddar North and Duddar South. These exposures are 258 and 274 meters long with an average thickness of 10 meters. The mineralization is stratiform, hosted by interbedded siltstone, mudstone and shale sequence of Anjira formation (Naseem *et al*., 2011; Zaigham and Mallick, 2000).

During mining, high grade variety of barite having specific gravity ranging from 4.1 to 4.35 is taken separately for direct use after grinding. But low grade ore with specific gravity below 3.9 is rejected. These low grade ores contain various gangue minerals which need to be removed in order to obtain a product suitable for industrial applications. There are mainly two processes that are commercially used to beneficiate low grade barite ores. Gravity concentration techniques like jigging, tabling, spirals, and dense media separation are generally used for coarse grained ores. Direct or reverse flotation technology is applied on finely disseminated ores to separate the barite mineral from the associated gangue components. A large number of barite producers utilize only flotation to recover and improve the grade of barite (Raju *et al*., 2004; Day, 2002; Davis, 1985).

The effects of important variables of flotation process on grade and recovery of barite concentrate were investigated. The rougher concentrate obtained was subjected to regrinding for further liberation of locked particles and two cleaning operations were employed in close circuit to achieve higher grade concentrate.

Table 1A. Barite production (thousand metric tonnes) country wise for the last 5 years

Country	Year 2010	Year 2011	Year 2012	Year 2013	Year 2014
Algeria	60	40	60	-	-
China	3,600	4,100	4,000	4,000	4,100
Germany	75	70	70	-	-
India	1,000	1,350	1,400	1,740	1,600
Iran	250	350	350	270	270
Kazakhstan	100	200	200	250	250
Mexico	140	157	160	344	400
Morocco	460	600	650	1,000	1,000
Pakistan	45	58	60	118	75
Peru	-	87	90	-	-
Russia	65	62	60	-	-
Turkey	150	230	250	250	270
United Kingdom	50	50	50	-	-
Vietnam	90	85	85	-	-
United States	670	710	654	700	720
Other Countries	160	220	220	558	575
Total	6,900	8,370	8,400	9,230	9,260

Mcrae (2015).

Materials and Methods

Sample preparation. A representative sample of barite ore of Duddar area, weighing about 100 kg packed in five cloth bags was supplied by Pakistan Mineral Development Corporation (PMDC), Karachi, for beneficiation test work. The whole of the ore sample included drill core pieces cut into quadrants. Processing experiments were carried out on laboratory scale in Mineral Processing Research Centre (MPRC) PCSIR Complex, Lahore, Pakistan. The ore was mixed and crushed in laboratory jaw crusher where opening was set at 12 mm. The jaw product having size less than 12 mm was further crushed in secondary rolls crusher to obtain a product size of finer than 8 mm. The roll product was thoroughly mixed and a head sample for chemical and XRD analysis was prepared by using a sample splitter. It was ground to minus 200 mesh size with the help of disc pulverizer. The remaining crushed composite ore sample was riffled to make smaller samples weighing one kg each for beneficiation studies.

Table 1B. Barite production (thousand metric tonnes) in Pakistan and World for the last 10 years

Barite production	2005	2006	2007	2008	2009	2010	2011	2012	2013	2014
Production by Pakistan	42	45	44	43	42	45	58	60	118	75
Total world production	7,870	7,960	7,730	8,200	6,130	6,900	8,370	8,400	9,230	9,260

Mcrae (2015); Miller (2011).

Chemical analysis. The head sample was analyzed for $BaSO_4$ and the associated gangue components. The quantitative chemical analysis of the head sample was done by gravimetric, volumetric and instrumental analytical techniques. The finely ground ore sample was fused with AR grade sodium carbonate in platinum crucible at 900 °C in muffle furnace. The fused mass was leached in hot water and filtered. The volume of filtrate was made up to the mark with distilled water and this was named as 'Solution A', and used for the determination of soluble components i.e., silica, alumina, zinc and sulphur. The residue was dissolved in dilute hydrochloric acid and diluted with water to make the volume up to the mark. This was named as 'Solution B' and utilized for the determination of barium, calcium, magnesium, iron and lead. Barium, sulphur and silica were estimated by gravimetric methods (Jeffery, 1989; ASTM: E 247-01, 2007). Iron was found by oxidation reduction titration using standard solution of potassium dichromate (ASTM: E 246-05, 2007), while aluminum, calcium and magnesium were determined by complexometric titration using standard solution of EDTA (ASTM: E 738-05, 2007; Jeffery, 1989). The minor elements were determined by Atomic Absorption Spectrophotometer (Model: 8000, Hitachi, Japan). Another 1 g of sample was heated in electric oven for 1 h at 110 °C to find out moisture. The same sample was ignited in electric furnace at 950 °C for 1 h to determine the loss on ignition. The chemical analysis of the representative sample is given in Table 2. Barium sulphate content of processed products was also determined by the same method. The chemical analysis of flotation concentrate and final leached barite concentrate was carried out by same techniques as applied for head sample of ore.

Table 2. Chemical analysis of the composite sample of Duddar barite ore

Constituents	Percentage
Barium sulphate ($BaSO_4$)	76.04
Silica (SiO_2)	10.77
Iron oxide (Fe_2O_3)	4.85
Aluminum oxide (Al_2O_3)	2.31
Calcium oxide (CaO)	1.65
Magnesium oxide (MgO)	0.88
Zinc (Zn)	0.08
Lead (Pb)	0.06
Sulphur (S) other than sulphate	2.33
Loss on ignition (LOI) other than sulphur	0.95

Mineralogy. A qualitative scan was performed by x-ray diffractometer (Model: D-5000, Siemens, Germany) in order to find out different mineral phases present in the composite ore sample. X-ray diffraction was performed @ 0.02 steps/sec. The scan angle was ranged from 5°-80° to get all the important peaks. X-ray diffractogram of the ore is illustrated in Fig. 1, while 2 θ, d values and relative intensities of various peaks are given in Table 3. The diffractogram obtained was matched with standard data provided with x-ray diffractometer to identify the minerals by search/match procedure. The major and minor minerals found in the ore are given in Table 3.

Gravity concentration tests. Wilfley shaking table (Mine & Smelter Supply Company, Serial No.13, USA) was used for gravity concentration tests. It has a flat deck (55 cm × 110 cm) having cleats on it which form riffles. It moves with a horizontal to and fro motion of 300 cycles per minute. Each cycle consists of a slow

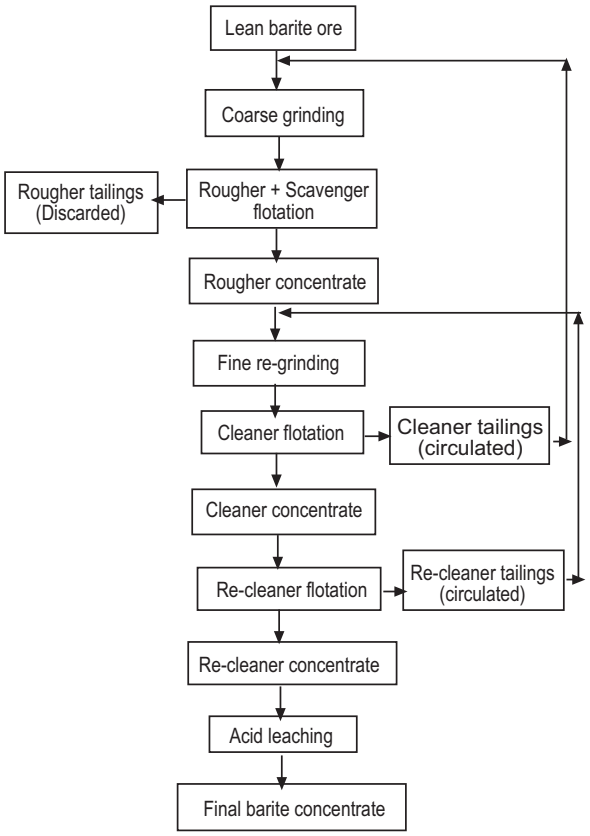

Fig. 1. Flow-sheet for the beneficiation medium grade barite ore of Duddar (Lasbela) Balochistan, Pakistan.

Table 3. Minerals identified in Duddar barite ore

Seq.	2 θ	d Value	Rel. I.	Minerals identified
1	20.31	4.37	9.26	gibbsite
2	20.74	4.28	19.68	quartz/gypsum
3	21.07	4.21	6.93	-
4	23.11	3.85	29.67	calcite
5	25.19	3.50	86.15	anhydrite
6	26.17	3.45	100.00	barite
7	27.15	3.33	85.85	quartz/barite
8	29.05	3.09	55.81	barite/galena/sphalerite
9	29.32	3.03	10.42	calcite
10	31.86	2.80	35.27	siderite/dolomite/ anhydrite/gypsum
11	33.322	2.68	25.99	pyrrotite/sphalerite/ galena/gypsum/pyrite
12	36.48	2.46	9.67	quartz/gibbsite/pyrite
13	38.91	2.33	6.74	anhydrite
14	41.13	2.19	13.09	dolomite
15	42.94	2.11	60.54	barite
16	43.20	2.09	51.45	barite
17	43.46	2.08	18.52	pyrrotite
18	44.37	2.04	10.66	-
19	49.38	1.84	12.01	calcite/quartz/sphalerite
20	51.27	1.78	6.70	dolomite
21	52.33	1.74	9.87	siderite/galena
22	53.18	1.72	5.58	pyrrotite
23	55.19	1.66	11.77	sphalerite
24	56.33	1.63	3.88	pyrite/sphalerite/galena
25	60.85	1.52	9.72	quartz/sphalerite
26	66.86	1.38	4.80	quartz

forward and rapid return motion along with slurry control system for stratification of materials. A few preliminary experiments were performed at feed rate of 15 kg/h, wash water flow rate of 10 L/min, deck inclination angle of 7° and stroke length of 8 mm. The results of gravity separation tests are given in Table 4.

Flotation tests. The froth flotation tests were conducted using laboratory flotation machine (Model: D-12, Denver, USA). The feed for the flotation tests was prepared by wet grinding of barite ore in a laboratory rod mill (Denver, USA size: 7"×14") with the addition of water in the mill to maintain the solid to liquid ratio of 1:1. The ground ore was transferred to stainless steel flotation cell of 4 L capacity. A number of batch type flotation tests were carried out at different sets of conditions so as to investigate the effects of important variables such as (a) grind size of the ore (b) pulp density (c) pH of the pulp (d) impeller speed (e) dosage of collector (f) amount of frother (g) quantity of regulator (h) conditioning time and (i) flotation time on the grade and recovery of the product. In all tests a scavenging flotation was conducted and scavenger concentrate was mixed along with rougher concentrate. After having optimizing rougher flotation recovery, the test work was done to produce required grade concentrate. The rougher concentrate was re-ground for further liberation and one cleaning flotation with addition of flotation reagents and another re-cleaning flotation without addition of flotation reagents was carried out. The concentrate produced was heated in oven at 250 °C to get rid of flotation reagents. The optimum parameters of flotation tests are reported in Table 5 while the metallurgical balance of typical test is given in Table 6. The complete chemical analysis of final barite concentrate produced by flotation is shown in Table 7.

Table 4. Metallurgical balance of a typical gravity concentration test of Duddar barite ore

Tabling products	Weight (%)	Grade (%) ($BaSO_4$)	Recovery (%) ($BaSO_4$)
Concentrate	54.26	84.07	60.08
Middling	17.50	78.60	18.10
Tailing	28.24	58.88	21.87
Head	100.00	76.06	100.00

Table 5. Flotation parameters and optimum conditions of Duddar barite ore processing

Flotation parameters	Optimum conditions		
	Roughing	Cleaning	Re-cleaning
Grind size (feed size) of ore	100% -75 µm	100% -65 µm	100% -65 µm
Pulp density (% solids)	25% Solids	15% Solids	10% Solids
pH of pulp (slurry)	~10.0	~10.0	~10.0
Agitation speed (aeration)	1100 rpm	1000 rpm	900 rpm
Collector (sodium oleate)	600 g/t	300 g/t	Nil
Frother (polypropylene glycol)	60 g/t	30 g/t	Nil
Gangue depressant (sodium silicate)	400 g/t	200 g/t	Nil
Galena depressant (sodium chromate)	Nil	20 g/t	Nil
Conditioning time	12 min	12 min	12 min
Flotation time	20 min	20 min	20 min

Table 6. Metallurgical balance of a typical flotation test of Duddar barite ore

Flotation products	Weight (%)	Grade (%) ($BaSO_4$)	Distribution (%) ($BaSO_4$)
Re-cleaner concentrate	65.11	95.83	82.06
Re-cleaner tailings	5.10	58.89	3.95
Cleaner concentrate	70.21	93.15	86.01
Cleaner tailings	8.98	53.69	6.34
Rougher concentrate	79.19	88.68	92.35
Rougher tailings	20.81	27.95	7.65
Head sample	100.00	76.04	100.00

Leaching tests. Acid leaching tests were performed on final flotation concentrate using different concentrations of commercially available hydrochloric acid (37%). About 100 g portions of concentrate were taken in 4 different Pyrex glass beakers (500 mL). These were treated with 100 mL diluted solution of 5, 10, 15 and 20% hydrochloric acid, respectively, with constant stirring on hot plate at 95 °C to boiling temperature for 1 h. These were cooled, filtered and washed with distilled water until free of acid. The residues left on filter paper were dried for 1 h in electric oven at 110 °C and evaluated for comparison of $BaSO_4$ content. The results obtained are shown in Table 8. The flow sheet developed for the overall process is shown in Fig. 1.

Results and Discussion

Chemical analysis of head sample (Table 2) indicates that $BaSO_4$ content in the ore is 76.04%. Main undesirable gangue impurity is silica which is 10.77%. The other relatively a lower impurity is iron oxide, whose concentration is 4.85% whereas, alumina and calcium oxide are found to be 2.31% and 1.65%, respectively. Other minor impurities include magnesium oxide which is less than 1%, heavy metal such as lead is 0.08% and zinc is 0.06%. It is obvious from the result that ore is medium grade and is not suitable for final application until beneficiated. In order to produce a commercial grade barite concentrate assaying more than 90% $BaSO_4$ with specific gravity around 4.2, some kind of beneficiation work is required for further up-gradation of this ore.

Mineralogy prior to the selection of beneficiation process is crucial parameter. It provides information about valuable and valueless minerals present in the ore deposit which in turn help to decide the process selection. Mineralogical characterization of the ore was carried out by x-ray diffraction technique. The x-ray diffraction (Fig. 2) of the head sample confirms that ore predominantly consisted of barite along with subordinate amount of quartz, anhydrite and gypsum minerals as major peaks of XRD correspond to standard values of these minerals. It was identified by JCP.CAT search and match programme of the x-ray diffractometer that the minor peaks corresponds to calcite, aragonite, dolomite, siderite, gibbsite, galena, sphalerite, pyrrotite and pyrite minerals (Table 3).

Many researchers attempted different mineral processing techniques and their combination in order to achieve the desired goal from wide variety of barite ore deposits.

Table 7. Chemical analysis of final Duddar barite concentrate and requirement of industries

Constituents	Flotation concentrate	Leached concentrate	Requirements of different industries
Barite ($BaSO_4$)	95.85%	98.86%	Min. 92.0% for drilling mud, 95.0% for all other
Silica (SiO_2)	1.30%	1.02%	Max. 2.50% for drilling mud, 1.50% for glass
Iron oxide (Fe_2O_3)	0.50%	0.02%	Max. 0.15% for glass, 1.0% for chemicals, 0.05% for paint
Aluminum oxide (Al_2O_3)	0.34%	0.025%	Max. 0.03% for drilling mud, 0.15% for glass
Calcium oxide (CaO)	0.94%	0.006%	Max 0.01% for drilling mud
Magnesium oxide (MgO)	0.36%	0.001%	Max 0.01% for drilling mud
Total heavy metals (Pb)	0.01%	Nil	Max 0.001%
Moisture content	Nil	Nil	Max 0.1%
Loss on ignition (LOI)	0.11%	0.07%	Max 0.5%
Colour	off white	Beige white	Beige white
Specific gravity	4.28 g/cm^3	4.35 g/cm^3	Min. 4.2 g/cm^3 for mud
Particle size	100.0% < 63 µm	100.0% < 63 µm	Max. 3.0% > 75 µm for drilling mud, Vary for others
Flotation chemicals	Nil	Nil	Nil for drilling mud

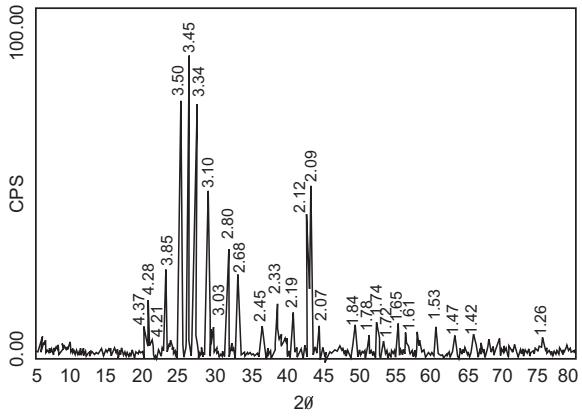

Fig. 2. XRD of Duddar barite ore representing the peaks of various minerals.

Ciccu *et al*. (1987) applied gravity concentration using jigs and flotation method with Na-Cetylsulphate to upgrade barite ore collected from Barega mine in Sardinia, Italy into a concentrate assaying 94-95% $BaSO_4$. Nwoko and Onyemaobi (1997) used gravity concentration using Wilfley Mineral Jig on Nigerian barite ore possessing 87% $BaSO_4$ to obtain a barite concentrate having 98% $BaSO_4$ for industrial use with 95% recovery. Hadjiev *et al*. (2000) applied magnetic separation to separate iron minerals and then froth flotation on tailings using OMC 199 and AERO 845 flotation reagents in ratio of 2:1 to obtain a barite concentrate ranging from 87% to 97% but with relatively low recovery of around 53% from Kremikovtzi ore-deposit, Bulgaria containing 32% $BaSO_4$. Khan *et al*. (2003) applied leaching process using 25% HCl to leach out the impurities from Gunga barite ore, District Khuzdar, Balochistan containing 92% $BaSO_4$ and produced a concentrate assaying 95% $BaSO_4$. Chemical processing could not minimize silica content and only minimized the iron, calcium and magnesium content. Moreover, it is more expensive as compared to physical processing when applied on low to medium grade ores due to more consumption of chemicals. Raju *et al*. (2004) applied direct flotation using oleic acid (anionic collector) as well as reverse flotation in the presence of Armoflote (cationic collector) and could produce barite concentrate of 96% purity from Mangampet barite deposit of Andhra Pradesh, the largest deposit in the world. Kumar *et al*. (2005) applied cationic flotation on Indian barite ore using Armoflote collector followed by dilute sulphuric acid leaching of 96% flotation concentrate and prepared a barite concentrate of 98% purity with 80% recovery. Udenko *et al*. (2011) upgraded a barite ore of Azara, Nasarawa State, Nigeria, from 75.40 to 91.90% content with recovery of 86% through flotation technique using palmitic acid as collector.

In order to minimize the impurities and as a consequence maximize the percentage of barium content in the ore, it was decided to use gravity concentration and froth flotation techniques for up gradation of this ore. Gravity concentration tests were performed employing laboratory sized Wilfley shaking table. It produced three products named as concentrate, middling and tailing. As can be seen from metallurgical balance of these results (Table 4) that barite was concentrated however, a significant fraction of the barite also reported to the middling and tailing products. The results of the gravity based test work revealed that the barite was not sufficiently liberated at coarser sizes so it could not produce desired grade concentrate with acceptable recovery. The most reasonable result obtained by gravity processing is a grade of 84.07% at a recovery of 60.08%. Obviously, gravity based separation could not be applied successfully to this ore due to fine-grained nature of this ore. Then froth flotation technique using Denver flotation machine was employed for up-gradation of $BaSO_4$ content. The froth flotation technique seemed to be a better option for attaining the desired grade and recovery.

Effect of feed size of ore. To study the influence of feed size, different feed sizes of the ore were prepared. The ore was wet ground in rod mill to achieve desired feed size with solid to liquid ratio of 1:1. The flotation tests were carried out on feed sizes of almost 100% passing 100, 150, 200 and 250 mesh sizes. The experiments were performed at arbitrarily selected values and reagents, i.e., at natural pH, 30% pulp density, 1000 rpm, 15 min conditioning period and 20 min of froth collecting time with sodium oleate as collector, polyglycol-400 as frother and sodium silicate as depres-sant. Figure 3 presents the results of the effect of particle size on the grade and recovery of $BaSO_4$ concentrate. This figure depicts a gradual increase in the grade of concentrate with an appreciable increase in the recovery of $BaSO_4$ with the decrease in particle size up to 200 mesh (75 μm). It was established that as the grind size became fine to finer i.e., from 200 to 250 mesh size, the grade improved a little with slight decrease of recovery. The best flotation recovery was obtained when the feed size was almost 100% passing 200 mesh size. This feed size was considered as optimum and selected for onward flotation tests. At still finer grinding i.e., after 200 mesh

size, it was noticed that more slimes were generated which had actually lowered the recovery of concentrate. Moreover, lower recovery as well as grade at coarse particle size revealed that barite was not sufficiently liberated from associated gangue and thereby reported to the tailings.

Effect of pulp density of slurry. In order to study the effect of pulp density on the flotation behaviour of the composite ore, a series of four experiments was conducted using 20, 25, 30 and 35% solids in the slurry. The flotation feed was conditioned initially at 60-65% solids. The slurry having grind size of 100% passing 200 mesh was conditioned for 15 min at 1000 rpm using appropriate quantities of sodium oleate as collector, polyglycol-400 as frother and sodium silicate as depressant at natural pH. The feed was then diluted to 20-35% solids. The test results are shown graphically in Fig. 4. It may be observed that pulp density variation has a significant influence on grade and recovery of $BaSO_4$. As the pulp density increased from 20 to 25% solids, recovery is improved profoundly with no fall in grade. But when it is further increased to 30% and then 35% solids, a slight change takes place resulting in lower grade and recovery. This behaviour may be due to the fact that a pulp density higher than 25% solids produced thick froth layer which was difficult to wash. It can be explained that the draining out of entrapped gangue particles was not proper at higher pulp densities (Jain, 2001). Accordingly, in subsequent experiments, the pulp density was fixed at 25% solids.

Effect of pulp pH. In a series of flotation experiments, pH of the pulp was varied using soda ash as pH modifier and keeping other variables constant. It was found that for different collectors, the froth formed in the pH range of 8-12. With sodium oleate collector it was found that better results were obtained near pH 10. The results attained at different pH values of pulp using sodium oleate as collector are shown in Fig. 5. The plot of barite recovery against pH showed that as the pH increased from 8 to 10, both grade and recovery were increased but after that grade and recovery were dropped slightly. This shows that at pH 10, the mineral-collector bond is more stable leading to maximum recovery. Moreover, at this point, the net adsorbed ion charges become zero so the surface of the barite particles for the adsorption of the collector becomes saturated with collector mono-layer (Zhao *et al*., 2014). It was accordingly, decided to maintain the pH at 10 for the subsequent flotation trials for the composite ore.

Effect of agitation speed. Some flotation experiments were carried out in order to observe the effect of agitation speed on the grade and recovery of barite concentrate keeping other variables constant and varying the agitation

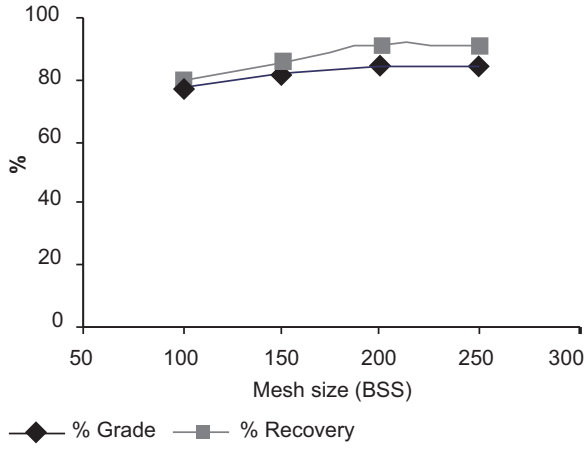

Conditions: (a) Pulp density: 30%; (b) pH of the pulp: Natural; (c) Impeller speed: 1000 rpm; (d) Collector (sodium oleate): 500 g/ton; (e) Frother (polyglycol-400): 50 g/ton; (f) Depressant (sodium silicate): 500 g/ton; (g) Conditioning time: 15 min and (h) Flotation time: 20 min.

Fig. 3. Effect of feed size on grade and recovery of barite rougher concentrate.

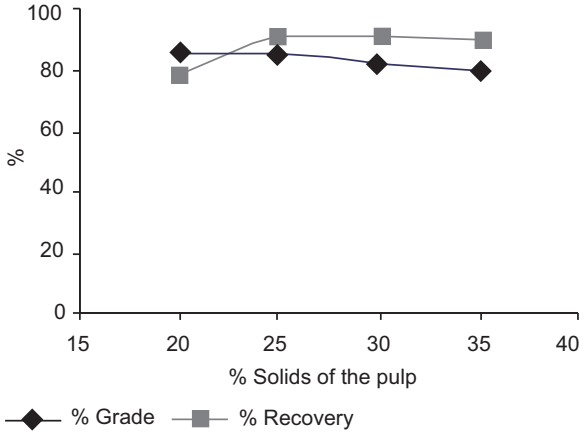

Conditions: (a) Grind size of ore: 100%-200 mesh; (b) pH of the pulp: Natural; (c) Impeller speed: 1000 rpm; (d) Collector (sodium oleate): 500 g/ton; (e) Frother (polyglycol-400): 50 g/ton; (f) Depressant (sodium silicate): 500 g/ton; (g) Conditioning time: 15 min and (h) Flotation time: 20 min.

Fig. 4. Effect of pulp density on grade and recovery of barite rougher concentrate.

speed. The flotation feed was conditioned at 25% solids at a pH of 10 which is achieved through the addition of sodium carbonate. The reagents were added and feed was conditioned for a minimum of 15 min prior to the flotation. The reagents used and their quantities are mentioned below the respective figure. The plot of percentage grade and recovery against agitation speed is shown in Fig. 6. It was found that impeller speed of 1100 rpm yielded the best grade concentrate along with high recovery indicating the adequate mixing and aeration in the pulp. Figure 6 elucidates that recovery increases with agitation speed up to 1100 rpm beyond which grade decreases. It was observed that at lower impeller speed (less than 1000 rpm) the surface is quite low so that froth height and its removal were improper leading to lower recovery. On the other hand, higher impeller speed (1200 rpm and above) spilled the pulp along with froth into the launder resulting in lower grade.

Effect of collector dosage. Various types of cationic and anionic collectors are used in flotation of barite ores. The cationic collectors, mostly primary fatty amines, may be used in the reverse flotation of silica and silicate impurities from barite ore when the ore is high grade. The anionic collectors, largely fatty acids and their salts are used in the flotation of barite mineral in case of low grade ores. Alkyl sulphonates or petroleum sulphonates are rarely used as collector for barite although they have greater selectivity but their collecting power is low. As flotation response of calcite and fluorite is similar with fatty acid collectors, the separation from these minerals present some problems. Many investigators have shown that sulphonate are more selective in these systems (Wills and Napier-Munn, 2006; Davis, 1985). The AERO 827 promoter has also been used for many years to float barite mineral. The AERO 845 promoter is particularly preferred where high selectivity against fluorite and calcite is required. The newest AERO 856 promoter has much greater selectivity and has exhibited a significant increase in recovery (Day, 2002).

For present medium grade barite ore, different anionic collectors such as tall oil, oleic acid, palmitic acid, Aero 845 (sulphosuccinamate), and sodium oleate were tried in separate batches in neutral and basic pH range, keeping other parameters constant. Sodium oleate yielded the best over all metallurgical performance in terms of grade and recovery. Although, AERO 845 collector gave a higher grade of concentrate than was obtained with sodium oleate collector but it gave substantially lower recoveries. It appears that sodium salt of fatty acid is more selective for barite than fatty acid collectors. For this test work, sodium oleate was used as the collector since it gave much higher recoveries

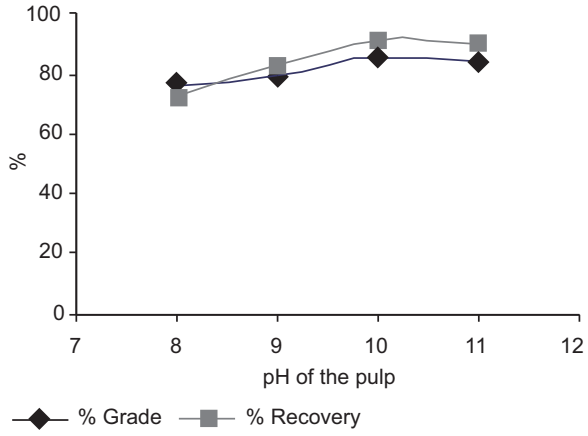

Conditions: (a) Grind size of ore: 100%-200 mesh; (b) Pulp density 25%; (c) Impeller speed: 1000 rpm; (d) Collector (sodium oleate): 500 g/ton; (e) Frother (polyglycol-400): 50 g/ton; (f) Depressant (sodium silicate): 500 g/ton; (g) Conditioning time: 15 min and (h) Flotation time: 20 min.

Fig. 5. Effect of pulp pH on grade and recovery of barite rougher concentrate.

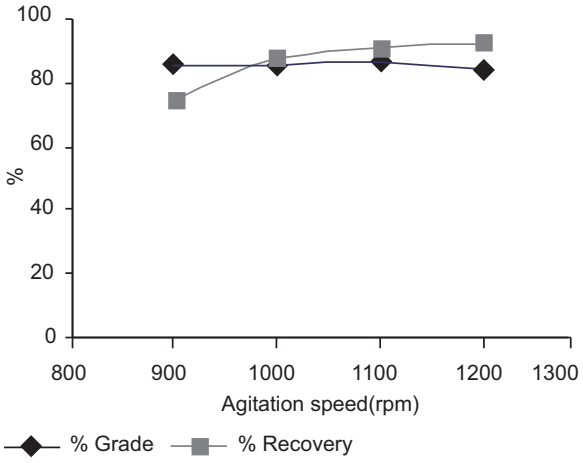

Conditions: (a) Grind size of ore: 100%-200 mesh; (b) Pulp density: 25%; (c) pH of the pulp: ~10; (d) Collector (sodium oleate): 500 g/ton; (e) Frother (polyglycol-400): 50 g/ton; (f) Depressant (sodium silicate): 500 g/ton; (g) Conditioning time: 15 min and (h) Flotation time: 20 min.

Fig. 6. Effect of agitation speed on grade and recovery of barite rougher concentrate.

in the rougher flotation. The results of flotation tests at different concentrations of collector are presented in Fig. 7. It can be seen from the obtained results that with increase in concentration of collector from 200 to 600 g/ton, higher recovery of barite results with a slight change in its grade. The collector sodium oleate yielded the best metallurgical results at a concentration of 600 g/ton and hence, it is the optimum value. This amount shows the starvation level i.e., the concentration required for making the monomolecular layer of collector on surface of particles and increased concentration tends to reduce the selectivity by collecting and floating other minerals (Wills and Napier-Munn, 2006).

Effect of frother dosage. A few flotation experiments were conducted to study the effect of type and dosage of frother on flotation behaviour of barite ore. Various types of frother such as pine oil (mainly terpineol), Cresol (cresylic acid), Aerofroth 65 (polypropylene glycol) and methyl isobutyl carbinol (MIBC) were tried. In a few earlier experiments, pine oil was used as frother in combination with sodium oleate collector, but no considerable change in froth stability was observed. The bubbles produced were of larger size and broke immediately after formation. Then cresylic acid was employed as frother in combination with sodium oleate collector, but the results with respect to grade and recovery were also poor leading to premature breakdown of froth. Results using methyl isobutyl carbinol were also similar showing no encouraging results. Then in another experiment a combination of polyglycol-400 with sodium oleate collector was used. This combination gave very good results in terms of stable froth with dense small size bubbles. Many flotation tests were performed by varying its concentration. The effect of frother dosage on the flotation of composite ore is shown in Fig. 8. The results describe that the best grade and recovery was obtained when 60 g/ton of polyglycol-400 was used as frother and further dosage has no pronounced effect.

Effect of depressant. Different contaminants present in barite ore were quartz, various carbonates and sulphides. In order to depress these gangue minerals, three different types of depressants were tried. These were sodium polyphosphate, sodium polyacrylate and sodium silicate. It was observed from these preliminary experiments that sodium silicate was the most effective depressant employed. Hence, further trials were continued using sodium silicate as a regulator. The results obtained using different quantities of depressant are shown graphically in Fig. 9. It is obvious from this figure that with increase in amount of the depressant from 100 to 400 g/ton both the grade and recovery of the concentrate were improved and after that value the grade improved a little but the recovery was decreased.

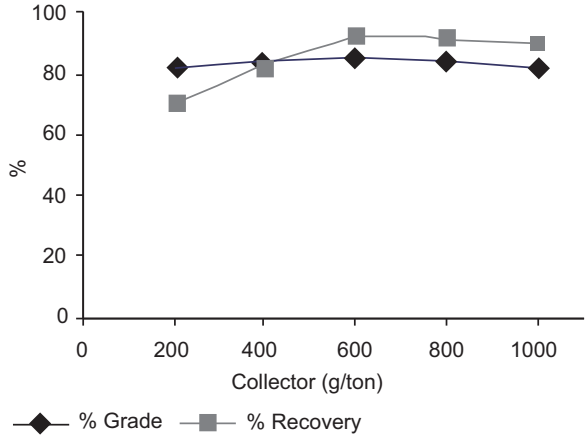

Conditions: (a) Grind size of ore: 100%-200 mesh; (b) Pulp density: 25%; (c) pH of the pulp: ~10; (d) Impeller speed: 1100 rpm; (e) Frother (polyglycol-400): 50 g/ton; (f) Depressant (sodium silicate): 500 g/ton; (g) Conditioning time: 15 min and (h) Flotation time: 20 min.

Fig. 7. Effect of collector dosage on grade and recovery of barite rougher concentrate.

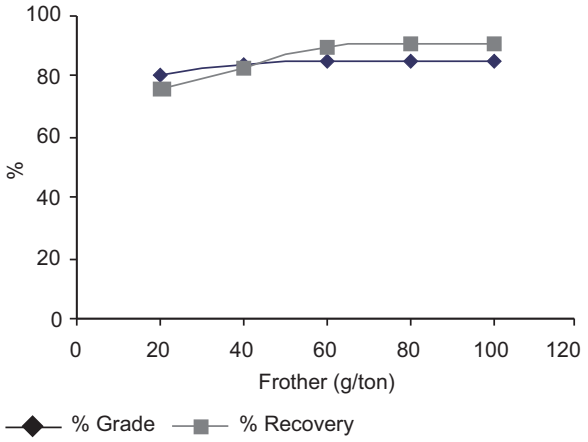

Conditions: (a) Grind size of ore: 100%-200 mesh; (b) Pulp density: 25%; (c) pH of the pulp: ~10; (d) Impeller speed: 1100 rpm; (e) Collector (sodium oleate): 600 g/ton; (f) Depressant (sodium silicate): 500 g/ton; (g) Conditioning time: 15 min and (h) Flotation time: 20 min.

Fig. 8. Effect of frother dosage on grade and recovery of barite rougher concentrate.

Hence, for further trials the depressant amount was kept fixed at 400 g/ton. This effect can be explained that sodium silicate efficiently depresses the gangue minerals with proportionate amount but excessive amount decreases the recovery due to an over coating of some middling particles (Wills and Napier-Munn, 2006).

Effect of conditioning period. Preliminary flotation experiments were conducted at an arbitrary selected value of 15 min after the addition of reagents. While later on, in order to determine the optimum conditioning period, it was varied from 8 to 16 min keeping other conditions constant. The plot of percentage recovery versus conditioning time is shown in Fig. 10. It indicates that recovery increases with time up to 12 min beyond which recovery decreases. It can be seen from this figure that, conditioning time of over 10 min and less than 14 min produces higher grade and recovery. It was found that maximum recovery of 92% could be obtained in rougher flotation at a conditioning time of 12 min. Increasing the conditioning time beyond this period reduced the recovery as well as the grade to some extent. This may be due to shearing of collector layer initially deposited on the particle's surface due to reverse process of desorption of the collector molecules from the surface of the barite particles (Raju *et al*. 2004). In the later tests a conditioning time of 12 min was considered as optimum and selected.

Effect of flotation time. After adjusting the other parameters constant i.e., feed size of 100% passing 75 µm, pulp density set at 25% solids and pulp pH of 10, conditioning time for 12 min, a series of four tests was performed to study the effect of flotation time, in which the froth collecting time was varied from 5 to 25 min. The froth was collected separately for these different time intervals. When froth became thinner, additional amount of collector was added and conditioned for another 5 min. This was collected as scavenger concentrate and mixed along with rougher concentrate. The results of this series of tests are recorded and presented in Fig. 11. It is evident from this figure, that most suitable condition was arrived in about 20 min when nearly all the froth was skimmed off and cell was completely barren.

Effect of cleaning flotation. After optimizing the rougher flotation parameters, it was decided to conduct one series of cleaning flotation tests to improve the grade of rougher barite concentrate. A few flotation tests were carried out at optimum conditions and a sufficient quantity of rougher concentrate was collected for this purpose. It was observed that about 90% of $BaSO_4$ was recovered in rougher concentrate whereas 10% was lost

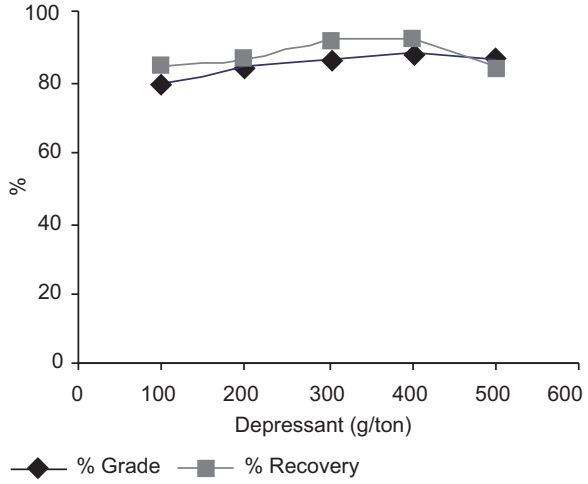

Conditions: (a) Grind size of ore: 100%-200 mesh; (b) Pulp density: 25%; (c) pH of the pulp: ~10; (d) Impeller speed: 1100 rpm; (e) Collector (sodium oleate): 600 g/ton; (f) Frother (polyglycol-400): 60 g/ton; (g) Conditioning time: 15 min and (h) Flotation time: 20 min.

Fig. 9. Effect of depressant quantity on grade and recovery of barite rougher concentrate.

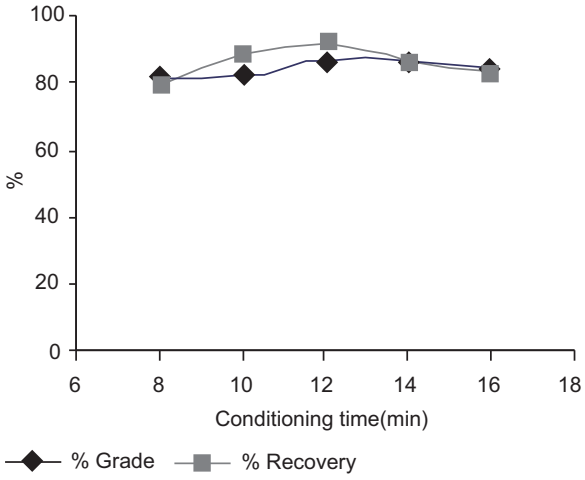

Conditions: (a) Grind size of ore: 100%-200 mesh; (b) Pulp density: 25%; (c) pH of the pulp: ~10; (d) Impeller speed: 1100 rpm; (e) Collector (sodium oleate): 600 g/ton; (f) Frother (polyglycol-400): 60 g/ton; (g) Depressant (sodium silicate): 400 g/ton and (h) Flotation time: 20 min.

Fig. 10. Effect of conditioning time on grade and recovery of barite rougher concentrate.

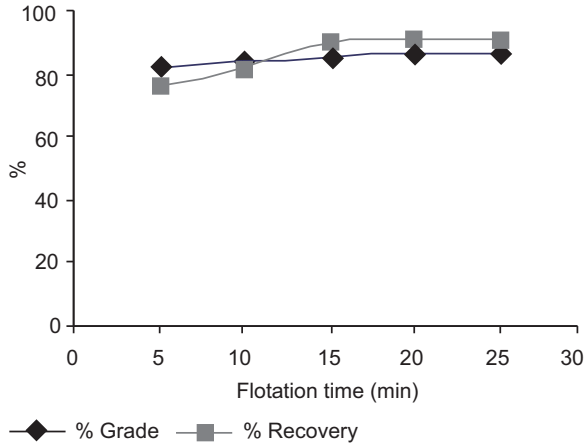

Conditions: (a) Grind size of ore: 100%-200 mesh; (b) Pulp density: 25%; (c) pH of the pulp: ~10; (d) Impeller speed: 1100 rpm; (e) Collector (sodium oleate): 600 g/ton; (f) Frother (polyglycol-400): 60 g/ton; (g) Depressant (sodium silicate): 400 g/ton and (h) Conditioning time: 12 min.

Fig. 11. Effect of flotation time on grade and recovery of barite rougher concentrate.

in rougher tailing. This loss was reduced to 7.65% by scavenging of tailings with the use of additional reagents (Table 6). The scavenging concentrate was mixed along with rougher concentrate to maximize the recovery up to 92.35%. The rougher concentrate obtained in the series of experiments was ground in a rod mill to get a product of 100% passing 250 mesh size (63 μm). The solid to water ratio was kept at 1:1.

The rougher concentrate was then subjected to cleaner flotation. In the cleaner flotation, additional amount of reagents was added to condition the newly liberated particles. A small quantity of sodium chromate (20 g/ton) was also added to depress galena (Jain, 2001). The cleaner flotation tests were carried out at pH 10 with 15% pulp density. Conditioning was done for 12 min at agitation speed of 1000 rpm. Recovery of $BaSO_4$ in the cleaner concentrate was found to be 86.01% at a grade of 93.17% $BaSO_4$. It can be seen in this comparison that cleaning of the rougher concentrate produces substantially higher grade in the cleaner concentrate at the expense of lower recovery (Table 6). Based on these results it was anticipated that the flow sheet for treating this ore would consist of multiple stages of flotation to improve the grade of barite concentrate.

The cleaner concentrate obtained was subjected to re-cleaner flotation without using any flotation reagents and further re-grinding (Table 5). The pulp density and agitation speed were slightly lowered down to 10% and 900 rpm, respectively, to get higher grade without considering the recovery. The results of re-cleaner flotation tests summarized in Table 6 describe that the cleaner concentrate after further re-cleaning step yielded a product assaying 95.83% $BaSO_4$ at about 82.06% recovery. Higher grade flotation product was achieved with re-cleaning flotation which decreased the recovery in final concentrate. It was observed that sodium chromate has successfully depressed the galena in cleaning stages. Overall recovery has been improved by recycling the cleaning and re-cleaning tailings. The developed flow sheet (Fig. 12) shows the multiple recycling of intermediate tailings at appropriate points to earlier stages of flotation. This has ensured a higher grade and recovery of the final concentrate by limiting the loss of barite to the discardable rougher tailings.

Table 6 presents the chemical composition of the final flotation concentrate. The production of barite concentrate with quality according to the requirements (API, 2010) demands the removal contaminants in barite, such as silica, iron oxide, aluminum oxide, calcium oxide, magnesium oxide and heavy metal sulphide which can cause problems in certain mud systems. Drilling-grade barite is expected to have a grade of at least 92% barium sulphate, specific gravity of 4.20 g/cm^3, maximum 3% residue left on 200 mesh screen (75 μm) and should be free of flotation reagents to meet standard API specifications. The concentrate produced contained 95.83% barium sulphate content having specific gravity of 4.28 g/cm^3 and was found free of flotation reagents. The particle sizes also fall predominantly in the range finer than 63 μm i.e., well within the required 75 μm limit. However, the impurities of iron (Fe_2O_3) and alkaline earth metals (CaO and MgO) are slightly higher in flotation concentrate but content of SiO_2 is lower than admissible limit. This is due to the reason that carbonaceous minerals such as siderite, calcite and dolomite also float to some extent with same collector and silica is depressed effectively by sodium silicate. Hence, it was decided to leach out these impurities.

Effect of acid leaching. The requirements of barite concentrate for different industries along with standard specifications are also summarized in Table 7 for comparison (Mills, 2006; Khan *et al*., 2003, Ahmad and Siddiqi, 1992). In the glass industry, the requirements are somewhat rigid but vary to some extent. The general requirements include $BaSO_4$ 96-98%, iron oxide 0.1-0.2% and no more than 1.5% silica and 0.15% alumina.

The barite used in paints should have minimum 95% $BaSO_4$ content and less than 0.05% iron oxide. The rubber industry requires product to be over 99.5% pure with traces of silica, iron oxide and alumina. For the manufacture of various barium chemicals, barite should have at least 95% $BaSO_4$ content, iron oxide less than 1.0% and only traces of fluorine (Mills, 2006; Ahmad and Siddiqi, 1992). Impurities are minimized because these affect the reduction reaction of barite by charcoal or natural gas at 850-950 °C and consequently lower the yield of barium sulphide which is the starting material of other barium chemicals (Khan *et al*., 2003). Silica and alumina when present in appreciable amounts form barium silicate and barium aluminate and keep barite in residue after leaching of barium sulphide with water. Iron is the main colour imparting component which may be present due to iron minerals as well as from abrasion of grinding mills. For paper, glass, ceramics and paint industry its removal is necessary.

Hydrochloric acid and sulphric acid are commonly used for leaching of barite (Kumar *et al*., 2005; Khan, 2003). Sulphuric acid leaching is preferred when ore contain witherite ($BaCO_3$) which is converted into barite on leaching. The main advantage of using hydrochloric acid is that it leaches out anhydrite mineral. Treatment of the final flotation concentrate with hydrochloric acid increases the grade from 95.83 to 98.86% and decreases the unwanted impurities of iron oxide, calcium oxide, magnesium oxide and aluminum oxide to permissible limits. Acid soluble salts of these metals go into the filtrate leaving behind comparatively pure barite. The concentration of 15% hydrochloric was found sufficient to leach out the objectionable impurities (Table 8).

This investigation highlights the applicability of various processes for the beneficiation of low to medium grade barite ore and gives conclusive result regarding the most suitable method for attaining the desired grade and recovery. The technology developed is economical and helpful for the beneficiation rejected and lean grade barite ore for commercial exploitation. The concentrate produced is useful for drilling mud, barite based chemical production and other industrial applications.

Table 8. Effect of acid concentration on the purity of final Duddar barite concentrate

Test no.	Conc. of dilute HCl	Purity of Barite ($BaSO_4$)
1	5%	97.63%
2	10%	98.05%
3	15%	98.86%
4	20%	98.87%

Conclusions

Mineralogical evaluation of the ore shows that it contains mainly barite as an economical mineral whereas the others are associated gangue minerals. The gravity concentration tests on Duddar barite ore using Wilfley shaking table show that it is not helpful for this ore due to heavy losses of barite in tailings which results in poor recovery. Even the best test resulted in insignificant grade of 84.07% with 60.08% recovery. The direct flotation results show that a barite concentrate assaying 95.85% $BaSO_4$ can be obtained with the recovery of 82.06% from this ore. The optimum grade and recovery of rougher concentrate was attained when the slurry of 100% passing 200 mesh size was conditioned for 12 min with 25% solids at pH 10 maintained with soda ash. The best reagents combination used in the flotation was found to be sodium oleate as collector at dosage of 600 g/ton, sodium silicate as depressant at 400 g/ton, Aerofroth 65 as frother at 60 g/ton. In the closed circuit, one roughing along with scavenging followed by regrinding and two consecutive cleanings operations produced maximum grade and recovery. It is concluded that direct flotation is the most suitable method for the up-gradation of this fine-grained ore for commercial exploitation. The obtained leached concentrate is suitable for the barium chemicals industry.

Acknowledgement

The authors are highly thankful to Director, Pakistan Mineral Development Corporation, for providing barite ore.

References

Ahmad, Z., Siddiqi, R.A. 1992. *Minerals and Rocks for Industry*, Geological Survey of Pakistan, Quetta, vol. **1,** pp. 770-771.

Ahsan, S.N., Quraishi, I.H. 1997. Mineral and rock resources of Lasbela and Khuzdar Districts of Balochistan, Pakistan. *Geological Bulletin, University of Peshawar*, **30:** 41-51.

API, 2010. API Spec 13A: *Specification for Drilling Fluids Materials Specifications and Testing*, 18th edition, *American Petroleum Institute*, pp. 7-9.

ASTM, 2007. Standard Test Method for the Determination of Iron in Ores and Related Materials by Dichromate Titration (E 246-05), ASTM International, 100 Barr Harbor Drive PO Box C700,

West Conshohocken, USA, *Annual Book of ASTM Standards*, vol. **03.05,** pp.154-162.

ASTM, 2007. Standard Test Method for the Determination of Iron in Ores and Related Materials (E 247-01), ASTM International, 100 Barr Harbor Drive PO Box C700, West Conshohocken, USA, *Annual Book of ASTM Standards*, vol. **03.05,** pp. 163-165.

ASTM, 2007. Standard Test Method for the Determination of Aluminum in Ores and Related Materials by Comlexometric Titrimetry, (E 738-05), ASTM International, 100 Barr Harbor Drive PO Box C700, West Conshohocken, USA, *Annual Book of ASTM Standards*, vol. **03.05,** pp. 560-562.

Blackburn, W.H. 1988. *Principles of Mineralogy*, 290 pp., 1st edition, W. C. Browns Publishers, Iowa, USA.

Ciccu, R., Curreli, L., Giuliani, S., Manca, P.P., Massacci, G. 1987. Optimization of an integrated flow sheet for barite processing. APCOM87. In: *Proceedings of the Twentieth International Symposium on the Application of Computers and Mathematics in the Mineral Industries*. vol. **2,** Metallurgy. pp. 281-293, SAIMM, Johannesburg, South Africa.

Day, A. 2002. *Mining Chemicals Handbook*, revised edition, pp. 172-173, Cytec Industries Inc. West Paterson, New Jersey, USA.

Davis, F.T. 1985. Barite, In: *SME Mineral Processing Handbook*, N. L. Weiss, (ed.), vol. **2,** Section 29, pp. 6, Society of Mining Engineers of American Institute of Mining, Metallurgical and Petroleum Engineers (AIME) Inc., New York, USA.

Hadjiev, A., Hadjiev, P., Georgiev, R. 2000. Flotation of Barite from Complex Iron Ore, In: *International Symposium on Processing of Fines (PROF-2000)*, November 2-3, P. K. Bhattacharyya, R. Singh and N. G. Goswami, (eds.), pp. 222-230, NML Jamshedpur, India.

Jain, S.K. 2001. *Mineral Processing*, 442 pp., 2nd edition, CBS Publisher and Distributor, New Delhi, India.

Jeffery, G.H. 1989. *Vogel's Text Book of Quantitative Chemical Analysis*, pp. 324, 328, 337, 448 458, 5th edition, Longman Scientific and Technical, Longman Group Limited, UK.

Khan, H., Kanwal, F., Aurangzaib, M. 2003. Studies on the beneficiation of Gunga barite with different concentrations of hydrochloric Acid. *Journal of Chemical Society of Pakistan*, **25:** 44-48.

Kumar, G.S., Ravi, B.P., Venugopal, R. 2005. Characterization and processing of low-grade barite, In: *Mineral Processing Technology (MPT-2005)*, R. Venugopal, T. Sharma, V. X. Saxena and N. R. Mandre (eds.), pp. 232-238, Tata McGraw Hill Publishing Company Limited, New Delhi, India.

Mcrae, M.E. 2011. Barite, In: *Minerals Commodity Summaries 2015*, United States Department of Interior, United States Geological Survey, Reston, Virginia, pp. 24-25. http://www.minerals.usgs.gov/minerals/pubs/mcs/2015/mcs2015.pdf

Mills, P. 2006. Barium Minerals, In: *The Industrial Minerals and Rocks, Commodities, Markets and Uses*, pp. 219-225, 7th edition, J. E. Kogal, N. C. Trivedi, J. M. Barker and S. T. Krukowski (eds.), Society for Mining, Metallurgy and Exploration, (SME) Inc., Littleton, Colorodo, USA.

Naseem, S., Bashir, E., Hussain, K. 2011. Evaluation of geotechnical characteristics of Lasbela barite deposits of Balochistan, Pakistan, as heavyweight aggregate. *Bulletin of Engineering Geology and the Environment*, **70:** 651-655.

Nwoko, V.O., Onyemaobi, O.O. 1997. Beneficiation study on a Nigerian barite ore for industrial use. *Journal of Material Science and Technology*, **13:** 76-78.

Raju, G.B., Probhakar, S., Rao, S.S. 2004. Studies on the beneficiation of barite, In: *International Seminar on Mineral Processing Technology (MPT-2004)*: G. V. Rao and V. N. Misra (eds.), pp. 322-329, Allied Publishers Private Limited, Mumbai, India.

Scott, P.D., Phillips, C., Robinson, L.H. 2010. Economic Considerations and Impacts for Using Low Grade Barite, pp. 1-7, *AADE Fluids Conference and Exhibition*, Hilton Houston North, Houstan, Texas, USA.

Singh, R., Banerjee, B., Bhattacharyya, K.K., Srivastava, J.P. 2007. Up-gradation of Barite Waste to Marketable Grade Concentrate, In: *Proceeding of the XXIII International Mineral Processing Congress (IMPC)*, pp. 2303-2307, Mineral Processing Division, National Metallurgical Laboratory, Jamshedpur, India.

Udenko, A., Gerald, A.C.O., Martins, O., Ausaji, A. 2011. Flotation recovery of barite from ore using palm bunch based collector. *International Journal of Chemical Sciences*, **9:** 1518-1524.

Wills, B.A., Napier-Munn, T.J. 2006. *Wills' Mineral Processing Technology*, pp. 270-276, 7th edition, Butterworth-Heinemann Publishers, Oxford, UK.

Zaigham N.A., Mallick, K.A. 2000. Bela ophiolite zone of southern Pakistan: Tectonic setting and associated mineral deposits. *Bulletin of Geological Society of America*, **112:** 478-489.

Zhao, Y., Liu, S.Q., Li, X.J., Li, T.T., Hou, K. 2014. Recovery of low grade barite ore by flotation in the southwest area of China. *Applied Mechanics and Materials*, **543-547:** 3865-3868.

Pak. j. sci. ind. res. Ser. A: phys. sci. 2017 **60**(1) 22-28

Experimental Investigation of Performance Characteristics of Compression Ignition Engine Fuelled with Punnai Oil Methyl Ester Blended Diesel

Mathan Raj Vijayaragavan*, Ganapathy Subramanian, Lalgudi Ramachandran, Manikandaraja Gurusamy, Rahul Kumar Tiwari and Sanat Kumar
Department of Mechanical Engineering, SRM University, Chennai, India

(received March 14, 2016; revised September 15, 2016; accepted October 18, 2016)

Abstract. Biodiesel is a renewable substitute to conventional diesel and offers cleaner performance. This paper deals with performance characteristics of four stroke, water cooled Compression Ignition (CI) engine fuelled with four different oils: diesel, diesel-punnai oil biodiesel 10% (B10), diesel-punnai oil biodiesel 20% (B20) and diesel-punnai oil biodiesel 30% (B30). The present research, experiments were conducted to study the effect of viscosity, cetane number, flash point, calorific value and density on performance characteristics of diesel, Punnai oil biodiesel and its different blends (B10, B20, B30). The experimental results of this study showed that the diesel has 2.6% and 4.6% higher brake specific fuel consumption (BSFC) as compared to B10 and B20, respectively at full load, whereas BSFC of diesel was same as B30 at higher load. Volumetric efficiency and mechanical efficiency of B10 was 1.2% and 7.5% higher as compared to diesel at full load condition. Brake Thermal Efficiency (BTE) and indicated thermal efficiency of B20 was 8.12% and 7% higher as compared to diesel at full load. From this study, it is concluded that Punnai oil biodiesel could be used as a viable alternative fuel in a single cylinder, four stroke, water cooled direct injection diesel engine.

Keywords: biodiesel, compression ignition engine, Punnai oil biodiesel, performance

Introduction

World energy demand is expected to increase due to the expanding urbanisation, better living standards and increasing population. At the same time when society is becoming increasingly aware of the declining reserves of fossil fuels beside the environmental concerns, it has become apparent that biodiesel is destined to make a substantial contribution to the future energy demands of the domestic and industrial economies. Moreover, a rapid decline in the fossil fuels has led scientists and researchers to look for new alternatives. Biodiesel is a suitable alternative for diesel and has an advantage over diesel because of its biodegradable nature, remarkable lubricity and better emission characteristics. The properties of biodiesel fuel mostly depend on the production technique and fatty acid composition of the oil. Although appropriate techniques are used in production of biodiesel, the properties of biodiesel fuel may not lie within the limits of the biodiesel standards due to the fatty acid composition of the oil (Serrano *et al*., 2013; Canakci and Sanli, 2008). So to conclude these challenges the most appropriate method to use the vegetable oils in Compression Ignition (CI) engines is by converting it into fatty acid methyl ester by the process of trans esterification (Agarwal and Dhar, 2013).

Vegetable oils have good ignition characteristics due to long chain hydrocarbon structure, however, they acquire high viscosity, lower calorific value, higher density and higher molecular weight. These physical properties cause poor thermal efficiency, while using vegetable oil in the engine. These properties can be changed by using different methods such as trans esterification, dilution and cracking method (Singh, 2012) that can be used to reduce the viscosity of vegetable oils. Punnai oil biodiesel and its different blends (B10, B20, B30) can be used on existing Compression Ignition (CI) engines to achieve both the energy and environmental benefits. There are different studies related to engine tests of biodiesel fuel blends. Rao *et al*. (2009) conducted experimental investigations on *Jatropha* biodiesel and its additive in a diesel engine. The results of the experiment showed that B100 had lower brake thermal efficiency mainly due to its high viscosity compared to diesel and B25 have closer performance to diesel. The brake thermal efficiency for B75 and B50 was found to be 14.5% and 24.45% higher

*Author for correspondence;
E-mail: mathanraj.v@ktr.srmuniv.ac.in

than that of diesel fuel. Ozer (2014) carried out the experiment on waste cooking oil and its blends B5 and B10 in a single-cylinder, direct injection, four-stroke, natural aspirated diesel engine. It was found that 5% and 10% biodiesel fuel addition resulted in slightly increment on break specific fuel consumption (up to 4%) and reduction on break thermal efficiency (up to 2.8%). Agarwal (2007) conducted experiment on a single cylinder, four stroke, constant speed, water cooled, direct injection diesel engine (typically used in agricultural sector) was used for the experiments. The acquired data were analysed for various parameters such as thermal efficiency, brake specific fuel biodiesel consumption (BSFC) and were nearly equal to diesel. How (2014) carried out the experiment and the result showed that the BSFC of B20E5 and B20 is higher than baseline diesel. In overall, B20E5 showed 2.0-2.7% higher BSFC compared to baseline diesel fuel at all engine loads. This was concluded due to the lower heating value of biodiesel and ethanol blends compared with that of baseline diesel. Masjuki *et al*. (2001) used preheated palm oil to run a CI engine. Better spray and atomization characteristics were obtained due to reduction in the viscosity of fuel while preheating it. Torque, brake-power, specific fuel consumption, and brake thermal efficiency were found to be comparable to those of mineral diesel. Raheman and Ghadge (2009) showed in his result that the reductions in brake specific fuel consumption together with increase brake power, brake thermal efficiency made the blend of biodiesel (B20) a suitable alternative fuel for diesel. Keeping these facts in mind, a set of engine experiments were conducted using Punnai oil biodiesel and different blends (B10, B20, B30) on an engine. Heating and transesterification were used to lower the viscosity of Punnai oil biodiesel and its different blends (B10, B20, B30) in order to eliminate various operational difficulties.

Materials and Methods

Biodiesel preparation. The production of biodiesel from Punnai oil was done by 2-step, trans esterification process. The first step acid, catalysed esterification reduces the free fatty acids (FFA) value of the oil to about 2%.

The second step, alkaline catalysed trans esterification process converts the products of the first step to its mono-esters and glycerol. In acid esterification, 1000 mL Punnai oil is heated to about 50 °C; 250 mL methanol is added and stirred for a few minutes. With this mixture 2% (v/v) of sulphuric acid (H_2SO_4) was also added and stirred at a constant rate with 50 °C for 1 h. After the reaction was over, the solution was allowed to settle for 24 h in a separating funnel. The excess alcohol along with sulphuric acid and impurities floated at the top surface and was removed. The lower layer was separated for further processing (alkaline esterification). In alkaline catalysed esterification, the products of the first step were again heated to about 50-55 °C. With this mixture, 5 g KOH dissolved in 250 mL methanol was added and stirred for 60 min. After the reaction was over, the solution was again allowed to settle for 24 h. The glycerin settled at the bottom and esterified Punnai oil rose to the top. This esterified Punnai oil (biodiesel) was separated and purified with warm water. After washing the final product was heated up to 60 °C for 10 min.

Experimental setup. An experimental setup was made to evaluate the performance of the engine. The overall view of the experiment setup is shown in Fig. 1. The present paper discusses the details of the experimental setup, instruments used and software needed for the work. Figure 2 shows a representation of diesel engine testing facility used to study engine performance and

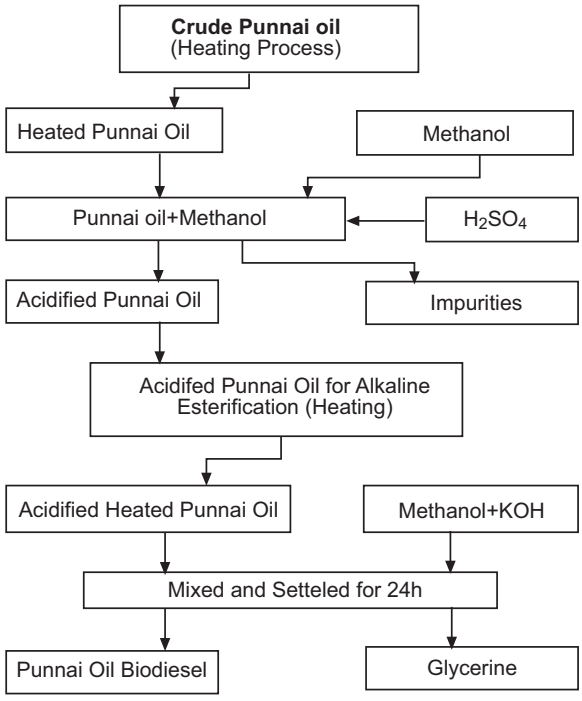

Fig. 1. Schematic representation of the 2-step transesterification.

combustion properties. All the specifications of engine are listed in Table 1. An eddy current dynamometer was connected with the engine and used to measure engine power. To evaluate the performance parameters, the important operating parameters were engine speed, power output and fuel consumption. Significant engine performance parameters such as brake specific fuel consumption (BSFC) and brake thermal efficiency (BTE) for biodiesel and its blends were calculated.

Computerised digital data acquisition system. The values of cylinder pressure and TDC signals were taken and stored on a high speed computer based digital data acquisition system. With specially designed software the stored signals were processed to obtain the performance parameters (B.P, volumetric efficiency, specific fuel consumption) and also other parameters like peak pressure, maximum rate of pressure rise etc.

Optical TDC positioning sensor. An electro optical sensor was used to give a voltage pulse exactly when the TDC position was reached. This sensor consists of a well aligned pair of infrared diode and phototransistor so that the infrared rays emitted from the diode fall on the phototransistor when not interrupted. Voltage signals from the optical sensor were fed to analogue to digital converter and then to data acquisition system along with pressure signals for recording.

Load and speed measurement. The engine was coupled to an eddy current dynamometer. The specification of the eddy current dynamometer is given in Table 1. The dynamometer unit basically comprises a rotor mounted on shaft running on bearings which rotates within a casing supported in ball bearing which forms the plate of the machine. The dynamometer load measurement is from load cell, speed measurement and a strain gauge is from a shaft mounted with a sixty tooth wheel and with magnetic pulse pickup. The voltage pulses from the sensor are sent to digital data rpm meter for pulse conversion and it displays the engine speed with an accuracy of 1 rev/min.

Table 1. Technical features of the test engine

Engine specification	Details
Number of cylinders	single cylinder
Cycle	four stroke
Ignition system	compression ignition
Bore x stroke	87.5 × 110 mm^2
Displacement volume	661 cm^3
Compression ratio	18:1
Valve arrangement	overhead
Rated power	3.5 kw@1500 rpm
Cooling medium	sater cooled
Eddy current dynamometer	60 kw

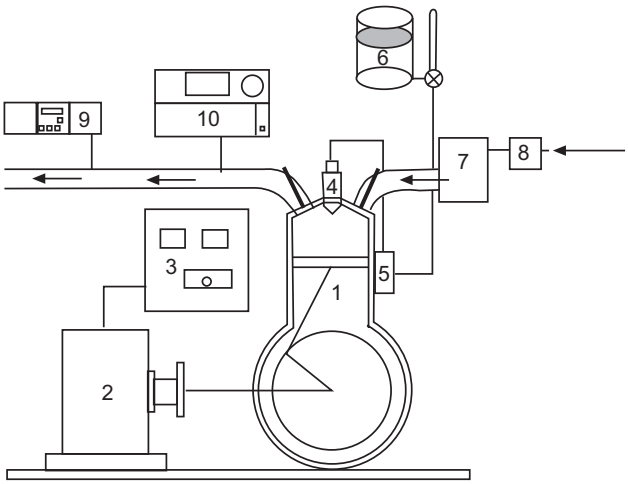

Fig. 2. Schematic diagram of the experimental step.

Fuel properties testing. Punnai oil biodiesel and its different blends (B10, B20, B30) were prepared in lab on volume basis and its main purpose was to replace diesel fuel in maximum quantity in order to increase the amount of fuel oxygen to maximum limit, but keeping the other essential properties (calorific value, pour point, density, Cetane index, flash point and viscosity) within the acceptable limits. These essential properties of biodiesel were measured experimentally. The viscosity was measured by using a dynamic viscometer, the fuel density was measured by weighing a known volume of fuel; the measurement principle consisted of measuring the time needed for a known volume of fuel to drop from a Viscometer. All properties were measured with standard procedure given in the ASTM standards

Results and Discussion

Fuel properties. Different fuel properties of Punnai oil biodiesel (B100) and its blends (B10, B20, B30) with diesel was found and summarized in Table 2. It can be seen from this Table that the fuel properties of B10 are comparable with those of diesel. The Punnai oil biodiesel (B100), however, was found to have much higher values of fuel properties, especially viscosity and density, way above any of these standard limits – thus restricting its direct use as a fuel for diesel engines.

Density. The density of the oil is important because it gives an indication of the delay between the injection and combustion of the fuel in a diesel engine. The densities of Punnai oil biodiesel (B100) and its blend (B10, B20, B30) was observed and found to be higher than that of diesel. Thus, density of Punnai oil biodiesel (B100) was about 9.25% higher than the diesel. The densities were observed to increase with the increasing concentration of biodiesel in the blends. Reason of higher densities of Punnai oil biodiesel and its blends as compared to diesel may be due to the higher molecular weights of triglyceride molecules and free fatty acid present in them.

Kinematic viscosity. Kinematic viscosity is the most important property of biodiesel since it effects the operation of fuel injection equipment. Moreover, high viscosity may lead to formation of soot and engine deposits due to insufficient fuel atomization. The kinematic viscosity of Punnai oil biodiesel (B100) and its blends (B10, B20, B30) was found to be higher than the diesel. However, the viscosity of blends increased with increasing concentration of biodiesel in the blends.

Calorific value. The gross calorific values of B100 were found to be 38.55 MJ/kg, respectively, which is 9.28% lower than 42.5 MJ/kg for diesel. This could be due to the difference in their chemical composition from that of diesel or the difference in the percentage of carbon and hydrogen content, or the presence of oxygen molecule in the molecular structure of Punnai oil and biodiesel. The calorific values of the blends proportionately decrease with the increase in biodiesel percentage.

Flash point. Flash point of the fuel is the temperature at which it will ignite when exposed to a spark or flame. Flash point varies inversely with the fuels volatility (Uriarte, 2010; Sanford *et al*., 2001). Flash point is the lowest temperature at which fuel emits enough vapour to ignite. The flash points of B10, B20, B30 and B100 were determined to be higher, respectively, and were not so high as compared to diesel. The flash points of all the blends were also higher than that of diesel. Thus overall flammability hazard of Punnai oil biodiesel (B100) is much less than that of conventional diesel.

Cetane number (CN). The CN is a measure of the ignition quality of the fuel during combustion ignition. It provides the information about the delay time of a fuel upon injection into the combustion chamber. High CN implies short ignition delay (Raj and Sahayaraj, 2010). Fuels

Table 2. Fuel properties of Punnai oil, Punnai oil biodiesel, blends of biodiesel and diesel

Fuel blend	Standard method	Diesel	Punnai oil	B10	B20	B30	B100
Density (kg/m^3)	ASTM D127	840	926.6	847.77	855	863.13	917.7
Viscosity (cST)	ASTM D445	2.87	12.5	3.11	3.27	4.23	5.97
Flash point (°C)	ASTM D93	51	218	59	88	124	172
Cetane number	ASTM D6890	45	-	45	49	45	64
CV (kJ/kg)	ASTM D240	42500	38511	42150	40362	41316.2	38554

with low CN cause knocking and show increased gaseous and particulate exhaust emissions due to incomplete combustion. The CN were observed to increase linearly with the increasing concentration of biodiesel in the blends. This is the reason why there is less emission found in biodiesel.

Engine performance. ***Brake specific fuel consumption (BSFC).*** Brake specific fuel consumption (BSFC) is a measure of volumetric fuel consumption for any particular fuel. The variation of brake specific fuel consumption with brake power output is shown in Fig. 3. The brake specific fuel consumption is determined by dividing the total fuel consumption per hour by the power developed. As seen from the Graph 1 that B30 has almost same fuel consumption at full load condition (Puhan *et al*., 2005; Raheman and Phatadare, 2004). This may be due to higher viscosity and higher density of the B30 as compared to other blends of Punnai biodiesel. The study showed that the diesel has 2.6% and 4.6% higher brake specific fuel consumption (BSFC) as compared to B10 and B20, respectively, at full load.

BSFC = ṙ/ṫw
BSFC = brake specific fuel consumption
ṙ = fuel consumption rate (g/s)
ṫ = Engine torque (N-m)
w = Engine speed (rad/s)

Total fuel consumption. The total fuel consumption is determined by measuring the volume or weight of fuel consumed by the engine under given test condition in a given time. The variation of total fuel consumption with brake power output is shown in Fig. 4. As seen from Fig. 4, B10 has the highest total fuel consumption as compared to diesel and different blends.

Brake mean effective pressure (Bmep). This is the average effective cylinder pressure that does useful work calculated from the brake power. The work accomplished during one engine cycle divided by the engine swept volume. The brake mean effective pressure is directly proportional to brake power and increases with load. As seen in Fig. 5 there is no particular change in the effective pressure of diesel and biodiesel.

Volumetric efficiency. Volumetric efficiency shows the breathing ability of the engine. More precisely, volumetric efficiency is a ratio of actual volume flow

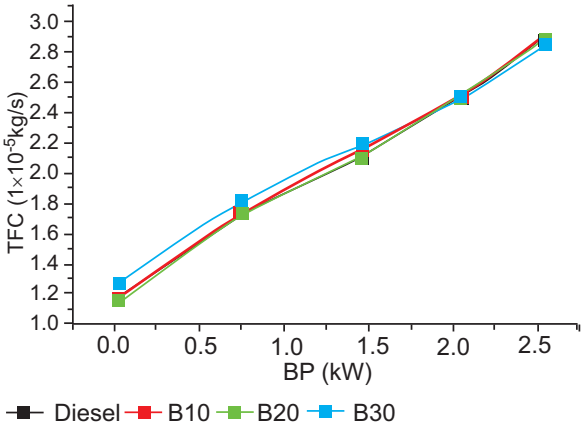

Fig. 4. Effects of biodiesel addition on total fuel consumption under different engine loads.

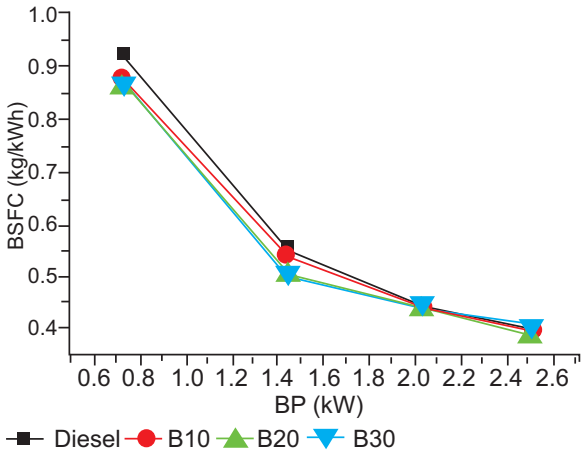

Fig. 3. Effects of biodiesel addition on brake specific fuel consumption under different engine loads.

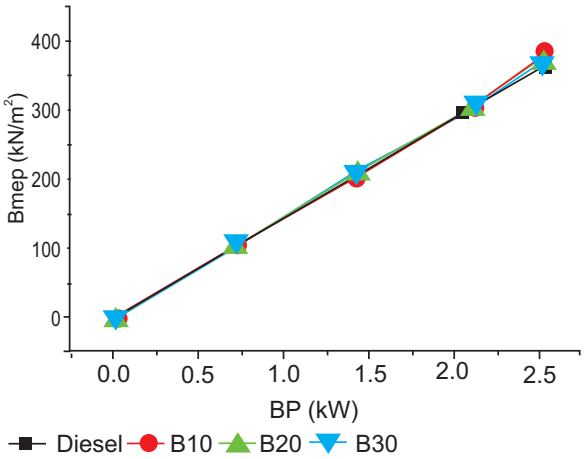

Fig. 5. Effects of biodiesel addition on brake mean effective pressure (Bmep) under different engine loads.

rate of air into the intake system to the rate at which the volume is displaced by the system. Figure 6 shows that there are no major changes at initial load, but there is a sudden drop in efficiency of B20 at full load condition. The reason may be due to improper mixing of B20 at full load condition. Whereas the result showed that B10 has 1.2% higher volumetric efficiency as compared to diesel at full load.

Mechanical efficiency. Mechanical efficiency measures the effectiveness of a machine in transforming the energy and power that is input to the device into an output force and movement. Mechanical efficiency is the ratio of brake thermal efficiency to indicated thermal efficiency. The mechanical efficiency is increased with the increase of engine load due to the remarkable improve in the fuel combustion quality at high engine load as shown in Fig. 7. As seen that B10 has 7.5% higher efficiency at full load condition as compared to diesel. The reason may be due to proper atomization of B10 and proper combustion at full load condition.

Brake thermal efficiency. The brake thermal efficiency is increased with the increase of engine load due to the remarkable improvement in the fuel combustion quality at high engine load as shown in Fig. 8. Increased brake thermal efficiency of Punnai oil biodiesel and its blends is attributed to increase in oxygen content of the fuel, resulting in improved combustion. The result showed that B20 was 8.12% higher than diesel at full load condition. Previous research works also shows that high kinematic viscosity and density fuels with lower calorific value tend to increase the brake specific fuel consumption and lower the brake power as it results in poor atomisation of fuel during spraying of fuels inside the combustion cylinder (Spataru and Romig, 1995; Wagner *et al*., 1984).

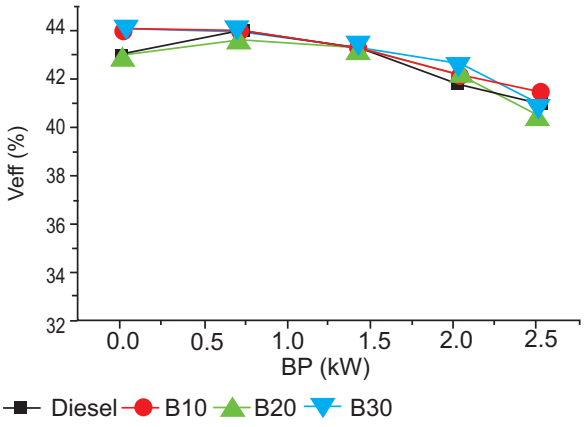

Fig. 6. Effects of biodiesel addition on volumetric fuel consumption (Veff) under different engine loads.

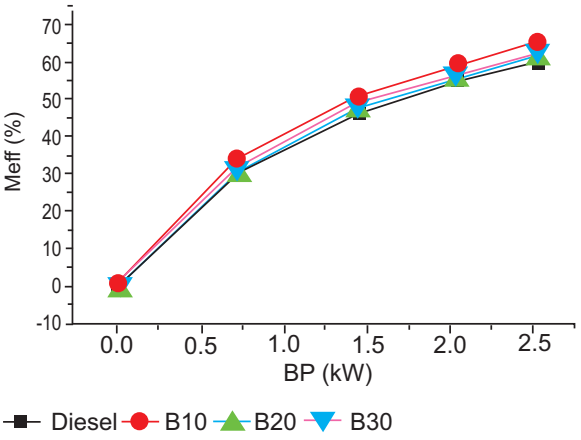

Fig. 7. Effects of biodiesel addition on mechanical efficiency under different engine loads.

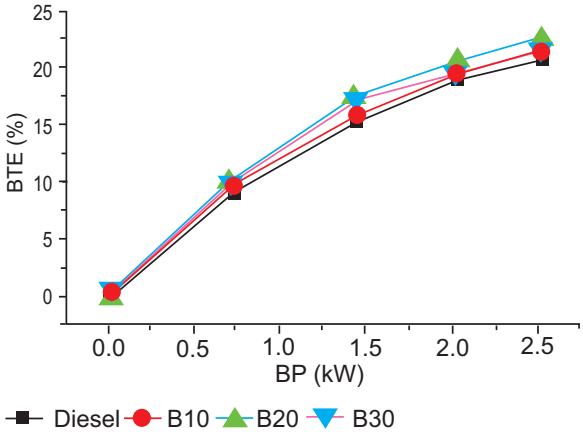

Fig. 8. Effects of biodiesel addition on brake termal efficiency under different engine loads.

Conclusion

Based on the experimental work on a compression ignition engine fuelled with Punnai oil biodiesel and its blends the following conclusions are drawn. The brake specific fuel consumption (BSFC) is increased with the increase of Punnai oil blending ratio in the blended fuels at full load. BSFC was almost same for B30 and diesel where B20 was 4.55% lower than the diesel at full load. The total fuel consumption increases

with increase in load. There are no such considerable changes in the Punnai oil biodiesel and diesel at full load condition but there is slightly greater TFC for B10. The break mean effective pressure increases with increasing load. There are no considerable changes in Punnai oil biodiesel and diesel at different load conditions. Volumetric efficiency of the Punnai oil biodiesel and its blends are same as compared to diesel at different load condition except B20 that showed 20% sudden decrease in volumetric efficiency at full load condition due to improper mixing. Mechanical efficiency increases with increasing load. Mechanical efficiency of B10 was 7.5% higher than diesel and other blends due to proper atomisation and combustion of the fuel. Brake thermal efficiency of the fuel increases with increasing load. Brake thermal efficiency of B20 was 8.12% higher due to proper combustion at different load condition.

References

Agarwal, A.K., Dhar, A. 2013. Experimental investigations of performance, emissions and combustion characteristics of Karanja oil blends fuelled DICI engine. *Renew Energy*, **52:** 283-291.

Agarwal, D. 2007. Performance and emissions characteristics of *Jatropha* oil (preheated and blends) in a direct injection compression ignition engine. *Applied Thermal Engineering*, **27:** 2314-2323.

Canakci, M., Sanli, H. 2008. Biodiesel production from various feedstocks and their effects on the fuel properties. *Journal of Industrial Microbiology & Biotechnology*, **35:** 431-441.

How, H.G. 2014. Engine performance, emission and combustion characteristics of a common-rail diesel engine fuelled with bioethanol as a fuel additive in coconut oil biodiesel blends. *Energy Procedia*, **61:** 1655-1659.

Masjuki, H.H., Kalam, M.A., Maleque, M.A., Kubo, A., Nonaka, T. 2001. Performance, emissions and wear characteristics of an I.D.I diesel engine using coconut blended oil. *Journal of Automobile Engineering*, **3:** 393-404.

Ozer, C. 2014. Combustion characteristics, performance and exhaust emissions of a diesel engine fueled with a waste cooking oil biodiesel mixture. *Energy Conversion and Management*, **87:** 676-686.

Puhan, S., Vedaraman, N., Ram, B.V.B., Sankarnarayanan, G., Jeychandran, K. 2005. Mahua oil (*Madhuca indica* seed oil) methyl ester as biodiesel-preparation and emission characteristics. *Biomass Bioenergy*, **28:** 83-87.

Raheman, H., Ghadge, S.V. 2009. Performance of compression ignition engine with Mahua (Madhuca indica) biodiesel. *Fuel*, **86:** 14-34.

Raheman, H., Phadatare, A.G. 2004. Diesel engine emissions and performance from blends of karanja methyl ester and diesel. *Journal of Biomass Bioenergy*, **27:** 393-397.

Raj, F.R.M.S., Sahayaraj, J.W. 2010. A comparative study over alternative fuel (biodiesel) for environmental friendly emission. Chennai, India: Recent Advances in Space Technology Services and Climate Change (RSTSCC), *IEEE Conference*, pp. 80-86.

Rao, H.Y.V., Voleti, R.S., Sitarama, Raju, A.V., Reddy, P.N. 2009. Experimental investigations on jatropha biodiesel and additive in diesel engine. *Indian Journal of Science and Technology*, **2:** 25.

Sanford, S.D., White, J.M., Shah, P.S., Wee, C., Valverde, M.A., Meier, G.R. 2001. Feedstock and Biodiesel Characteristics Report, Available from:/http://www.regfuel.com/pdfs/Feedstock%20and%20Biodiesel%20Characteristics%20Report.pdf

Serrano, M., Martinez, M., Aracil, J. 2013. Long term storage stability of biodiesel: influence of feedstock commercial additives and purification step. *Fuel Processing Technology*, **116:** 135-141.

Singh, S. 2012. Study of various methods of biodiesel production and properties of biodiesel prepared from waste cotton seed oil and waste mustard oil. *M.E. Thesis in Thermal Engineering*, Thapar University, India.

Spataru, A., Romig, C. 1995. Emissions and engine performance from blends of soya and canola methyl esters with ARB#2 diesel in a DCC 6V92 TA MUI engine. *SAE Paper No. 952388*, DIO:10.4271/952388.

Uriarte, F.A.J. 2010. Biofuels from Plant Oils; Available from:/http://www.asean foundation.org/documents/books/biofuel.pdf.

Wagner, L.E., Clark, S.J., Schrock, M.D. 1984. Effects of soybean oil esters on the performance, lubricating oil and water of diesel engines. *SAE Paper No. 841385*, Warrendale, PA, USA.

Pak. j. sci. ind. res. Ser. A: phys. sci. 2017 **60**(1) 29-33

Qualitative Analysis of Siro-spun and Two Fold Yarns Tensile Properties under the Influence of Twist Factor

Muhammad Qamar Tusief [a]*, Nasir Mahmood[a], Nabeel Amin[b] and Akmal Saeed[a]
[a]Department of Fibre & Textile Technology, University of Agriculture Faisalabad, Pakistan
[b]School of Textile and Design, University of Management and Technology, Lahore, Pakistan

(received August 22, 2016; revised September 26, 2016; accepted September 30, 2016)

Abstract. Siro yarns are spun from two separate roving of same type of materials. Similarly in textile arts, folding is a process used to create a strong and balance yarn by putting together two separate yarns. Hence, this research study was carried to analyse the quality of Siro-spun and two fold yarns under the influence of twist factor with special reference to their tensile properties. The results disclosed better tensile properties of yarn made from Siro spinning technique as compared to two plied yarn. This indicates the supremacy of Siro-spun yarn over two fold yarn. These findings enhance the fact that Siro spinning technique produces better quality yarn as compared to conventional ring spinning technique.

Keywords: Siro-spun twist multiplier, two fold yarn, yarn tensile properties

Introduction

Tensile properties of yarns are one of the most important characteristics desired by the spinners. These properties play significant role in determining the quality of the end product. In addition to raw material (fibre) characteristics, different spinning techniques and twist factor have vital role in defining the tensile properties of the yarn. Siro spinning is a technique which is being predicted to have profound influence on the yarn spinning industry. Siro-spun yarns are manufactured on a conventional ring frame by feeding two roving, drafted simultaneously into the apron zone at a pre-determined separation. The two strands are twisted together to form a two ply structure, when emerge from the nip point of the front rollers. This is an important spinning technique invented by the laboratories of the Commonwealth Science International Research Organization (CSIRO), Division of Textile Industry in Australia (Xuzhong *et al.*, 2015; Huo, 2008). A number of investigations have been made during the last two decades to analyse the properties of Siro-spun yarns and their edges over the conventional yarns. It has been depicted from all these studies that Siro-spun yarns have better properties in many ways as compared to the conventional yarns (Soltani, 2012). Most of these researches have covered the yarn appearance and mechanical properties in comparison with conventional ring spun yarn. However, there exist great research deficiency in the area of comparing quality parameters of Siro-spun yarn with two fold yarn.

In the textile fields, folding is a process, which is used to produce a strong, balanced yarn. It is made by taking two or more strands of yarn that each has a twist to them and putting them together. The combined strands are twisted in the opposite direction than that in which they were spun. Many newness yarns are made by using special plying techniques to produce their special effects. Textile industry extensively uses the folded yarns. Folded yarns are used in many woven and knitted fabrics (Bashir, 2010). Folded yarns are better in quality than single yarns because in single yarns in order to improve their strength and appearance some kind of sizing material is applied but in case of folded yarns sizing can be eliminated. The folded yarns get desired strength and appearance due to the folding of two single yarns which make them to bind each other completely reducing the hairiness of the resulting yarn and increase its abrasion resistance property (Palaniswamy and Mohamed, 2006).

The twist of yarns and threads influences their form and structure. This feature creates the thread's properties, and at the same time is conclusive regarding the processing throughout. Yarn folding that is twisting together some component fibre streams, causes an increase in tenacity, a lowering of the bending stiffness, a decrease in the linear mass irregularity, an increase in the abrasion and lowering of the thread's tendency

*Author for correspondence; E-mail: qamartosif@yahoo.com

to pilling formation. Consequential to these favourable circumstances, twisting positively influences the thread's making throughout and the barrier ability of the fabrics made from such a yarns (Rosiak and Przybyl, 2004).

Hence, keeping in view the above interface of Siro-spun and two fold yarns, the present research study was planned to explore the qualitative comparison of the tensile properties of these yarns under the influence of various twist factors. This could be helpful to set an optimum quality level of these two yarns for their better tensile properties to decide the best use of these yarns in making good quality end products.

Materials and Methods

The cotton yarn samples of two types Y1=Siro-spun yarn and Y2= two fold yarn were made for the same count of 20s at three twist levels T1= 3.5, T2= 3.7 and T3= 3.9, respectively. The folded twist of the two ply was inserted equal to that of its corresponding Siro-yarn, the folded twist of two ply was set at 70% of that of the single yarn as suggested by Cheng and Yuen (1997). Yarn samples so made were tested for their tensile properties (single yarn strength, rupture per kilometer, elongation percentage) using the following testing instrument and method.

Tensile properties of yarn. Tensile properties i.e., single end strength, elongation and rupture per kilometer were observed with Uster Tensorapid-3 which works on the principle of constant rate of extension (CRE). The principle describes the fact that the moving clamps are displaced at constant velocity as a result of which the specimen caught in between the stationary and moving clamps extended by a constant rate. The breaking tenacity was measured from the maximum force which was applied anywhere between the beginning of the test and the final rupture of the specimen. The breaking elongation of yarn was measured from the clamp displacement at the point of peak force. The procedure was adopted according to the ASTM (American Society for Testing and Materials) Standard for tensile properties of yarns by the single strand method D 2256-02 (ASTM, 2008).

Analysis of data. Duncan's multiple range test was applied in the analysis of variance of data for testing the differences among various quality characteristics as suggested by Montgomery (2009) applying statistical package for social sciences (SPSS) using micro-computer statistical programme.

Results and Discussion

Single yarn strength (g). The statistical analysis of variance and comparison of individual treatment means of the data regarding single yarn strength is given in Table 1 and 1(a), respectively. The results indicates that the main effects of yarn type (Y) and twist multiplier (T) were found significant while the interaction effect of (Y × T) was non-significant at 0.05 % level of significance.

As the interaction effect is non-significant, it leads to the multiple means comparison of main significant effects. As this experiment was done under control conditions so the chances of error were less. The Duncan's multiple range test was selected for mean comparison of treatments.

Duncan's multiple range test and the comparison for individual mean values regarding single yarn strength under different yarn types are given in Table 1(a) which indicate a maximum value of single yarn strength for Siro-spun yarn (Y1) i.e., 476.91 g followed by 469.85g i.e., for the two fold yarn (Y2), respectively. These findings are well supported by a previous study that the Siro-spun yarn was stronger than two plied yarn at all twist multipliers (Sun and Cheng, 2000). Moreover, in another research study it was concluded that Siro-spun yarns had better yarn tenacity and yarn elongation (%) values (Temel and Celik , 2010).

Table. 1 Analysis of variance for single yarn strength

S.O.V	D.F.	S.S.	M.S.	F. value	P
T	2	54.611	27.3057	1164.42	0.000**
Y	1	74.765	74.7654	3188.29	0.000**
Y×T	2	0.041	0.020	0.89	$0.005963^{N.S}$
Error	2	0.047	0.0235	-	-
Total	7	129.464	-	-	-

S.O.V= Source of variance; D.F = Degree of freedom; S.S = Sum of square; M.S= Mean square; P = Probability; F.value = F ratio value; ** = Highly significant; * = Significant; N.S = Non Significant

Table 1a. Comparison of individual treatment means for single yarn strength (g)

Yarn Types (Y)	Means	Twist Multiplier (T)	Means
Y1	476.91^{a}	T1	469.86^{c}
Y2	469.85^{b}	T2	473.07^{b}
		T3	477.23^{a}

Any two values not sharing a letter in common differ significantly at 0.05 level of probability.

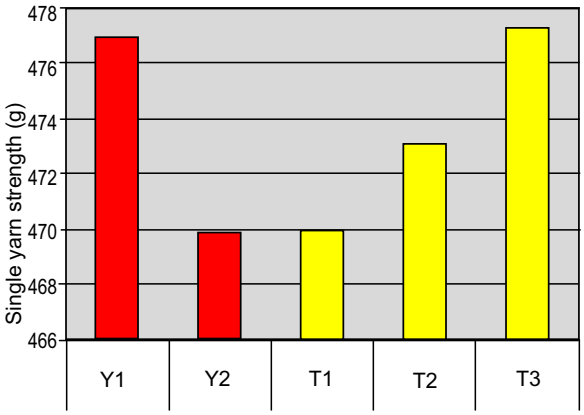

Fig. 1. Graphical representation of individual mean values for single yarn strength (g).

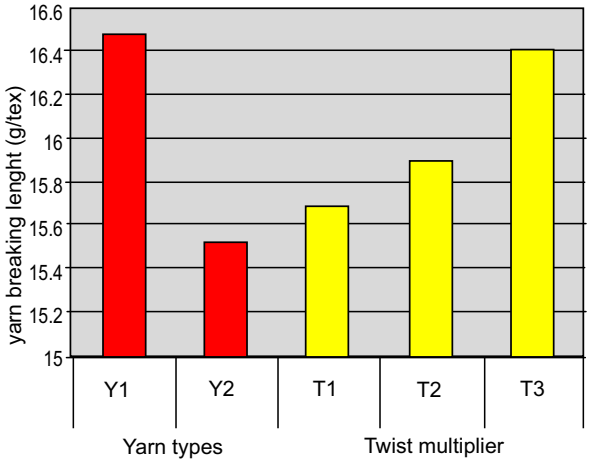

Fig. 2. Graphical representation of mean values for yarn breaking length (g/tex).

The comparison for individual mean values regarding single yarn strength for different twist multiplier by applying Duncan's multiple range test is given in Table 1a and elaborated in Fig. 1. The results show that the highest value regarding single yarn strength was recorded for twist multiplier T3(3.9) i.e., 477.23 g followed by 473.07g and 469.86 g for T2(3.7) and T1(3.5), respectively. The result of these values discloses a significant difference. It is clear from the results that the single yarn strength increased with the increase in twist in the yarn. These results are in line with the findings that the tenacity of yarn increased with the twist multiplier when it did not exceed the optimum twist multiplier (Lei, 2003). Similarly, in another study it was found that as the twist level increased, the yarn strength increased up to a certain level, beyond which the increase in twist actually decreased the strength of staple yarn (Palaniswamy and Mohamed, 2006).

Yarn breaking length {RKM value (g/tex)}. The statistical analysis of variance and comparison of individual treatment means of the data regarding breaking strength (RKM) is given in Table 2 and 2(a), respectively. The results indicate that the effect of yarn types (Y) and twist multiplier (T) are significant while the effect of interaction between the (Y×T) is found to be non- significant on yarn breaking length.

Duncan's multiple range test and comparison for individual mean values regarding yarn breaking length for different yarn types is presented in Table 2(a) which indicates that the maximum value of RKM for Siro-spun yarn (Y1) is 16.48 g/tex followed by 15.53 g/tex for two fold yarn (Y2), respectively. These results depict that RKM value for Siro-yarn is more than that of two fold yarn. These results get support from the findings that the breaking strength of Siro-spun yarn was higher than that of the two fold yarns of equivalent linear density due to the particular Siro-yarn structure in which fibres are being more firmly bound within the yarn structure. The twisted strands of the drafted fibres caused some surfaces fibres to be trapped into the Siro yarn so as to increase the inter fibre cohesion in the yarn which withstand higher breaking forces (Cheng and Yuen,

Table 2. Analysis of variance for yarn breaking length

S.O.V	D.F.	S.S.	M.S.	F. value	P
Y	1	1.36327	1.36327	1573.00	0.0006*
T	2	0.56493	0.28247	325.92	0.0031*
Y×T	2	0.00261	0.001305	1.5	$0.15931^{N.S}$
Error	2	0.00173	0.00087	-	-
Total	7	1.93254	-	-	-

S.O.V= Source of variance; D.F = Degree of freedom; S.S = Sum of square; M.S= Mean square; P = Probability; F.value = F ratio value; * = Significant; N.S = Non significant

Table 2a. Comparison of individual treatment means for yarn breaking length (g/tex)

Yarn types (Y)	Means	Twist multiplier (T)	Means
Y1	16.480_a	T1	15.690^c
Y2	15.527_b	T2	15.900^b
		T3	16.420^a

Any two values not sharing a letter in common differ significantly at 0.05 level of probability

Table 3. Analysis of variance for yarn elongation

S.O.V	D.F.	S.S.	M.S.	F. value	P
Y	1	0.20167	0.20167	12100.0	0.0001*
T	2	0.08923	0.04462	2677.00	0.0004*
Y×T	2	.000072	.000036	1.8	$0.3217^{N.S}$
Error	2	0.00003	0.00002	-	-
Total	7	0.29100	-	-	-

S.O.V= Source of variance; D.F = Degree of freedom; S.S = Sum of square; M.S= Mean square; P = Probability; F.value = F ratio value; * = Significant; N.S = Non significant

Table 3a. Comparison of individual treatment means for yarn elongation (%)

Yarn types (Y)	Means	Twist multiplier (T)	Means
Y1	6.4800^{a}	T1	6.18^{c}
Y2	6.1133^{b}	T2	6.245^{b}
		T3	6.465^{a}

Any two values not sharing a letter in common differ significantly at 0.05 level of probability.

1997). In the same lines it was observed that the Siro-spun yarn was stronger with more yarn tenacity and elongation % than two plied yarn at all twist multipliers (Temel and Celik, 2010; Sun and Cheng, 2000).

Duncan's multiple range test and the comparison for individual mean values regarding yarn breaking length at different twist multiplier is given in Table 2a and further illustrated in Fig. 2. It is clear from the findings that the highest value of yarn breaking strength (RKM)

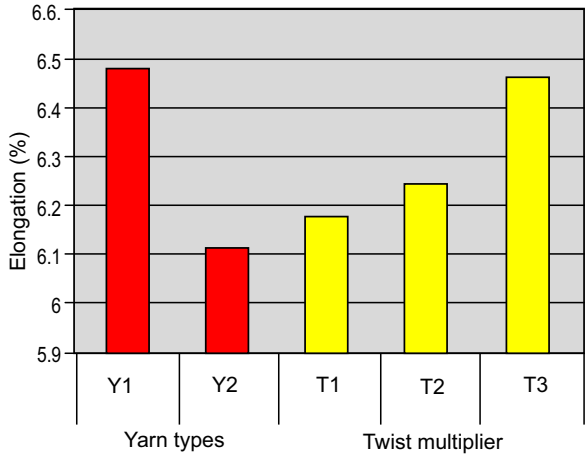

Fig. 3. Graphical representation of individual mean values for elongation (%)

i.e., 16.42 g/tex is recorded for T3 followed by 15.90 and 15.69 g/tex for T2 and T1, respectively. These results differ significantly from each other. It is clear from the observation that as the yarn twist increased, the RKM value increased. These results are in line with the findings that the tenacity of yarn increased with the twist multiplier when it did not exceed the optimum twist multiplier (Lei, 2003).

Yarn elongation %. The statistical analysis of variance and comparison of individual treatment means of the data regarding yarn elongation (%) is given in Table 3 and 3(a), respectively. The results indicate that the effects of twist multiplier (T) and the yarn types (Y) on elongation of yarn are significant while the effect of interaction of (Y×T) is non- significant on elongation.

The comparison of mean values for yarn elongation for different yarn types by applying Duncan's multiple range test is shown in Table 3a and in Fig.3. The elongation values for Y1 (Siro-spun) and Y2 (two fold) are 6.48 and 6.11 %, respectively. It is clear from the results that elongation of Siro-spun yarn is more as compared to that of two fold yarn. These results are in acccordance with the findings of earlier researchers that the Siro-spun yarn had better yarn elongation (%) and tenacity than two plied yarn at all twist multipliers (Temel and Celik, 2010; Sun and Cheng, 2000)

Duncan's multiple range test and the comparison of individual treatment means concerning to yarn elongation (%) for different twist multiplier (T) is given in Table 3(a). The highest value of yarn elongation was noted for T3 i.e., 6.46(%) followed by 6.24 and 6.18 (%) for T2 and T1, respectively. These results differ significantly from each other and match with the observations that the increase of twist factor and spindle speed increased the elongation percentage of yarn (Shabir, 2008; Subramaniam *et al.,* 1989; Sharma *et al*., 1987).

Conclusion

The present research was planned to explore qualitative analysis of Siro-spun and two fold yarns with special reference to their tensile properties. The respective yarns of same count i.e., 20s were made for various twist levels. The findings disclosed the fact that all yarn tensile properties i.e., single end strength, breaking length (RKM) and elongation percentage were better for Siro-spun yarn as compared to that of two fold yarn with increasing twist levels. This is because of the better handling of fibres into the yarn surface in Siro yarn

spinning technique which increases the compactness of the yarn and ultimately enhances its tensile properties.

References

ASTM Committee. 2008. *Standard Test Method for Measurement of Yarn.* ASTM Designation D: 2256-02. American Society for Test & Material, Philadelphia, U.S.A.

Bashir, M. S. 2010. Comparison of Hybrid Folded Cotton Yarn Quality from Different System Spun Yarns and its Effect upon Knitted Fabric. *M.Sc. Thesis,* Department of Fiber Technology, University. of Agriculture, Faisalabad, Pakistan.

Cheng, K.P.S., Yuen, C.H. 1997. Siro and two-fold yarns. Research Journal of Textile and Apparel **1:** 64-70.

Huo, L. 2008. Study on siro spunning system to reduce the hairiness of yarn. *Modern Applied Science*, **2:**133-138.

Lei, C. H. 2003. Continuous spun-like textured yarn processed with various plied filaments and different stages of Emery wheels. *Textile Research Journal*, **73**: 1046-1051.

Montgomery, D. C. 2009. *Design and Analysis of Experiments*. Arizona State University. ISBN: 978-0-470-12866-4.

Palaniswamy, K., Mohamed, P. 2006. Effect of the single-yarn twist and ply to single-yarn twist ratio on the hairiness and abrasion resistance of cotton two-ply yarn. *Autex Research Journal*, **6:** 59-71.

Rosiak, D., Przybyl, K. 2004. Twisting of multi-folded yarns and threads manufactured by means of new spinning technologies. *Autex Research Journal*, **4:**113-117.

Shabir, M. 2008. Optimization of Twist Ratio of Single Yarn and Ply to Single Yarn for Different Counts. *M.Sc. Thesis,* Department of Fiber Technology, University of Agriculture, Faisalabad, pp. 25-30.

Sharma, I. C., Gupta, N. K., Agarwal, B. R., Patnaik, N. R. 1987. Effect of twist factor and stitch length of open-end spun cotton yarn on properties of rib knitted fabrics. *Textile Research Journal,* **57**: 73-81.

Soltani, P., Johari,M.S. 2012. A study on siro, solo, compact and conventional ring spun yarns. Part I: structural and migratory properties of the yarns. *The Journal of the Textile Institute*, **103:** 622-628.

Subramaniam, V., Srinivasamoorthi, V.R., Mohamed, A. P. 1989. Effect of processing parameters on the properties of double-rove spun yarn produced on a short staple spinning system. *Textile Research Journal*, **59:** 762-767.

Sun, M. N., Cheng, K. P. S. 2000. Structure and properties of cotton siro spun yarn. *Textile Research Journal*, **70:** 261-268.

Temel, E., Celik, P. 2010. A research on spinnability of 100% polyester and polyester cotton blend siro spun yarns. *Journal of Textile and Apparel,* **20:** 23-29.

Xuzhong, Su., Weidong, G., Xinjin, L., Chunping, X., Bojun, X. 2015. Rsearch on the compact siro spun yarn structure. *Fibers & Textiles in Eastern Europe*, **3:** 54-57.

Pak. j. sci. ind. res. Ser. A: phys. sci. 2017 **60**(1) 34-41

Appraisal of Drinking Water Quality in Lahore Residence, Pakistan

Khalid Mahmood[a]* and Muhammad Asim[b]
[a]Remote Sensing and GIS Group, Department of Space Science, University of the Punjab, Lahore, Pakistan
[b]Department of Space Science, University of the Punjab, Lahore, Pakistan

(received February 14, 2016; revised June 8, 2016; accepted August 11, 2016)

Abstract. A comprehensive study for the spatial distribution of drinking water quality had been conducted for residential area of Lahore, Pakistan. The study had made use of the geographic information system (GIS) for geographical representation and spatial analysis of groundwater quality. Physicochemical parameters including electric conductivity, pH, TDS, Cl, Mg, Ca, alkalinity and bicarbonates from 73 of the water samples had been included in the analysis. Water quality data had been geo-referenced followed by its interpolation using inverse distance weighted (IDW) for each of the parameters. Very high alkalinity and bicarbonates values were observed in most parts of the area. For the comprehensive view, water quality index map had been prepared using weighted overlay analysis (WOA). The water quality index map was classified into five zones of excellent, good, poor, very poor and unfit for drinking as per WHO standards of drinking water. 21% region had excellent quality of the underground water and 50% was found good for drinking. Poor quality of water was found in southeastern part, covering 27% of the study area. Only 2% of the area was found under the very poor and unfit water quality conditions for drinking.

Keywords: drinking water quality, groundwater, water quality index, GIS, weighted overlay

Introduction

Groundwater is one of the most important resources available to humanity for their social and economic growth (Nwanwoala *et al*., 2012; Christophoridis *et al*., 2011). It is the most suitable form of fresh water as it contains almost balanced salt concentration, which is good for human use. Despite the fact that earth has a lot of water, only 2.5% of the earth's total water is fresh and only one-third of this small amount of fresh water is available for human use (PCRWR, 2007; Hassan *et al*., 2005). Recent developments in living standard, agriculture and industrialisation have greatly increased the demand of the groundwater (Mahmood *et al*., 2013). In arid and semi-arid regions the total water withdrawn for human usage has almost tripled from 1382 km^3/year in 1950 to 3973 km^3/year in 2000 and the worldwide projection has predicted that human water consumption would reach to 5235 km^3/year by 2025 (Clarke and King, 2004).

Any addition of undesirable substances to groundwater by human or natural activities is called contamination. Once a local aquifer is contaminated, it is almost impossible to clean it up as the cost of its purification is usually very high. Owing to its unique characteristics such as hydrogen bonding and polarity, water has ability to dissolve many components which leads to its contamination. The quality of groundwater is equally important as its quantity (Mahmood *et al*., 2013; Majandang and Sarapirome, 2013; Rehman, 2008), therefore, environmental protection policies give highest priority to its monitoring (Mahmood *et al*., 2013). Monitoring of water resources for its quality is necessary to avoid any outbreak of water born diseases (Ullah *et al*., 2013). Groundwater always moves by the force of gravity from recharge areas to the areas of its discharging. Its movement in most areas is slow as few feet per year, but in more permeable areas such as channels in limestone, movement could be as much as several feet per day.

Listed parameters by researchers that can alter groundwater contamination are pH, electric conductivity (EC), turbidity, salinity, total dissolved solids (TDS), alkalinity, bicarbonates, chloride, calcium, oil, grease and heavy metals (Brindha *et al*., 2014; Singh *et al*., 2014; Verma *et al*., 2013; Usali and Ismail, 2010). Groundwater is monitored in many parts of the world, mainly by measuring groundwater levels, groundwater recharge, and its contamination level. The results of these measurements are often interpolated and combined with other information to produce various groundwater thematic maps at local and regional scales. Over the time, many countries and states have developed groundwater mapping programmes for their entire territory or

*Author for correspondence; E-mail: khalid.m270@yahoo.com

for areas in which their most important groundwater resources are located. World-wide Hydro-geological Mapping and Assessment Programme (WHYMAP) thus bring together the huge efforts in hydro-geological mapping at regional, national and continental levels.

It is widely reported that degradation of groundwater is arising due to overexploitation of groundwater in Pakistan, India and other developing countries (Moench and Dixit, 2004). Currently fresh water stress in Pakistan has reached over 40% and the situation is going to get worse by the year 2025, just like other countries of the world. Lashari *et al*. (2007) estimated that about 60-70% population of Pakistan depends directly or indirectly on groundwater for its livelihood.

The mega city Lahore, Pakistan is facing serious challenges for the provision of safe and sufficient drinking water and the situation is predicted to be getting more severe in coming days.

The present study therefore, was conducted for spatial analysis of groundwater quality in this area.

Materials and Methods

Study area. The mega city of Lahore with an area of 17,000 hectares is provincial capital of Punjab and second largest city of Pakistan. It lies between Bari Doab and Rechna Doab, and is located along bank of river Ravi. It is located between 31°15′-31°45′N and 74°01′and 74°39′E with an average height of 217 m above the mean sea level (Fig. 1). It is delimited on the north with the Sheikhupura district, in the east with Wagah boarder and in the south with Kasur district. The river Ravi flows on the northern and western out skirts of the city (Mahmood *et al*., 2013).

The climate of the study area is hot and semi-arid with long and intensely hot summers, dry and warm winters, monsoon and mud storms. The average rainfall is about 575 mm/year but it can vary in the range of 300-1200 mm providing 40% recharge to the groundwater.

The area is underlain by 300 m thick bed of alluvial deposits, as investigated by WASID during the period of 1961-62 (WAPDA, 1980). The major recharge source for local aquifer is river Ravi, that flows now occasionally and BRBD Canal on the aquifer behaves as a single contiguous, unconfined aquifer. Underlying strata wise the area consisted predominantly of sand, silt and thin lenses of clay.

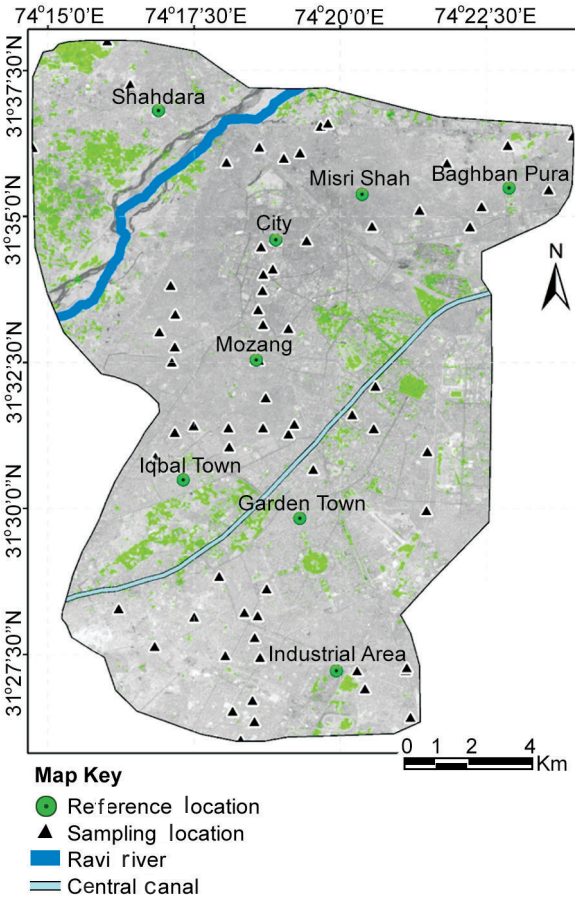

Fig. 1. Study area.

Provision of water supply to most of the study area is responsibility of Water and Sanitation Agency (WASA), Lahore. Water quality data for the year 2012 was acquired from WASA, Lahore, which periodically collects water samples from their installed tube wells in residential area of Lahore. They analysed collected water samples in their laboratory for 19 of the drinking water quality parameters. The analyses of the water samples carried out through standard methods for examination of water (APHA-AWWA-WPCF) as per WHO guildlines for drinking water (WHO, 2011). The analysed parameters include temperature, odor, colour, taste, pH, turbidity, TDS, conductivity, total hardness, Ca, Mg, alkalinity, Cl, NO_2, NO_3, CO_3, HCO_3 and *E. coli* (Table 1).

A total of 73 well seperated groundwater samples from residential area of the city had been chosen to carry out this work. Parameters considered for this study include pH, total dissolved solids (TDS), chloride (Cl), electrical conductivity (EC), bicarbonates (HCO_3), alkalinity (alk),

Table 1. Water quality data used in the study

No.	Location	Subdivision	pH	Alkalnity	TDS	EC	Ca	Mg	Cl	HCO_3
1	2-D-1 Green Town	Green Town	8.1	204	350.2	556	11.2	7.68	16	204
2	3-C-1 Township	Green Town	7.8	324	396.9	630	25.6	15.4	27	324
3	3-D-1 Green Town.	Green Town	8.1	202	385.5	612	11.2	10	17	202
4	5-D-1 Green Town	Green Town	7.8	366	687.9	1,092	38.4	27.8	32	366
5	5-D-2 Kir Kalan Village	Green Town	7.8	344	652.6	1,036	28.8	24.5	30	344
6	A3 Johar Town	Johar Town	7.8	424	720	1,143	32.8	29.7	24	424
7	A-Block Gulshan Ravi	Krishan Nagar	8.1	210	372.9	592	36	24.9	28	210
8	Abu Bakar Block.	Garden Town	8	370	517.8	822	38.4	27.3	35	370
9	Adda Crown Bus	Anarkali	8	242	618.6	982	33.6	30.7	46	242
10	Aibak Park Mozang	Mozang	7.8	296	849.8	1,349	72.8	48	10	296
11	Akbari Gate (New)	City	7.8	414	652.6	1,036	14.4	24.5	103	414
12	Alia Town	Baghban Pura	7.8	200	280.3	445	49.6	24.5	31	200
13	Aslam Iqbal Park	Mozang	8.1	246	392.4	623	32.8	18.7	45	246
14	Awa Pahari Queens Rd Mozang	Mozang	8.1	148	495.1	786	60	21.1	103	148
15	Awami Colony	Industrial Area	8	244	447.9	711	19.2	13.9	25	244
16	Aziz Colony Chatha Park	Farrukhabad	7.9	360	553.7	879	64.8	36.5	84	360
17	Bank Stop Main Fazal e Haq Co	Industrial Area	7.9	370	669	1,062	24	21.6	55	370
18	B-Block, Gulberg II	Gulberg	7.8	180	395	627	19.2	13.4	23	180
19	Cattle Park	Anarkali	7.8	252	293.7	625	60	36.5	49	252
20	C-Block, Faisal Town	Garden Town	8.1	302	380.5	612	25	18	15	302
21	Chah Motia Data Nagar	Data Nagar	7.8	216	249.4	396	49.6	19.7	39	216
22	China scheme	Misri Shah	7.9	188	248.8	395	24.8	16.3	15	188
23	Clifton Colony	Iqbal Town	8.1	190	299.8	476	19.2	10	20	190
24	D-Block, Faisal Town.	Garden Town	8	220	301	478	16.8	10.6	20	220
25	Dhobi Mandi	Anarkali	7.8	304	406.3	646	57.6	32.2	65	304
26	Dhoop Sari	Krishan Nagar	8	164	175.1	278	28.8	17.8	11	164
27	E-Block Johar Town	Johar Town	7.9	334	746.1	1,213	32.8	24.5	20	334
28	F-1 Block Johar Town	Johar Town	8.3	324	463	735	43.2	27.4	24	324
29	Faisal Park	Farrukhabad	7.8	200	202.2	321	35.2	19.7	28	200
30	Fareed Colony	Industrial Area	7.9	400	714.4	1,134	40.8	29.3	48	400
31	Fareed Kot	Anarkali	7.8	350	933.6	1,482	80	48	68	350
32	Farrukhabad	Farrukhabad	8.1	184	332.6	528	39.2	17.2	23	184
33	FC Block Gulberg II	Gulberg	8	160	282.2	448	16.8	15.8	19	160
34	Foot Ball Ground Gulshan Ravi	Krishan Nagar	8	170	176.4	280	32.8	15.4	17	170
35	G IV Block Johar Town	Johar Town	8.3	158	299.2	475	12.8	10	14	158
36	General Hospital	Industrial Area	8.2	282	479.4	761	21.6	11.5	24	282
37	Hanif Park Tonda Phatak	Data Nagar	8	122	190.8	303	20	10.8	15	122
38	Huma Block	Iqbal Town	7.8	180	261.4	415	24.6	13.4	34	180
39	Hussain Park	Data Nagar	8.2	164	223	354	40.8	18.9	15	164
40	Jahanzaib Block	Iqbal Town	7.8	160	245.7	390	25.6	11.5	13	160
41	Jinnah Park Sultan Pura	Misri Shah	8.2	186	395.6	628	48.8	20.6	67	186
42	Kamran Park	Farrukhabad	8.1	160	240	381	66	12	23	160
43	Kanchi Stop	Industrial Area	7.8	446	834.1	1,324	40	24.5	40	446
44	Kanji House Gujjar Pura	Misri Shah	7.8	162	332	527	26.4	15.8	14	162
45	Karmabad, Rehman Pura	Ichra	8	242	249.4	396	21.6	7.2	18	242
46	Khokhar Road # 3	Data Nagar	8.1	126	163.1	259	32.8	11.5	10	126
47	Lahori Gate	City	7.8	222	400.6	636	58.4	24.5	45	222
48	Madhulal Hussain	Baghban Pura	8.3	184	364.1	578	24.8	11.5	22	184
49	Makkah Colony (New)	Gulberg	7.8	284	492.6	782	27.2	19.7	30	284
50	Match Factory	Farrukhabad	8.1	246	369.8	587	51.2	19.6	13	246
51	Mehmood Booti Disposal	Baghban Pura	8.1	180	199	316	25.6	15.8	10	180
52	Mori Gate	City	7.9	186	243.8	387	192	19.7	18	186
53	Napier Road	Anarkali	7.8	346	824	1,308	60	21.1	130	346
54	Nargis Block	Iqbal Town	7.9	270	553.1	878	46.4	26.9	48	270
55	N-Block, Model Town Ext.	Garden Town	7.8	400	589	935	43.2	26.4	32	400
56	Neelum Block	Iqbal Town	7.8	234	518.4	823	35.2	20.6	59	234
57	Nisar Press Gulberg	Gulberg	7.8	462	817.1	1,297	45.6	34.1	55	462
58	Rasool Park	Ichra	8.3	126	422.7	671	47.2	22.1	105	126
59	Rehman Pura	Ichra	8	226	545.5	866	16.8	9.6	23	226
60	Rustam Park	Krishan Nagar	7.8	230	454.8	722	32	20.6	51	230
61	Saad di Mill	Baghban Pura	8.1	240	287.2	456	34.4	15.4	15	240
62	Saadi Park	Mozang	8.2	294	355.9	565	35.2	16.3	56	294
63	Sawami Nagar (Old)	Misri Shah	8.1	206	510.9	811	41.6	32.6	98	206
64	Shah di Khoi	Johar Town	7.8	382	481.9	765	48	12.9	22	382
65	Shah Kamal (New)	Ichra	8	184	521	827	17.6	11.4	18	184
66	Siddique Pura	Data Nagar	8	134	204.7	325	24.8	12.5	10	134
67	Surria Jabeen Park	Baghban Pura	7.8	202	477.5	758	44	23.5	34	202
68	Takia Lehri Shah	Ichra	7.8	234	600.3	953	40.8	20.6	58	234
69	Takia Mehmood Shah	Krishan Nagar	8.1	242	166.9	265	27.2	17.3	15	242
70	Timber Market	City	7.9	220	228.6	363	15.2	10.1	28	220
71	Usman Block	Garden Town	7.9	254	430.9	684	34.4	17.8	62	254
72	Wasan Pura	Misri Shah	8	168	252.6	401	28.8	18.7	20	168
73	Zafar Ali Rd Gulberg V	Gulberg	8	194	367.9	584	16	10.1	23	194

Magnesium (Mg) and Calcium (Ca). All this collected data is shown in Table 1 and their corresponding statistics are given in Table 2.

An overview of the used methodology is given in Fig. 2. The spatial reference to each of the sampled location had been measured using global position system (GPS). The used model of GPS for ground survey was GPSmap-76CSx receiver, having horizontal accuracy of ±3 m. All the quality data were then georeferenced using the location data in the form of a point shapefile

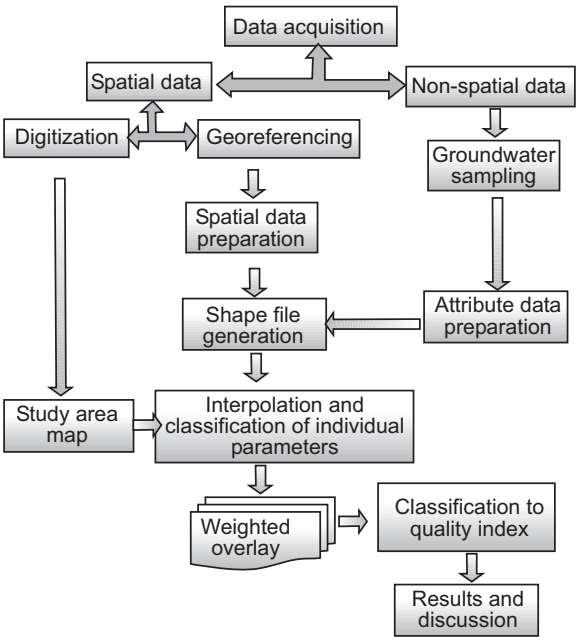

Fig. 2. Flow chart of methodology.

in ArcGIS 9.3. The point data was then interpolated to generate continuous rasters for each of the selected water quality parameters. The used technique of interpolation, Inverse Distance Weighted (IDW) belongs to deterministic family of interpolators as suggested by a number of previous studies (Bairu *et al*., 2012; Latha *et al*., 2012; Abulhakeem *et al*., 2011; Balakrishnan *et al*., 2011; Singh *et al*., 2011; Latha *et al*., 2010).

IDW is based on the fact that the nearby values are more related to each other than values that are far apart. In other words, for this spatial interpolation technique the influence of a known data point is inversely related to the distance from the unknown location, being estimated (Shepard, 1968). The mathematical expression of the inverse distance weighted is given as:

$$z_o = \frac{\sum_{i=1}^{s} z_i \frac{1}{d_i^k}}{\sum_{i=1}^{s} z_i \frac{1}{d_i^k}}$$

where:

z_o = estimated value at point-o; z_i = the value at known point-i; d_i = is the distance between point-i and point-o; s = the number of known points used in estimation and k = the specified power.

Boundry of the Lahore residents is marked/digitized using Quick Bird imegery having spatial resolution of 2.6 m, improved to 0.6 m by high resolution merging. Layers obtained from the interpolation contains continuous values for each of the parameters which make

Table 2. Data statistics and applicable classification scheme

Parameter	Min	Max	Mean	Range	Assigned value	Weight
Eletric conductivity (EC) (µS/cm)	260	1469	864.5	< 500	1	12
				500 – 1000	2	
				> 1000	3	
pH	7.80	8.29	8.05	7.5 – 8.0	2	16
				> 8.0	3	
TDS (mg/L)	169	929	549	< 500	1	28
				500 – 1000	2	
HCO_3 (mg/L)	122	481	301.5	< 240	1	9
				240 – 400	2	
				> 400	3	
Cl (mg/L)	10	129	69.89	< 250	1	8
Ca (mg/L)	11	191	101	< 75	1	8
Mg (mg/L)	7.2	47.7	27.45	< 30	1	8
				30 – 75	2	
Alkalanity (mg/L)	122 l	481	301.5	< 200	1	12
				240 – 400	2	
				> 400	3	

data more complex. To overcome this problem of diversity in parameteric values all the rasters have been classsified as per WHO standard classification. This three-classes scheme of WHO for each of the parameters has been used by a number of researchers for groundwater quality assessment (Bairu *et al*., 2013; Latha *et al*., 2012; Abulhakeem *et al*., 2011; Balakrishnan *et al*., 2011; Singh *et al*., 2011; Latha *et al*., 2010).

Finally the water quality index (WQI) is calculated through weighted overlay analysis (WOA). WOA is a GIS based framework to conceptulize a spatial phenomenon depending over more than one geographic parameters as is the case of groundwater quality. Weights have been assigned to each of the constituting quality parameter showing their relative importance in overall quality indexing. These weights have been assigned to the parameters following earlier studies by Bauru *et al*. (2013) and Latha *et al*. (2012). The assigned weights are shown in Table 2.

Maximum weight of 28 had been assigned to TDS showing its dominating significance in water quality assessment. Cl, Ca and Mg are assigned the minimum weight of 8, as they have relatively low importance in the overall quality assessment of groundwater (Bairu *et al*., 2013; Latha *et al*., 2012). Other parameters like, electric conductivity, bicarbonates and pH are given weights between 8 and 28 depending on their relative significance for the phenomenon. Ratings and weights are multiplied to calculate final output. Finally the water quality index is computed through WOA and had been classified as excellent, good, poor, very poor and unfit for drinking purpose depending on their degree of fitness for human consumption.

Results and Discussion

The study has prepared thematic maps for each of the studied quality parameters and then their common representation has been made using WQI map for the year 2012. Variation of the EC was within the permissible limit of 1,500 µS/cm at 25 °C as suggested by WHO. However, lower values were mostly concentrated in northern parts of the study area comprising of Farrukhabad (Shahdra), Data Nager, Baghban Pura, Krishan Nager and few patches of westerly located Iqbal Town, and Johar Town as well. Higher values were found in Gulberg, Industrial area, Mozang, Anarkali and a portion of Johar Town sub-divisions. Spatial distributions of electric conductivity (EC) of the underground aquifer is shown in Fig. 3A.

All of the study has been found well within the range of maximum acceptable limit of pH for drinking water i.e., 9.2 as per WHO standards. In this way groundwater of the area is mainly neutral to slightly alkaline in nature. As per WHO classification scheme only two classes were formed in the measure range of the pH value. Second ranked category covers the maximum area while Class 3 has some portions of Furrakhabad, Krishan Nager, Mozang, Johar Town, Green Town and Industrial area sub-divisions. Spatial distributions of pH concentrations are shown in Fig. 3B. Spatial concentration of Cl is given in Fig. 3C, where all the sample data lies in a single class. The permissible limit for HCO_3 is 240 mg/L and only 21% of the study area is found under this permissible limit. Spatial distribution of HCO_3 is shown in Fig. 3D. Maximum of the study area is found with 500 mg/L of TDS, whereas higher values are found in parts of Anarkali and Mozang sub-divisions as shown in Fig. 3E. Dissolve magnesium in water is the most common mineral that makes water hard, 98% of the groundwater samples were found within the desirable limits (30 mg/L), whereas higher values had been found in Mozang, Misri shah, Gulberg, Anarkali and Furrakabad

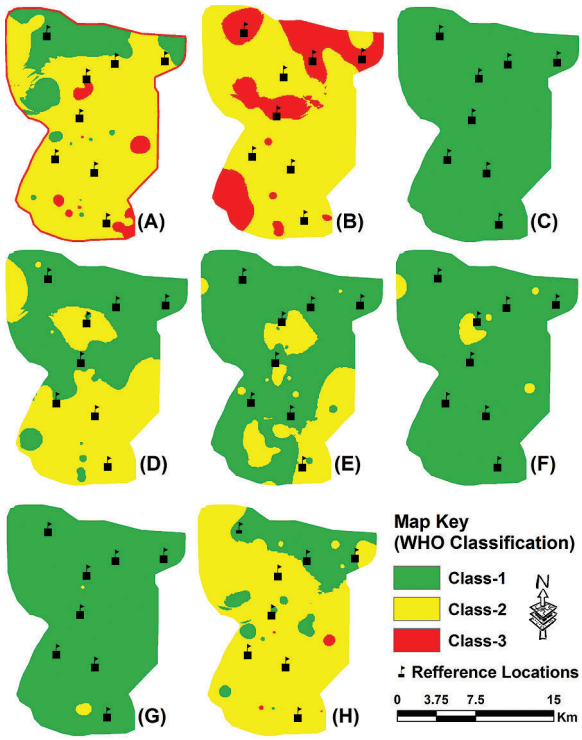

Fig. 3. Spatial distribution of individual parameters (A)-EC; (B)-pH; (C)-Cl: (D)-HCO_3; (E)-TDS; (F)-Mg; (G)-Ca: (H)-alkalanity.

sub-divisions as shown in Fig. 3F. There are two spots of higher Ca concentration, one found between Anarkali and Mozang and the other at southern side of the study area, as shown in Fig. 3G.

About 21% of the study area was under permissible limits of alkalinity and the areas under relatively extreme conditions were distributed over patches of Johar Town and Gulberg sub-divisions as shown in Fig. 3H. High concentration of alkalinity in these areas may be the result of huge construction work including under passes and a flyover, involved heavy drilling in ground. All the measured and predicted values of Cl are almost similar and fall in one of the three classes defined by WHO. Similarly Ca is within the permissible limits and formed two of WHO classes. It is notable that the common regions for extreme measures of majority of the parameters are Mozang and Anarkali subdivisions.

Water quality index. The water quality index values have been divided into classes of excellent, good, poor, very poor and unfit for drinking. Layer generated in this way is further subjected for calculation of areas corresponding to each of the class which shows that 21% of the study area is under excellent conditions, 50% is good, 27% is poor, less than 2% is very poor and a very small portion of the region is found unfit for drinking. This area wise comparison of different classes is depicted in Fig. 4.

The hot spot that is classified as unfit for drinking is found at the same region which was stated to have the deepest groundwater levels in the Lahore (Mahmood *et al*., 2013). The same region is found prominent in most of the individual parameters maps (TDS, HCO_3, EC and alkalinity) for their high values as shown in Fig. 2. Very poor quality of groundwater is centered at the depression centre of ground water in the city and its chunks have also been found at out skirts of the study area including parts of Gulberg, Johar Town and Anarkali subdivisions. Poor quality groundwater is found mostly in south eastern parts of the study area however, its patches are also found in Anarkali, Misri Shah and Furrakabad subdivisions. 71% of the study

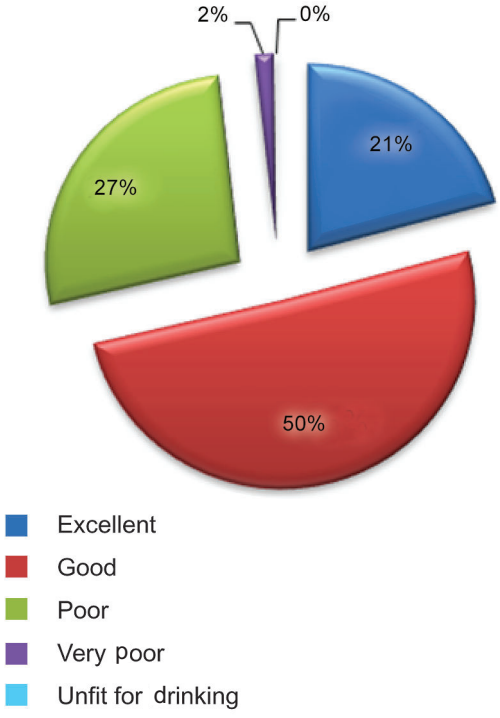

Fig. 4. Drinking water suitability area comparison chart as per WHO standard classification.

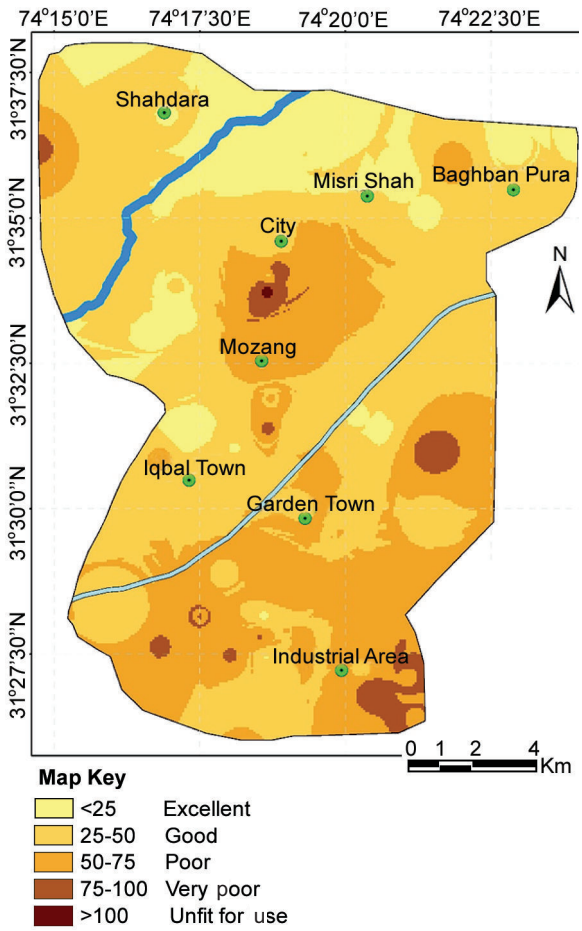

Fig. 5. Water quality index map.

area is found under good and excellent groundwater conditions that is located in the north, the only exception exist around the central depression zone.

The existence of concentering zones of gradually degrading water quality in the central portion of the study area as shown in Fig. 5 shows that the quality of extracted water is somehow linked to over exploitation of the fresh water resource. There is no recharge from this portion of the area and water reached there, by the lateral movement of the recharge from edges of the city. In this way degradation of the water quality seems to be occurring during its path through the underground materials.

Conclusion

This study concludes that groundwater quality parameters including pH, electric conductivity, Ca, Cl and TDS are well within the permissible limits defined by WHO for the drinking water. However alkalinity, HCO_3 and Mg are crossing their respective safe limits in some parts of Lahore residence.

Groundwater in subdivisions of Gulberg, Anarkali and Mozang sub-divisions, is found to be marginally fit for drinking purpose. So these areas need special attention of authorities regarding provision of the safe drinking water to the community. Surrounding areas of the above mentioned locations have also been spotted to be touching upper limits of the safety margins, so in near future these regions of groundwater may also become unsuitable for human use. Estimation of the health damage done by intake of the polluted water can be made by the field observation, showing increased use of filtration plants in the Lahore residence.

Visible correlation between distribution of poor quality of groundwater and impervious surfaces along with high abstraction rates of water reflects that urbanisation is the root cause of all this environmental damage. High abstraction rates along with increasing pervious surfaces has already been reported to cause a cone like depression in under-ground aquifer cantered between Muzang and Anarkali subdivisions. This cone like depression causes the water to flow latterly from remote areas of recharge to discharge zones. This lateral flow may be the reason of dissolving substances from underlying lithology. The possible solution to the issue for the local government is to minimize this lateral flow, ultimately, reduce the depression. It is possible through locally distributed groundwater recharge facilities in the study area and controlling pumping rates. People awareness plans are necessary to stop unnecessary wastage of this precious fresh water resource for the sustainable development of the mega city of Lahore.

References

Abulhakeem, A., Ishaku, J.M., Ahmed, A.S. 2011. Mapping of water quality index using GIS in Kaltungo, Northeastern Nigeria. *Journal of Environmental Sciences and Resource Management*, **3:** 94-106.

Bairu, A., Tadesse, N., Amare, S. 2013. Use of geographical information system and water quality index to assess suitability of groundwater quality for drinking purpose in Hewane Area, Tigray, Northern Ethiopa. *Ethiopian Journal of Environmental Studies and Management*, **6:** 110-123.

Balakrishnan, P., Saleem, A., Mallikarjun, N.D. 2011. Groundwater quality mapping using geographic information system (GIS): A case study of Gulbarga City, Karnataka, India. *African Journal of Environmental Science and Technology*, **5:** 1069-1084.

Brindha, K., Vaman, N.K.V., Srinivasan, K., Babu, S.M., Elango, L. 2014. Identification of surface water-groundwater interaction by hydrogeochemical indicators and assessing its suitability for drinking and irrigational purposes in Chennai, Southern India. *Applied Water Science*, **4:** 159-174.

Christophoridis, C., Bizani, E., Fytianos, K. 2011. Environmental quality monitoring, using GIS as a tool of visualization, management and decision-making. Applications emerging from the EU water framework directive EU 2000/60. (http://www.irma-international.org/viewtitle/70522/). pp. 1554-15560.

Clarke, R., King, J. 2004. *The Water Atlas*, 98 pp. The New Press, New York, USA.

Hassan, R., Scholes, R., Ash, A. 2005. *Ecosystems and Human Well-Being: Current State and Trends*, vol. **1,** 170 pp. Island Press, Washington, DC., USA.

Lashari, B., McKay, J., Villholth, K. 2007. Institutional and legal groundwater management framework: Lessons learnt from South Australia for Pakistan. *International Journal of Environmental and Development*, **4:** 45-59.

Latha, H.T., Kumar, P.G.N., Lakshminarayana, P., Anil, A. 2012. Assessment of groundwater quality index for upper Pincha basin, Chittoor district, Andhra Pradesh, India using GIS. *International Journal of Scientific & Engineering Research*, **3:** 1-8.

Latha, S.P., Rao, N.K. 2010. Assement and spatial distribution of quality of groundwater in zone –II and III , Greater Viskhapatnam, India using Water Quality Index (WQI) and (GIS). *International Journal of Environmental Sciences*, **1:** 198-212.

Mahmood, K., Daud, A., Tariq, S., Kanwal, S., Ali, R., Haider, A., Tahseen, T. 2013. Groundwater levels susceptibility to degradation in Lahore metropolitan. *Science International*, **25:** 123-126.

Majandang, J., Sarapirome, S. 2013. Groundwater vulnerability assessment and sensitivity analysis in NongRua, KhonKaen, Thailand using a GIS-based SINTACS Model. *Environment Earth Sciences*, **68:** 2025-2039.

Moench, M., Dixit, A. 2004. Adaptive capacity and livelihood resilience, Adaptive strategies for responding to floods and droughts in South Asia. ISET (Institute for Social and Environmental Transition), Boulder, Khatmandu, Nepal.

Nwankwoala, H.O., Eludoyin, O.S., Obafemi, A.A. 2012. Groundwater quality assessment and monitoring using geographical information system (GIS) in Port Harcourt, Nigeria. *Ethiopian Journal of Environmental Studies and Management (EJESM)*, **5:** 583-596.

PCRWR, 2007. *Water Quality Monitoring, Fifth Monitoring Report (2005-6)*. ISBN 978-969-8469-18-4, Pakistan Council of Research in Water Resources (PCRWR), Pakistan.

Rahman, A. 2008. A GIS based DRASTIC model for assessing groundwater vulnerability in shallow aquifer in Aligarh, India. *Applied Geography*, **28:** 32-53.

Singh, P., Khan, I.A. 2011. Ground water quality assessment of Dhankawadi ward of Pune by using GIS. *International Journal of Geomatics and Geosciences*, **2:** 688-703.

Singh, U.V., Abhishek, A., Singh, K.P., Dhakate R., Singh, N.P. 2014. Groundwater quality appraisal and its hydrochemical characterization in Ghaziabad (a region of Indo-gigantic plain), UP, India. *Applied Water Science*, **4:** 145-157.

Ullah, Z., Khan, H., Waseem, A., Mahmood, Q., Farooq, U. 2013. Water quality assessment of the river Kabul at Peshawar, Pakistan: Industrial and urban wastewater impacts. *Journal of Water Chemistry and Technology*, **35:** 170-176.

Usali, N., Ismail, M.H. 2010. Use of remote sensing and GIS in monitoring water quality. *Journal of Sustainable Development*, **3:** 228-238.

Verma, A., Thakur, B., Katiyar, S., Singh, D., Rai, M. 2013. Evaluation of ground water quality in Lucknow, Uttar Pradesh using remote sensing and geographic information systems (GIS). *International Journal of Water Resources and Environmental Engineering*, **5:** 67-76.

WAPDA, 1980. Development Credit Agreement. Third Water and Power Development Authority (WAPDA), Power Project, International Development Association and Pakistan, *United Nations-Treaty Series*, **1256:** I-20601.

WHO, 2011. *Guidelines for Drinking Water Quality*, 4th edition. http://www.unicef.org/cholera_toolkit/chapter_4_prevention/01_WHO_G/guidelines_for_drinking_water_quality.pdf.Access date: 13-02-2014.

Pak. j. sci. ind. res. ser. A: phys. sci. 2017 **60**(1) 42-49

Sulphide Removal from Sewage Wastewater by Oxidation Technique

Muhammad Tahir Butt*, Naz Imtiaz, Naeem Abbas and Rauf Ahmad Khan
CEPS, PCSIR Laboratories Complex, Ferozepur Road Lahore-54600, Pakistan

(received August 19, 2015; revised March 31, 2016; accepted April 08, 2016)

Abstract. In this study sewage wastewater samples were collected from different areas of Lahore, Pakistan from the WASA sewer system and then different chemical oxidizers: O_2, $KMNO_4$, H_2O_2 were used to remove the sulphides from these samples for selection of suitable oxidizer for treatment. From these results, it was observed that H_2O_2 was found effective and suitable for treatment and it can be used for this purpose. Theoretical and experimental doses required for treatment were similar. The $KMNO_4$ oxidation reactions were completed in five minutes time while H_2O_2 required more time and removed sulphide completely with slow chemical reaction. Different doses of oxidizer such as 1 to 6 g of oxygen, 1 to 14 g of $KMNO_4$,1 to 11 g of H_2O_2 with different ratios were used and H_2O_2 was found suitable. Using 11 g of H_2O_2 dose, 100 % sulphides were removed, H_2O_2 as an oxidizer was found more suitable for sulphide removal from wastewater.

Keywords: treatment, sulphide removal, wastewater, oxidation technique

Introduction

Wastewater treatment is a major challenge to the industrial advancements and treatment of the wastewater in efficient way has also become very vital problem. The organic and inorganic pollutants in the liquid wastes can be treated by various techniques like activated sludge process, membrane separation and adsorption (Sunil and Jayant, 2014). In case of contaminants like H_2S vapours, chemical treatments, adsorption, oxidation, bio-filtration. and membrane technology can be used for treatment. The pollutants in the wastewater include hydrogen sulphide, sulphur dioxide, carbon dioxide, and carbon monoxide.

Maata *et al.* (2005) used aqueous metal sulphate as absorbent for hydrogen sulphide (H_2S) removal. Premkumar and Krishnamohan (2013) also used bio filters for removal of H_2S from the wastewater stream. H_2S generation in wastewater streams depend on the temperature and pH of wastewater.

H_2S gas in the sewer may be adsorbed in the thin film of water that usually covers the sewer walls and may be incompletely oxidized to sulphuric acid by bacteria (Hvitved-Jacobson, 2002; Tanaka *et al.,* 2000). Bacteria in urban or industrial wastewater with favourable nutrient doses combined with facultative environments, i.e., space above the water causes the development of bacterial colonies. These bacterial colonies tend to lower the pH and oxidize H_2S to produce sulphuric acid, which causes corrosion. This sulphuric acid induced corrosion can deteriorate cement and iron piping very quickly. To prevent the spread and development of the bacterial biofilm in cement and iron pipes, root cause of this issue need to be focussed.

*Author for correspondence; E-mail: pcsir322@gmail.com

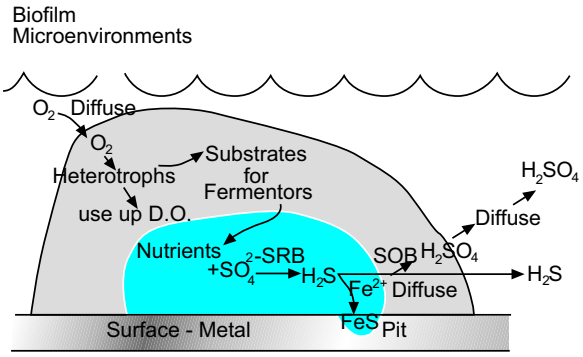

Bio film in collection system (Nielsen *et al.,* 2005; Hvitved-Jacobson, 2002)

Generally the sulphide produced from anaerobic sulphate decreases biofilms covering the wetted sewer walls (Hvitved-Jacobson, 2002). The sulphides produced in the biofilms will diffuse the water phase and if dissolved oxygen is higher in concentration, the sulphide will be oxidized in the external parts of the biofilm (Kamp *et al.,* 2006). Sulphide does not enter the water phase if dissolved oxygen concentration is above 1 g/L. Metal sulphides gathered in the biofilm can no longer be released (Nielsen *et al.,* 2005 ; Hvitved-Jacobson, 2002).

Corrosion and odor problems in sanitary sewers are due to high sulphate concentrations. Sulphide corrosion in sewers may be controlled by oxidation reduction potential in the sewage water, through addition of oxygen and other chemical oxidizers. Oxygen may be introduced as pure oxygen or as air into main sewers systems. Oxygen may also be injected to sewer. H_2O_2 provides residual oxidizer protection for up to one hour without pressurization. Chlorine gas, hypochlorite and $KMNO_4$ are also powerful oxidizers. These chemicals are used for effective sulphide control in sewers (Hampton Roads Manual, 2011; Calf and Eddy, 2009; Hvitved-Jacobson, 2002). However, blend of two or more of these chemicals may be counterproductive for sulphide control. Chemical requirements for complete sulphide oxidation depend on pH of solution and temperature. Corrosion in sanitary sewers is caused by oxidation of H_2S to sulphuric acid in the environment above wastewater. The sulphide from wastewater is generally removed by different treatments such as aeration, chemical oxidation and H_2O_2 but these do not actually remove the sulphur/ sulphide molecules from the system. Because the reduction of sulphur into H_2S or oxidation to sulphuric acid causes odor and corrosion problem. The high toxicity associated with H_2S is due to its ability to bind iron centers in enzymes, which effectively stops cellular respiration and deprives essential organs of energy (Hampton Roads Manual, 2011). Corrosion of metal and concrete is a major issue associated with the generation and oxidation of H_2S.The higher level of sulphuric acid that is produced as a result of oxidation of H_2S, which lowers the pH and, contributes to the declining of concrete, and stimulates ferrous pipe corrosion (Marry, 2005; Kerry *et al.,* 1989). The rate of concrete corrosion depends on the permeability of concrete and the amount of gaseous H_2S that is adsorbed to the moist sewer walls. Signs of prolonged exposure to mild acid attack include rust bleeding and cracking of the concrete (Davit *et al.,* 1998).

H_2S is a result of the breakdown of organic substances by bacteria, typically insufficient O_2 in environment such as municipal sewer system. Controlling this hazardous gas is one of the most challenging problems faced today. Anaerobic microorganisms must have a food to stay alive. Within this environment, the richest source of food for anaerobic bacteria is sulphate. When these sulphates are consumed by the anaerobic bacteria, H_2S is produced (Calf and Eddy, 2009). These sulphide-containing pollutants will either be oxidized, or released

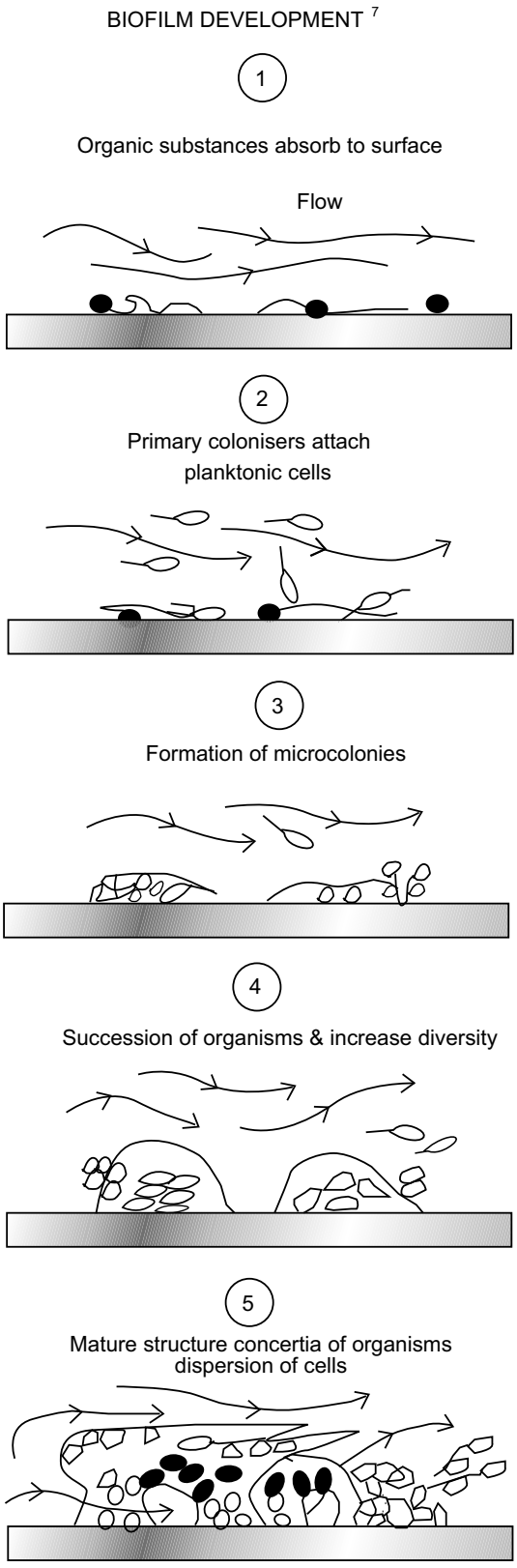

Bio film in collection system (Nielsen *et al.,* 2005; Hvitved-Jacobson, 2002)

into the sewer atmosphere (Zhu *et al.,* 2009; Tanaka *et al.,* 2000).

Oxidation by low cost oxidizers like ozone, chlorine, hydrogen peroxide and potassium permanganate was also used. This technique is easy to use and control. In case of high dose requirements, cost ineffectiveness for small amount of sulphide removal is a drawback of this method (Gholami *et al.,* 2009). The aim of this study was to remove the sulphide from wastewater to control bacterial biofilms because corrosion damages the refrigerators and air conditioners in the study area.

Materials and Methods

Sampling. The sampling was made according to the standard methods for the examination of water and wastewater method No. 4500-F **(**Marry, 2005). The sampling was made in Lahore city, Pakistan from the main holes on the sewerage system laid down by the Water and Sanitation Agency (WASA), Lahore. The samples were collected in the 1.5 liter plastic bottles and preserved according to the standard methods and transported to the CEPS, PCSIR Laboratories complex, Lahore for chemical analysis.

Sample handling and preservation

i. Plastic bottles were used for sampling and it was carefully observed that the material suspension should not stick to container walls.
ii. Samples were preserved using zinc acetate and sodium hydroxide solution.

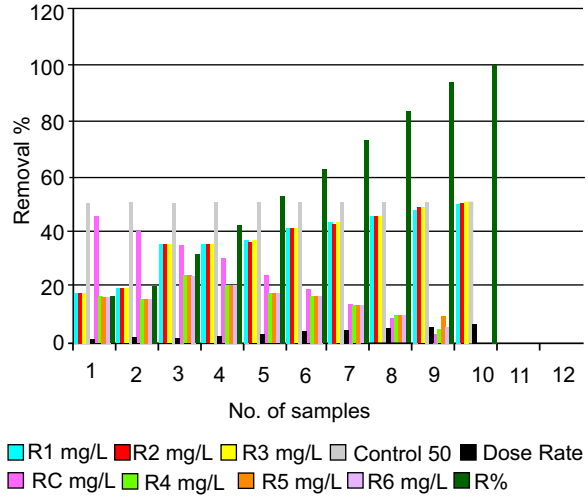

Fig. 1. Sulphide removal using different oxygen dose rates (area A)

iii. 0.2 mL of 2N zinc acetate solution for 100 mL sample was used.
Volume of zinc acetate solution was increased if the sulphide concentration is expected to be greater than 64 mg/L.
iv. The pH was adjusted at 9 using NaOH solution 5%.
v. Bottles were filled completely and stoppered.
vi. 5 mL of potassium iodide solution was taken in a titration flask and 100 mL of water was added, then by pipette 20 mL of 0.025N potassium iodate was added in the flask. Then 10 mL of diluted sulphuric acid was added and titration was done using 0.025N thiosulphate. When solution becomes pale yellow few drops of starch solution were added in the flask and titration was done until the blue colour disappears (Marry, 2005; Kerry *et al.,* 1989).

Calculation

One milliliter 0.025 N iodine solutions react with 0.4 mg S^{2-}

$$\text{mg } S^{2-}/\text{L} = \frac{[(A \times B) - (C \times D)] \times 16000}{\text{mL sample}}$$

where:

A = Iodine solution (mL)
B = Normality of iodine solution
C = $Na_2 S_2O_3$ solution (mL)
D = Normality of $Na_2 S_2O_3$ solution

Samples were brought to room temperature 32 °C before analysis. Samples were analysed in replicate.

Results and Discussion

The results before and after treatment with O_2, $KMNO_4$ and H_2O_2 along with control samples of 50 g and 100 g are presented in Figs. 1-10. The treatment was made with 1.0 mg/ min for samples and control, removal rate was 10.36 %. The concentration of H_2S before and after treatment was 18.3 mg/L and 16.47 mg/L .The maximum dose of 5 mg/L of O_2 was used for the treatment of sulphide removal from 50 mg/L to 3.01 mg/L removal percentage for control sample was 93.97% and for unknown samples 47.38 mg/L and at dose rate of 6 mg/L removal was 100 %.

The results of sulphide removal before and after treatment with O_2 as oxidizer for unknown and control samples are presented in Fig. 4 and 7 respectively, which are similar for removal percentage with dose rate of 1 g dose, removal of H_2S in controls were from 89.64 to 100 g with percentage removal 10.36 % and in

unknown samples at the similar dose rate results were 32.56 to 29.19 g with removal percentage 10.36%. The reduction in sulphide values in controls and unknown samples were from 100 to 6.57 and 100 to 6.03 g, 60.98 to 3.68 g and 62.27 to 3.75 g with O_2 dose rate of 5 g/g of O_2.

In Figs. 2, 4 and 8 the treatment was given with $KMNO_4$ to control and unknown samples, the removal in control and unknown samples at dose rate of 1 g/g removal was 6.66 % in both type of samples result of before and after treatment were 50g to 46.67 g ,100 mg to 93.34g and unknown were 18.30 to 17.11,73.6 to 68.7 and 32.56 to 30.39 g and at dose rate of 9 g,12 g 14 g results of controls and unknown samples before and after treatment were 50 to 4.03 mg, 100 to 8.05 g in unknown samples sulphide reduction was 47.82 to 3.82 g,60.96 to 4.91g and 62.27 g to 5.01 g at 10.5g dose rate. The sulphide removal was 100% in both categories at O_2 dose of 14 g/g.

In Figs. 3, 6 and 9 control and unknown samples were treated with H_2O_2 at various dose rates, at dose rate of 1 g and 50 to 39.01mg, 21.99 %, 100 to 78.01 mg, 99.51%, 100 to 0.49 mg, at dose rate of 5.5 removals was 100 %. In unknown samples results with similar

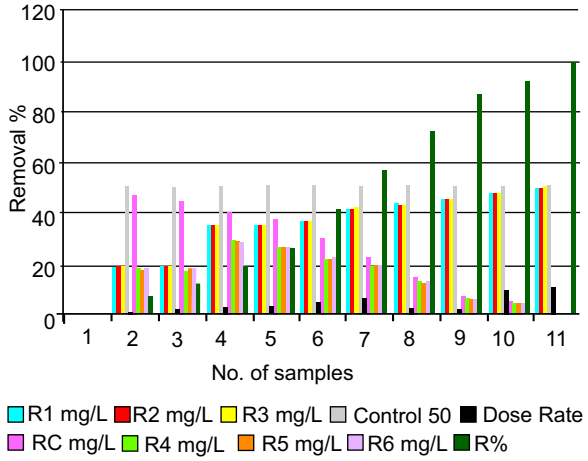

Fig. 2. Sulphide removal using different $KMNO_4$ dose rates (area A)

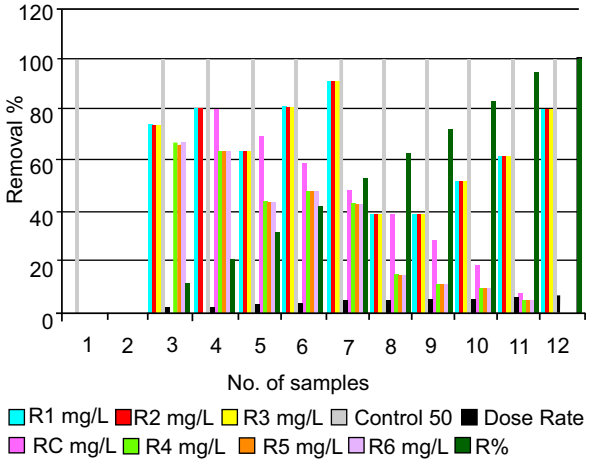

Fig. 4. Sulphide removal using different oxygen dose rates (area B)

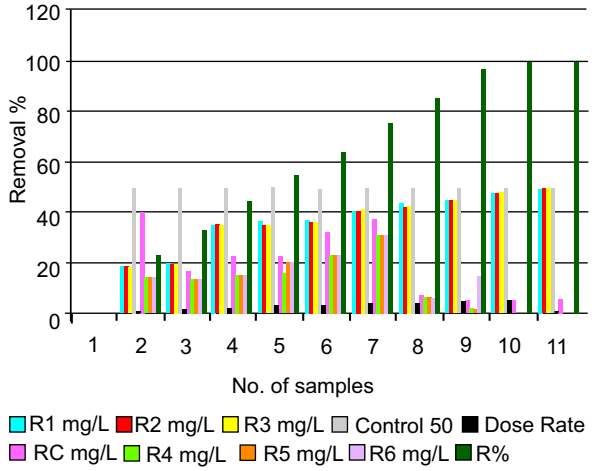

Fig. 3. Sulphide removal using different H_2O_2 dose rates (area A)

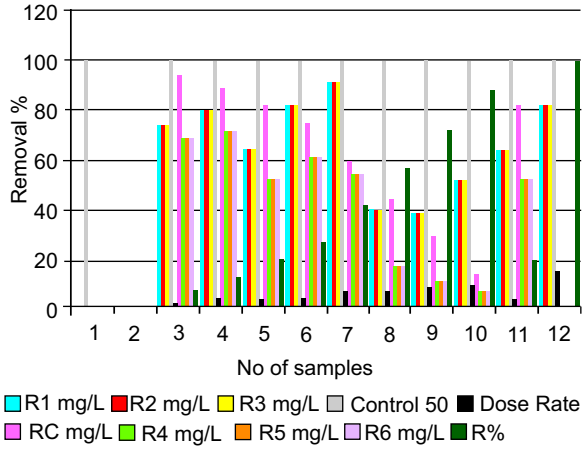

Fig. 5. Sulphide removal using different $KMNO_4$ dose rates (area B)

dose were 18.30 to 14.27g, 60.96. to 0.3g and 62.27 g to 0.31 g and at 5.5 g removal was 100 %. The treatment of these known and unknown samples with different oxidizers such as O_2, $KMNO_4$ and H_2O_2 were tried and H_2O_2 was found most suitable for treatment with respect to dose rates, while O_2 and $KMNO_4$ were less effective for this treatment. The experimental results before and after treatment along with controls for oxidation of free sulphides with chlorine compounds, $KMNO_4$ and H_2O_2 are presented in Figs. 1 to 9. Results presented in these figures show sulphides removal efficiencies after equilibrium was attained for various oxidizers to free sulphides percentages. For the tests with strong oxidizers chlorine compounds and $KMNO_4$, equilibrium conditions occurred five minutes after chemical addition. Oxidation of sulphides by H_2O_2 is a slower process requiring 30 min to reach equilibrium. Results presented in these figures correspond to values obtained at 5 min for strong oxidizers and contact time 30 min for the H_2O_2 tests. The wastewater used during the chlorine oxidation studies contained different concentrations of free sulphides before chemical addition. The figure shows that minimum dose required for complete sulphides removal in a typical wastewater sample is approx. 5.5g of sulphides in solution. This experimentally determined demand is well within the theoretical limits.

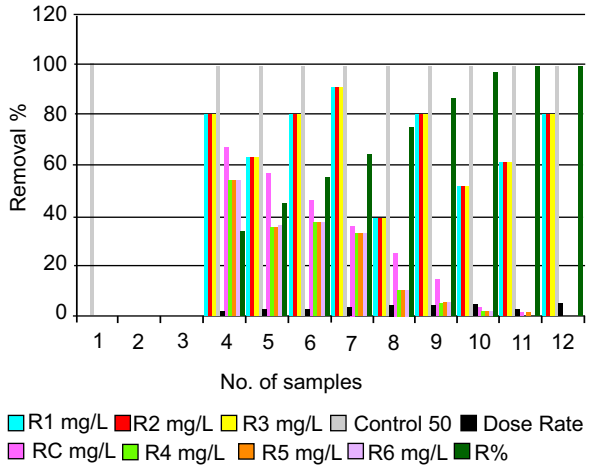

Fig. 6. Sulphide removal using different H_2O_2 dose rates (area B)

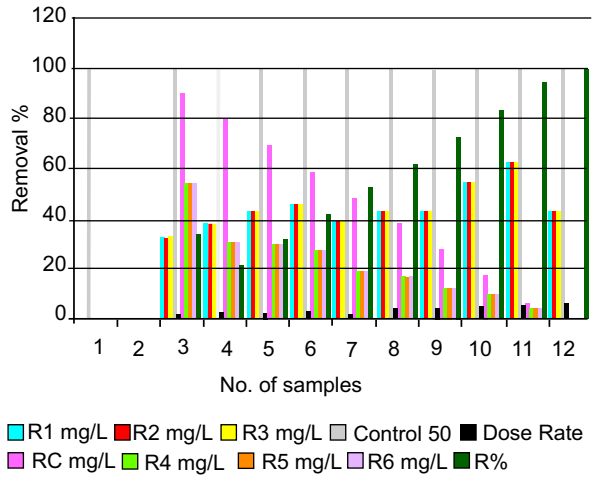

Fig. 7. Sulphide removal using different oxygen dose rates (area C)

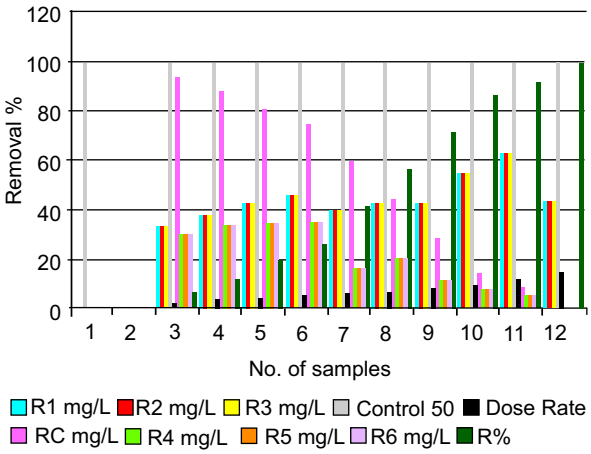

Fig. 8. Sulphide removal using different $KMNO_4$ dose rates (Area C)

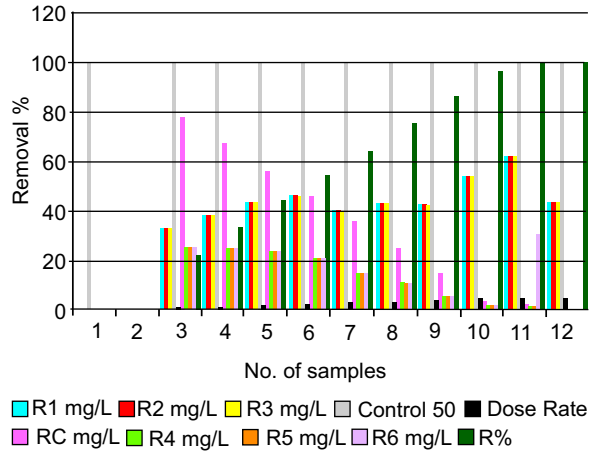

Fig. 9. Sulphide removal using different H_2O_2 dose rates (Area C)

Figures 2, 4 and 8 also show results of the sulphide oxidation tests with potassium permanganate. The minimum potassium permanganate required for free sulphides removal was approximately 14 g of sulphides oxidized. This optimum dose ratio also falls within the theoretical limits. Measured sulphides concentration in the H_2O_2 tests depend on both the H_2O_2, H_2S ratio and the contact time. Free sulphides concentration for different tests (where H_2O_2 was used as oxidizing agents) are reported as functions of H_2O_2: H_2S ratio, even at the highest H_2O_2: So^{2-} rates. Free sulphides concentrations in the absence of oxidizers were also measured as a function of time.

Initial and final removal of sulphides concentration is presented in Figs 1 to 9.This trend occurs as long as H_2O_2 actively oxidizes H_2S. This continues until the chemical is totally consumed. No additional sulphides removal is observed after this time. The residual effect of H_2O_2 is more marked at H_2O_2: H_2S ratios greater or equal to 5.5 g/g where oxidation continues after 30 min. On the other hand, at ratios lower than 1.2 g/g the oxidation reaction stops in less than 5 min. Termination of the reaction is possible because of the total consumption of the oxidizer.

The applicability of H_2O_2 is limited to field situations, where the oxidation kinetic exceeds the generation ratio; sulphides produced in sewers are faster than the rate at which they can be removed by H_2O_2. Oxidation may be protected by using other strong oxidizers. It is interesting to observe that H_2O_2 is completely depleted H_2O_2: Sulphide ratios, lower than 5.5 g/g of sulphides in less than 30 min. Thus the minimum H_2O_2 required for the complete oxidation is approx. 5.5 g of pure H_2O_2 of free sulpdides. Equilibrium reactions between three supplied spices are represented by the following reactions (Marry, 2005).

Consequently H_2S is the main dissolved component at pH values below 7, while HS- predominates at pH values between neutrality and 14. Sulphide induced order control in wastewater works may be accomplished by the use of various oxidizing agents which commonly include hypochlorite, chlorine and $KMNO_4$, H_2O_2, and O_2 (Hampton Roads Mannual, 2011; Calf and Eddy, 2009) end products and oxidizer demands are dependent on solution pH and redox potential (E-).Oxidizers increased the redox potential of the solution. Sulphides may be converted to more oxidizing forms such as sulphates and elemental sulphur by increasing solution of chemical oxidizer O_2 unless excessive oxidizer doses are applied, oxidation of sulphides in the acidic range is incomplete, which results in elemental sulphur production. In the basic range sulphate is the end product of oxidation reaction. On the other hand complete oxidation of sulphide occurs at pH value above 7.5 resulting in the formation of SO_4. Therefore, lower oxidizer doses are common in the acidic range because elemental sulphur possesses a lower oxidation potential then SO_4.Therefore, oxidizer does typically increases with the increasing solution pH. Therefore, hypochlorite salts and chlorine may be used for the oxidation of sulphides in well buffered waters where the pH of the solution will be very significant because of the introduction of the oxidizer. Addition of chlorine or hypochlorite to wastewater results in OCl production. This radical in turn reacts with H_2S to form the sulphur. On the stoichiometry reactions between 2.1 and 8.4 g of elemental chlorine are oxidized 1 g sulphides of H_2S. The lower value for the chlorine demand is required in the acidic range. The larger demand value is required at pH values higher than 7.5 when sulphate is produced. Hypochlorous of ion requirement to fully complete the reactions are 1.5 and 6.1g of sulphides oxidized corresponding chemical requirements of pure calcium hypochlorite vary from 2.1 and 8.4 g while those for pure sodium hypochloride are between 2.2 and 8.8 g of sulphides oxidized.

The oxidation rate of sulphide with H_2O_2 is relatively slow. 20 to 30 min contact times are normally required for a completed reaction .In the absence of bacteria H_2S reaction directly reacts H_2S as shown by the reaction J and K. Reaction J occurs in the neutral and acidic range (pH < 7.5). According to the stoichiometry of these reactions, between 1 to 4 g of pure H_2O_2 are required to oxidize 1g of H_2S.

$$H_2S+H_2O_2 \text{ ------} 2H_2O + S^o \text{ if pH} < 7.5 \text{ ----------(A)}$$

$$H_2S+4H_2O_2 \text{ ----} SO_4^{2-} + 4HO_2 + 2H + \text{ if pH} > 7.5 \text{ ----(B)}$$

The mechanism of oxidation of H_2S by H_2O_2 in wastewater is not well understood. Others suggest that direct oxidation of sulphides using H_2O_2 reaction A and B is unlikely in the presence of larger concentrations of bacterial catalase in wastewater. H_2O_2 first reacts with the bacterial catalase producing O_2 and water (Nielsen *et al.,* 2005; Hvitved-Jacobson, 2002). Sulphides in wastewater are oxidized by the dissolved O_2 generated

during gradual decomposition of H_2O_2 the stoichiometric requirement should be identical, regardless of the oxidation reaction path way. Therefore, reactions A and B are also commonly accepted for sulphides oxidations in wastewater. H_2O_2 is manufactured as fluid in concentrations as high as 15 % pure hydrogen per oxide has a specific gravity of 1.2 cm^3/ g at 20 °C. The stoichiometry requirement to satisfy reactions A and B are 1.7 and 6.7 mL of 50% H_2O_2/ g of H_2S, respectively.

Oxidation of H_2S with chlorine, $KMNO_4$ and H_2O_2 was conducted under controlled laboratory conditions. The pH of the wastewater samples used in the study varied between 7.2 and 7.5. Oxidation reactions were maintained at approximately 25 °C ±1°C. Free sulphides were analyzed using standard method with the preliminary investigations chlorine compounds and $KMNO_4$ reacted rapidly in dissolved sulphide in solution. Oxidation of sulphides with the strong oxidizers occurred in 5 min after chemical addition. On the other hand the kinetics of sulphides oxidation with the H_2O_2 was significantly slower. Two different experimental procedures were designed to evaluate the effectiveness of oxidizers. In the first experimental procedure sodium hypochlorite, commercial and in liquid form containing 7.5% elemental chlorine and $KMNO_4$ industrial grade, 97% pure were used to prepare dilute stock solutions for the oxidation tests. Different volumes of stock solution were dispensed into replicate 300 mL bottles previously filled up to capacity. The bottles were carefully stoppered to evacuate the gas. Concentration of free sulphides was measured before tests 5 min after each oxidizer was added. Two small reactors were used in the second phase (Bowker, 1985; Waltrip and Snyder, 1985; Parthum, and Leffel, 1979; Dague, 1972). During the H_2O_2 tests shown in the figure the DO and pH of the solution were measured. Precision of pH and DO measurement was 0.01 pH units and 0.1 mg/L, respectively. DO and temperature of solution was measured by DO meter and thermometer.

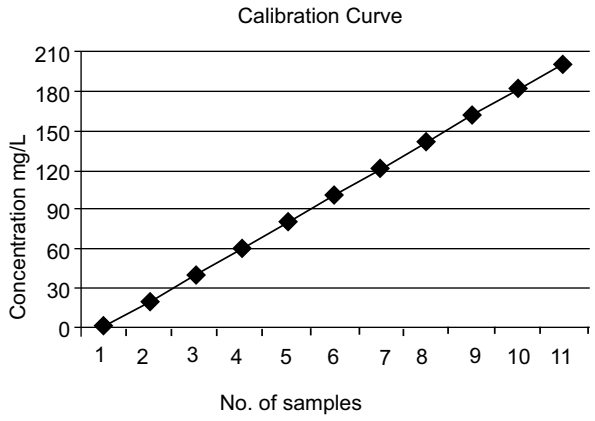

Fig 10. Calibration curve for sulphide

Conclusion

Kinetics of sulphides oxidation with chlorine compounds and $KMNO_4$ very rapidly attained in five minutes after addition of oxidizer. Oxidation of sulphides with H_2O_2 is a relatively slow process. This oxidation reaction proceeds as long as residual per oxide remains in solution. Minimum dose of oxidizer required to remove one g. of free sulphides are equal to 11.0, 6.0 and 5.5 g of H_2O_2, O_2 and $KMNO_4$, respectively. Because of the relatively slow reaction rate, H_2O_2 provides extended sulphides protection while O_2 and $KMNO_4$, removed sulphides rapidly without providing a residual protection. Effective sulphides control in sewers using H_2O_2 is limited to conditions where sulphides generation is relatively slower than the removal rates. Stronger oxidizers may be used in more adverse conditions. Thus H_2O_2 is recommended for the sulphide removal treatment.

Acknowledgement

We are thankful to WASA, Lahore for providing assistance and map of Lahore sewer system.

References

Bowker, R.P.1985. Odor and corrosion control in sanitary sewerage systems and treatment plants EPA. 625/I-85/18.U. S. EPA, Cincinnati, Ohio, USA.

Calf, M., Eddy, 2009.*Wastewater Engineering, Treatment and Reuse.* 70 pp., 4th edition Tata, Mc Graw-Hill Education Private Limited West Patel Nagar, New Delhi, India.

Dague, R. R. 1972. Fundamentals of odor control. *Journal of Water Pollution Control Federation*, **44:** 583-594.

Davit, P., Applebee, M., Craiglacher, Bessie, J.1998. Low parts per billion determination of sulfide by colourimetric argentometry. *Environmental Science & Technology,* **32:** 1734.

Gholami, Z., Torabi, A.M., Gholami, F., Razavi, A.S.A. 2009. Reactive absorption of hydrogen sulphide in aqueous ferric sulfate solution. *World Academy of Science, Engineering and Technology,* **3:** 01-24.

Hampton Roads Sanitation District Coatings Manual. 2011. Appendix A: Basics on corrosion in wastewater collection and treatment system: Management, Operations, and Maintenance Program Revised July 2011.

Hvitved-Jacobson, T. 2002. *Sewer Processes - Microbial and Chemical Process Engineering of Sewer Networks*. CRC Press, Florida, USA.

Kamp, A., Stief, P., Schulz-Vogt, H. N. 2006. Anaerobic sulphide oxidation with nitrate by a freshwater Beggiatoa enrichment culture. *Applied and Environmental Microbiology,* **72:** 4755-4760.

Kerry, L., Tusla, S., Maron, O., Woolsey, E., Okala, T., Frances, S,M., Okla, T ., Montgomery, A., Antonio,S ., Michael, T., Mcinerney, J., Okla, N. 1989. Microbial Control of H_2S Production by Sulphate Reduction Bacteria. Patent no. 4879240. USA Patents.

Maata, H.T., Hogendoornb, J.A., Versteeg, G.F. 2005. The removal of hydrogen sulfide from gas streams using an aqueous metal sulphate absorbent. *Separation and Purification Technology*, **43**: 199-213.

Marry, A.H.F .2005. *Standard Methods for Examination of Water & Wastewater*. 21st edition, AWWA/ APHA. P.4 -170 to 4 -176.

Nielsen, A., Yongsiri, C., Hvitved-Jacobsen, T., Vollertsen, J. 2005. Simulation of sulphide buildup in wastewater and atmosphere of sewer networks. *Water Science and Technology,* **52:** 201-208.

Parthum, C.A., Leffel, R.E. 1979.Odor Control for Wastewater Facilities. *Manual of Practice* No.22, pp. 1-13, Water Pollution Control Federation Washington, D.C. USA.

Premkumar, R., Krishnamohan, N. 2013. Biological elimination of volatile hydrogen sulphide compounds in bio filters. *International Journal of Chemical Technology Research,* **5:** 56-64.

Sunil, J.K., Jayant, P.K. 2014. Removal of cadmium from wastewater by groundnut shell adsorbent-batch and column studies. *International Journal of Chemical Engineering Research,* **6:** 27-37.

Tanaka, N., Hvitved-Jacobsen, T., Horie, T. 2000. Transformations of carbon and sulfur wastewater components under aerobic-anaerobic transient conditions in sewer systems. *Water Environment and Research,* **72:** 665-674.

Waltrip, G. D., Snyder, E. G. 1985. Elimination of odor at six major wastewater treatment plants. *Journal of Water Pollution Control Federation,* **50:** 1027-1032.

Zhu, H. T., Wen, X. H., Huang, X. 2009. Effect of ozone on membrane fouling in water and wastewater treatment: a research review. Huan jing ke xue Huanjing kexue/[bian ji, Zhongguo ke xue yuan huan jing ke xue wei yuan hui" *Huan jing ke xue" bian ji wei yuan hui,* **30:** 302-312.

Pak. j. sci. ind. res. Ser. A: phys. sci. 2017 **60**(1) 50-58

The Study of PM_{10} Concentration and Trace Metal Content in Different Areas of Karachi, Pakistan

Durdana Rais Hashmi*, Akhtar Shareef and Farooq Ahmed Khan
Centre for Environmental Studies, PCSIR Labs Complex, Karachi-75280, Pakistan

(received August 6, 2015; revised April 4, 2016; accepted April 8, 2016)

Abstract. Atmospheric particulate matter may exert serious health hazards because of its chemical characteristics. Aim of this study was to determine the concentrations of particulate matter (PM) with an aerodynamic diameter ≤10 μm (PM10), and air transmitted particulate trace metals in different areas of Karachi's ambient air, for the period of 01 year *viz.* June 2011 to June 2012. Furthermore, the present work compares the levels of particulate matter and trace metals with the proposed limiting values from the U.S. Environmental Protection Agency (65 μg/m^3 for PM10). The sampling for PM_{10} was performed by using a high volume air sampler. The PM_{10} levels were determined by gravimetry and the metals by graphite furnace. Arithmetic means of 361.0 μg/m^3 was determined for PM_{10} in commercial areas, 275.0 μg/m^3 in residential areas, 438.0 μg/m^3 in industrial areas and 68.9 μg/m^3 in background areas of Karachi. Trace metal content in PM_{10}, such as lead (Pb) and cadmium (Cd) were also analysed separately during the same period using atomic absorption spectrometry. The average concentration of Pb were found in commercial zone 1.36 μg/m^3, in residential zone 1.0 μg/m^3, in industrial zone 1.46 μg/m^3 and in urban background zone 0.6 μg/m^3, whereas; Cd concentration in commercial zone 0.10 μg/m^3, in residential zone 0.02 μg/m^3, in industrial zone 0.25 μg/m^3 and in urban background zone 0.01 μg/m^3, respectively.

Keywords: trace metal, atmospheric particulate matter, ambient air, Karachi

Introduction

Airborne particulate matter composed of wide range of chemically and physically diverse substances variable in size, chemical composition, formation, origin and concentration, and is variable across space and time. The particulates may include a broad range of chemical species, ranging from metals to organic and inorganic compounds (Park and Kim, 2005; Tsai and Cheng, 2004). The sources, characteristics, and potential health effects of particulate matter with aerodynamic diameter less than 10 μm (PM_{10}) are very different. The particulate emitted by stationary and mobile sources have a range of health effects that are known for a long period of time (Sharma and Maloo, 2005). One of the most important components of the air pollution mixture that contributes in a various adverse health outcomes as well as general environmental effects is urban particulate matter (PM) (Van Der Zee *et al*., 1998). Regarding the size of urban particulate matter, it tends to be divided into three principal groups: coarse, fine, and ultrafine particles. Particulate matter air pollution has both natural and anthropogenic sources.

Coarse particles normally divided into rural and natural crustal material for example dust due to 1) kicked up by vehicles (called resuspended dust), 2) construction and demolition, 3) industries, and 4) biological sources. It contains biological matter, hydrocarbons, both organic and inorganic compounds, acid deposition and several trace metals (de Kok *et al*., 2006). Fine particles may be emitted directly as a result of combustion process or may be due to some chemical reactions of different gases such as nitrogen dioxide, sulphur dioxide and some of organic gases.

A number of epidemiological studies show strong relation between elevated concentrations of inhalable particles (PM_{10}) and increased mortality and morbidity (Namdeo and Bell, 2005). Health hazards associated with particulate matter (PM_{10}) are linked to pulmonary and cardiovascular diseases (Callen *et al*., 2009). It is demonstrated that trace metal content of PM_{10} can be toxic to living organism at certain levels. They occur naturally and also emitted from different sources such as industrial emission, mining industries, fossil fuels burning, solid waste incineration, garbage dumping, tobacco smoke and transportation. Several trace metals, such as Cd, Pb, Co, Cu, and Cr, are considered to be very harmful that can accumulate in the human body, with a relatively long half-life. For example, it has been stated that Cd has a half-life of 10 years in the human body. Cadmium can produce acute toxic effects on

*Author for correspondance; E-mail: drhpakr@yahoo.com

various organs such as the kidney, liver, pancreas, and lung (by inhalation) and the toxicity of lead may largely be explained by its interference with different enzyme systems; lead inactivates these enzymes by binding to SH-groups of its proteins or by displacing other essential metal ions (Benoff *et al*., 2000).

Several researches have been conducted on Pb, Cd, Cr, Hg, and other trace metal levels in air and their toxic effects (Onder and Dursun, 2006), which shows a wide inconsistency in the intake of some metals through air by breathing, drinking water and food (e.g., seafood). High concentration of airborne trace metals such as Pb, Cd, other trace metals and organic pollutants may also cause neuro-developmental and behavioural defects in children. Thus, in this study, the levels of PM_{10}, and two most important trace metals (Pb and Cd) have been investigated in the atmospheric air in Karachi. Also, the trace metal content of PM_{10} has been compared with other parts of the world.

Materials and Methods

Study area. Karachi lies between 24°45′N in longitude and 66°37′E in latitude. It has an area of 3,640 km² and is located along the cost of the Arabian sea. It is the largest metropolitan city of Pakistan, has an estimated population of over 23.5 million people as reported in 2013. With respect to the population, Karachi is the 2nd largest city in the world. Karachi has a moderately temperate climate with a generally high relative humidity that varies from 58% in December (the driest month) to 85% in August (the wettest month). In winter, the average temperature of the city is about 21°C while in summer it reaches up to 35°C. Karachi receives about 256 mm of average annual rainfall (Sajjad *et al*., 2010).

Karachi is the financial and commercial capital of Pakistan as well as the major sea port. It plays an important role in the economy of Pakistan and is considered as the economic and financial gateway of Pakistan. Karachi has several large industrial zones such as Karachi export processing zone (KEPZ), Sindh industrial trading estate SITE, Korangi industrial area (KIA), Landhi industrial trading estate, Northern by-pass industrial zone (NIZ), Bin Qasim and North Karachi industrial zone (KNIZ), located on the fringes of the main city (Sajjad *et al*., 2010). Its primary industries are textiles, pharmaceuticals, steel, and auto-mobiles. Due to industrialisation, business activities and employment opportunities Karachi has been facing mass scale rural-urban migration from all over Pakistan.

Ambient monitoring. *Sampling*. Sampling was carried out at one hundred eight (108) locations consisting of main roads, side road, round abouts, and open places along the busy roads of Karachi (Fig. 1) from 2011 to 2012 for PM_{10}. Selected locations were categorized as commercial, residential, industrial and background areas of the Karachi. Samples were collected on glass fibre filters (203×254 mm) by using high volume air sampler with an average flow rate of 1.0 m^3/min. Eight hour average sampling was done in duplicate at each location during the year 2011 to 2012. The high volume is considered a reliable instrument for measuring the weight of PM_{10} in ambient air (USEPA-Method 40 CFR). Relevant features of air quality stations are shown in Table 1.

Mass concentration. In addition to the determination of elemental concentrations, airborne particle masses of PM_{10} samples were measured using analytical balance (KERN, ALS 220-4). The filter papers were weighed under controlled conditions of humidity and temperature before and after collection of particulate matter. Weights for the blank filters were also recorded. Prior to weighing, all filter papers (glass fiber filter paper) were left to equilibrate their humidity and temperature conditions for at least 24 h in a desiccators. The collected particle mass was calculated by subtracting pre–weight from post–weight of the filter.

Sample analysis. Acid digestion method for metals determination by atomic absorption spectrophotometer (Hitachi Z-8000), with Zeeman effect background correction was carried out according to a standard procedure. Acid digestion was performed by following these steps: (1) samples of dry filters were dissolved in

Table 1. Relevant feature of the air quality stations

Location code	Remarks
C-01 to C-54	Vehicular movement and other commercial activities. Road traffic and commercial activities
R-01 to R-36	Railway siding, vehicular movement, transport on paved road and unpaved road, haul road and exposed dump/ exposed pit surface, domestic waste burning and residential activities etc.
I-01 to I-14	Vehicular emission, waste incineration, Stack emissions and other industrial activities.
UB-01 to UB-04	Low vehicular movement and transport on unpaved road and solid waste dumping.

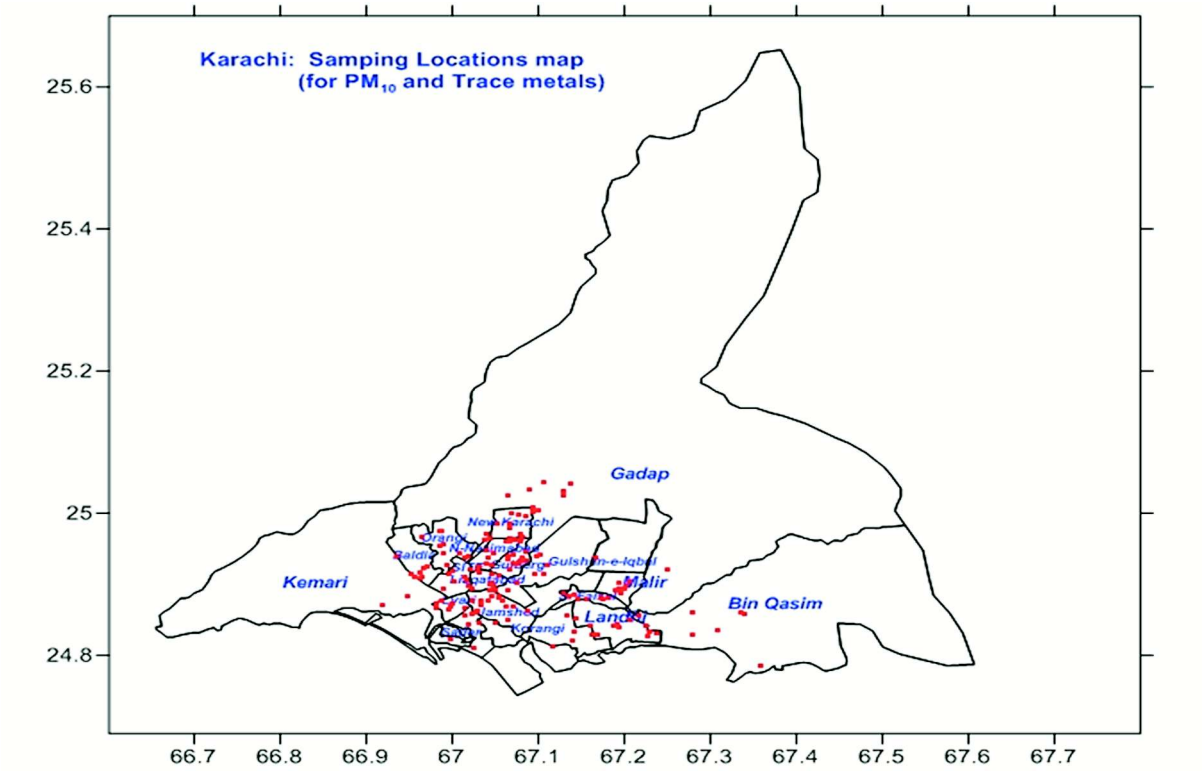

Fig. 1. Location map.

nitric acid and perchloric acid (10:4), (2) digestates were evaporated till white fumes arose and reduced to 2-3 mL, (3) the content was filtered through a Whatman filter 42 and the final volume was make up to 50 mL by double distilled water.

A series of blanks were prepared using the same digestion method. Metals and reagents used for standard solutions were of AR grade. The reagents used were HNO_3 71% (specific gravity=1.41, Pb and Fe=0.00002%, Mn=0.00004%, while Cu=0.00001%) and $HClO_4$ 40% (specific gravity 1.13). The filtrates were analysed for trace metals using AAS. The trace metal amounts in the samples were calculated by subtracting the blank value for the respective metal. The detection limit of various trace metals for the AAS were Pb (0.01 ppm) and Cd (0.004 ppm).

Before analysing the samples, the instrument was calibrated for Pb and Cd. As per the USEPA method 40 CFR, stock solutions (BDH, 1,000 ppm) were used and diluted to the range of working standards for individual metal just before their utilisation. Using these working standards, the calibration graphs were prepared in the linear range of the optical density (0.04-0.8). The instrument was calibrated at three different levels (0.5, 1.0, and 1.5ppm) for both metals. Exactly the same extraction and analysis procedure was employed for PM_{10} filter papers in order to examine the trace metal content of blank filter paper.

Quality assurance. Precision and accuracy of the results were confirmed through an average value of three replicates for each reading and cross checking of the blank or standard at ten sample intervals. The calibration curves of standard solutions of metals were used to justify the quantification. The minimum detection limit for Pb and Cd is 0.30 and 0.01 µg/m^3, respectively. The precision of the analysis of standard solution was better than 5% in all the readings.

Results and Discussion

PM_{10} concentration. The statistical distribution parameters for PM_{10} and trace metals (Pb and Cd) for commercial, residential, industrial and background areas are given in Table 2. The particulate matter concentrations varied from 68.3-719.3 µg/m^3 for commercial areas, 69.1-491.4 µg/m^3 for residential areas, 109.6-736.6 µg/m^3 for industrial areas, while 47.2-98.3 µg/m^3 for background areas. In commercial areas PM_{10} concentrations were higher at locations C-6, C-7, C-28

Table 2. Statistical distribution of PM_{10} and trace metals levels ($\mu g/m^3$) in particulate matter of study areas

Pollutants	Range ($\mu g/m^3$)	Arithmetic mean	Median
Commercial areas			
PM10	68.3-719.3	361.0	325.9
Pb	0.182-2.46	1.36	1.35
Cd	0.008-0.723	0.10	0.052
Residential areas			
PM10	69.1-491.4	275.0	297.0
Pb	0.30-1.80	1.0	1.06
Cd	0.003-0.073	0.023	0.017
Industrial areas			
PM10	109.6-736.6	438.0	479.35
Pb	0.844-2.15	1.46	1.39
Cd	0.038-0.944	0.25	0.1045
Background areas			
PM10	47.2-98.3	68.9	65.0
Pb	0.40-0.70	0.60	0.006
Cd	0.00-0.01	0.01	0.5

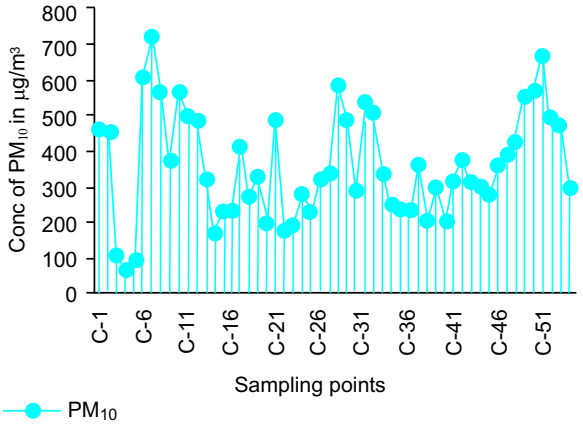

Fig. 2. Concentration of PM_{10} in commercial areas.

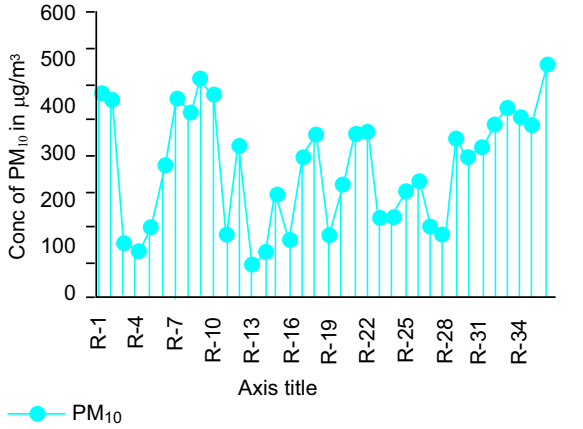

Fig. 3. Concentration of PM_{10} in residential areas.

and C-51. These locations are surrounded by roundabouts having automobile repairing shops, unplanned rickshaws stand and they are receiving higher emissions due to vehicles and commercial activities (Fig. 2). In residential areas PM_{10} concentrations were higher at locations R-1, R-2, R-7, R-9, R-10 and R-36, surrounded by shopping centers with food court producing emission due to

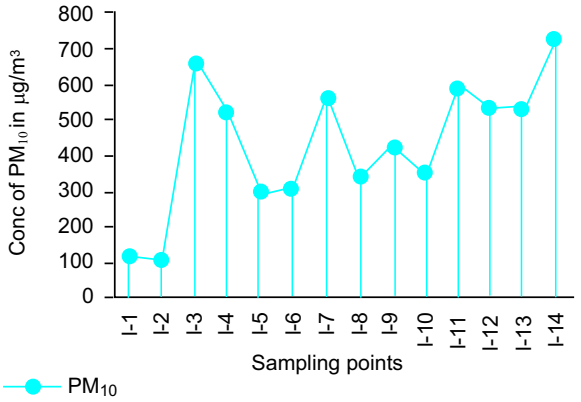

Fig. 4. Concentration of PM_{10} in industrial areas.

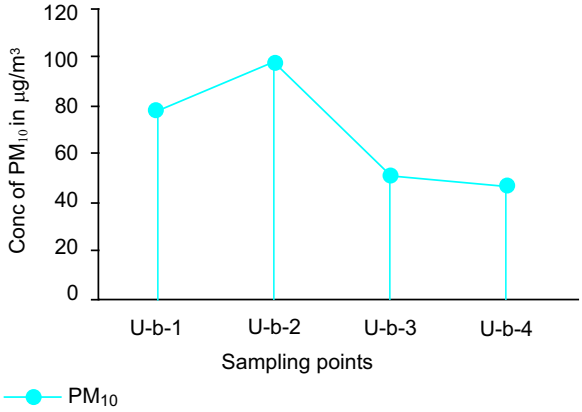

Fig. 5. Concentration of PM_{10} in background areas.

commercial activities (Fig. 3). In industrial areas PM_{10} concentrations were higher at locations I-3, I-7, I-11 and I-14 and receiving higher emissions due to industrial and vehicular emission (Fig. 4) whereas in background areas PM_{10} concentrations were higher at location UB-2 due to impact of vehicular emission from nearby superhighway (Fig. 5). Mean concentration of PM_{10} at various locations of commercial, residential, industrial and background areas were 361.0, 275.0, 438.0 and

68.9 µg/m^3, respectively (Table 2), giving an overall mean of 285.7 µg/m^3 for Karachi region.

Elemental concentrations. Average concentrations for trace metals (Pb and Cd) at various locations (commercial, residential, industrial and background areas) are shown in Fig. 6-9 for the study areas**.** The highest mean concentration of Pb (Table 2) was found 2.46 µg/m^3 in commercial area, 1.83µg/m^3 in residential area, 2.15µg/m^3 in industrial area and, 0.7µg/m^3 in urban background area and Whereas highest mean concentration of Cd (Table 2) was found 0.72 µg/m^3 in commercial area, 0.073µg/m^3 in residential area, 0.94 µg/m^3 in industrial area and, 0.01µg/m^3 in urban background area, respectively. On the average, the decreasing elemental concentration trend for Pb and Cd in Karachi was: commercial > industrial > residential >urban background areas.

Source apportionment. One hundred eight (54+36+14+4) samples of particulate matter were collected from the main roads, side road, round about, and open places along the busy roads of Karachi (Fig. 1), and these locations were categorised as commercial (54 locations), residential (36 locations), industrial (14 locations) and urban background zones (04 locations) of the Karachi city. Analysis of these particulate matter samples were carried out for lead and cadmium, respectively.

Figure 6 shows the concentration of lead and cadmium in commercial areas of Karachi. Maximum average concentration of lead and cadmium found at location C-52 (2.46 µg/m^3 Pb) and (0.723 µg/m^3 Cd), respectively. These high concentrations of lead and cadmium may be due to the large parking place for hundreds of vehicles near this round about with very high traffic density. Moreover; the roads are narrow and congested with high traffic density. The lowest concentration of lead and cadmium in commercial areas was found at location C-4 (0.18 µg/m^3 Pb) and (0.008 µg/m^3 Cd), respectively. The low concentration at this location may be because this is an open place on wide road having low traffic density with low emissions. All the sampling points in commercial areas were on the busiest intersections in Karachi and are surrounded by multistoried buildings both for commercial offices and residential buildings on main roads and round about having high traffic density.

Figure 7 shows the concentration of lead and cadmium at 36 locations in residential areas of Karachi. Maximum concentration of lead and cadmium found at location R-11 (1.8 µg/m^3 Pb) and (0.073µg/m^3 Cd), respectively. The factors responsible for high values at R-11 are multistoried buildings located at both sides of the roads which produce tunnel effect in this area and high traffic density, whereas, the lowest concentration of lead and cadmium found at location R-3 (0.3µg/m^3 Pb) and (0.003 µg/m^3 Cd), respectively due to open place with low vehicular emissions. Residential areas are densely populated having high traffic density. The sampling points in residential areas are also covered with the busiest intersections in Karachi and surrounded by single and mostly multistoried buildings for residence. The populations living around the selected locations were middle and high income group and also have high emission of vehicles.

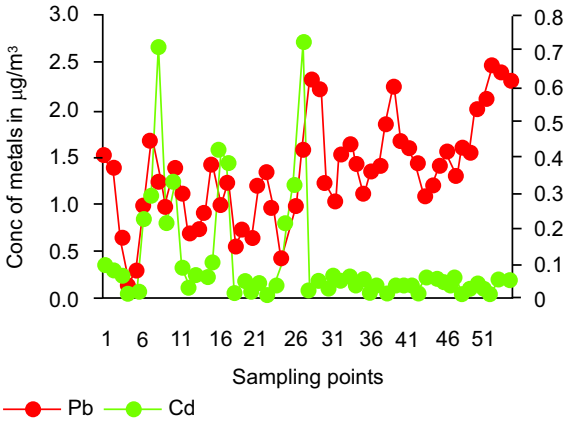

Fig. 6. Concentration of Pb and Cd in commercial area.

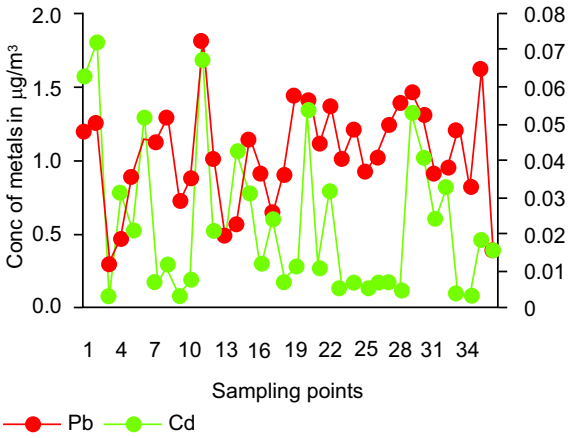

Fig. 7. Concentration of Pb and Cd in residential areas.

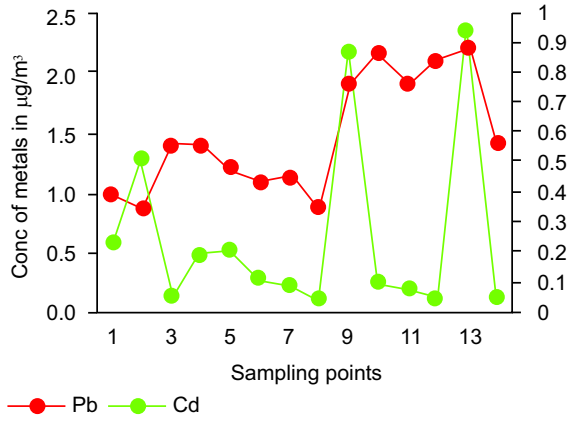

Fig. 8. Concentration of Pb and Cd in industrial areas.

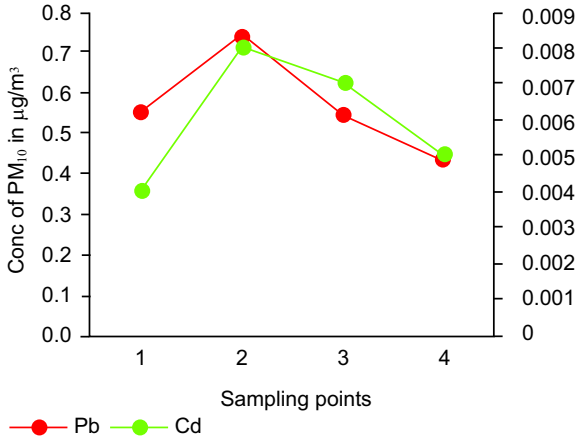

Fig. 9. Concentration of Pb and Cd in industrial areas.

Figure 8 shows the concentration of lead and cadmium at 14 locations in industrial areas of Karachi. Maximum concentration of lead and cadmium found at location I-13 (2.2 µg/m^3 Pb) and (0.944 µg/m^3 Cd), respectively. Increase in trace metal pollution at this location may be due to high traffic density and emission from the industries which are located on main roads of the city. Whereas, lowest concentrations of lead and cadmium found at location 1-8 (0.84 µg/m^3 Pb) and (0.038 µg/m^3 Cd), respectively. The low values found here may be because these industrial areas have relatively open place and situated on the intersection of very wide road. The sampling points in industrial areas have different types of industries. The areas covered are SITE, LITE, KIA and Port Qasim. Approximately 60% of the industries are textile mills, while other involve pharmaceuticals, chemicals, detergents, iron and steel, sulphur refining, vegetable oil, beverages and food products.

Figure 9 shows lead and cadmium concentrations at 04 locations in background areas of Karachi. Maximum concentrations of lead and cadmium in urban background areas was found at location U-B-2 (0.7 µg/m^3 Pb) and (0.008 µg/m^3 Cd) whereas, minimum concentration was found at location U-B-4 (0.4 µg/m^3 Pb) and (0.004 µg/m^3 Cd), respectively. The low values found here may be due to the locations selected in urban background areas are relatively open places and situated on wide roads having low traffic density. The sampling points UB-2 and UB-3 in urban background areas are 390 km away from the main super highway whereas UB-1 and UB-4 are situated on wide road. The areas around the sampling site are sparsely populated having low vehicular traffic.

Lead has been found to be one of the major toxic elements generated through the motor vehicle exhaust using leaded gasoline. It is non degraded pollutant and it not only accumulates in the body but also modifies itself as it moves through biological cycles and food chain. The relatively high lead concentration in Karachi could predominantly originate from burning of solid waste and from large number of vehicles. Emission from road or wind-blown dust, or other industries may also have significant contribution to the lead pollution in Karachi city. Previously, much attention has been paid towards lead in the atmosphere due to wide spreads use as an anti-knocking agent in gasoline (Jones, 1991). Presently, however, after the introduction of the regulations requiring the reduction in the lead content in gasoline markedly decreased from 0.64 g/L in 1966 to 0.14 g/L in 1986, this decrease of lead concentration in gasoline also decrease the addition of lead to the environment by using it in the motor vehicles. Whereas, previously deposited lead concentration in the environment is a main source of lead in present environment. Even though the concentration of lead decreases in the gasoline but due to increase of vehicles in the city also increase the emission of lead in the environment of the city.

The average concentration of cadmium at some points exceeded the WHO guidelines value (0.005 µg/m^3) in commercial and industrial areas at selected points in Karachi. The higher cadmium concentration in industrial

areas of Karachi may be due to the release of cadmium from different industrial and mechanical processes. Whereas in commercial areas may be due to the vehicular traffic. The sources of cadmium are diesel and lubricating motor oil, tyres and galvanized part of the vehicles. Diesel oil contains 0.07 to 0.1 ppm of Cd, whereas lubricating oil contains 0.26 ppm. The wear and tear of automobile tyres, which contain 20-90 ppm Cd, is main source of Cd pollution (Qureshi, 2000). However, the cadmium concentration has the lowest concentration than the measured concentration of lead in this study. Care should be taken about the sources and remedy of the high level of cadmium pollution in Karachi as it has serious impact on human health.

Table 3 shows that various studies on trace metals (lead and cadmium) level in PM_{10} samples have been undertaken in different countries of the world. Khillare and Sarkar (2012) reported the Pb concentration in particulate matter in urban residential areas within the range 0.27 to 0.46 µg/m^3. In the present study (Table 3) average concentration of lead in residential areas was recorded 0.96 µg/m^3 which is higher from Delhi, India (Shridhar *et al*., 2010), Coimbatore, India (Vijayanand *et al*., 2008), Beijing China (Khan *et al*., 2010) and Tocopilla, Chile (Jorquera, 2009). In urban background areas, was recorded as 0.01 µg/m^3, which is higher than that reported for urban background of Italy (Contini *et al*., 2010) and UK (Heal *et al*., 2005). Level of lead and cadmium also analysed in the samples collected from industrial and commercial areas of Karachi city. The average concentration of lead in industrial areas was found to be 1.46 µg/m^3 whereas in commercial areas of Karachi was found to be 1.36 µg/m^3, respectively. Khillare and Sarkar (2012) also

Table 3. Comparison of metal concentrations (µg/m^3) in Karachi with other parts of the world

Location/Site type	Typography	Cd	Pb	References
Karachi, Pakistan	Commercial	0.10	1.36	Present study
	Residential	0.03	0.96	
	Industrial	0.25	1.46	
	U-background	0.01	0.6	
Delhi, India,	Residential	0.01-0.02	0.27-0.46	Khillare and Sarkar (2012)
Coimbatore, India	Residential	BDL	0.21-0.62	Vijayanand *et al*. (2008)
Agra, India	Urban	NR	1.1	Kulshrestha *et al*. (2009)
Delhi, India	Urban	0.01	0.44	Shridhar *et al*. (2010)
Lahore, Pakistan	Urban	0.08	4.4	von Schneidemesser *et al*. (2010)
Beijing, China	Residential	0.005	0.33	Khan *et al*. (2010)
Tocopilla, Chile	Residential	NR	0.01	Jorquera (2009)[a]
Istanbul, Turkey	Urban	0.001	0.07	Theodosi *et al*. (2010)
Lecce, Italy	Urban background	NR	0.008	Contini *et al*. (2010)
Vienna, Austria	Urban	0.0005	0.01	Limbeck *et al*. (2009)
Bratislava, Slovakia	Urban	0.0001	0.02	Meresova *et al*. (2008)
Huelva, Spain	Urban	0.0006	0.02	Sanchez de la Campa *et al*. (2007)
Edinburgh, UK	Urban background	0.0003	0.01	Heal *et al*. (2005)[b]
Los Angeles, USA	Urban	NR	0.002	Singh *et al*. (2002)

NR=not reported; BDL=below detection limit; a=sampling in March-April 2006; b=median values

Table 4. Comparison of metal concentrations (µg/m^3) with USEPA and WHO guidelines

Metals	Commercial (present study)	Residential (present study)	Industrial (present study)	U-background (present study)	WHO	USEPA
	(µg/m^3)	(µg/m^3)	(µg/m^3)	(µg/m^3)	(µg/m^3)	(µg/m^3)
Pb	1.36	0.96	1.46	0.6	0.500	1.500
Cd	0.008	0.10	0.03	0.25	0.01	0.006

reported the concentration of cadmium in particulate matter range from 0.01 to 0.02 $\mu g/m^3$. Table 3 shows that in the present study the average concentration of Cd in residential areas was recorded as 0.03 $\mu g/m^3$ which is higher from Delhi, India (Shridhar *et al*., 2010), Coimbatore, India (Vijayanand *et al*., 2008), Beijing China (Khan *et al*., 2010) and Tocopilla, Chile (Jorquera, 2009), in urban background areas was recorded as 0.60 $\mu g/m^3$ which is higher than that reported for urban background of Italy (Contini *et al*., 2010) and UK (Heal *et al*., 2005), in industrial areas was found to be 0.25 $\mu g/m^3$ whereas in commercial areas of Karachi was found to be 0.10 $\mu g/m^3$, respectively.

In the atmospheric air, toxic metals cannot be destroyed or shattered and can be inhaled during breathing. Various studies on atmospheric metal concentration and their health hazards have been carried out in different cities of the world which shows variation in the concentration of toxic elements like lead and cadmium (Freitas *et al*., 2010). Both these toxic metals causes different types of health hazards as slowing of heart rate, different types of cancer, bronchitis and leukemia (Khillare and Sarkar, 2012; Jorquera, 2009). Lead is one of the well known man made environmental pollutant and causes chronic obstructive pulmonary diseases, lungs cancer, bronchitis and chief source of asthma both in young and older citizens even a very small amount of lead exposure becomes physiologically active and results into its accumulation in the food chain. Adverse health effects on humans particularly on infants' central nervous system (CNS) have been well established.

Cadmium is carcinogenic to human body and inhalation of Cd, causes lung cancer, different types of cardio-vascular diseases, acute and chronic kidney diseases etc. Other effects due to cadmium exposure due to breathing for a long time are lung damage and fragile bones (Järup and Alfvén, 2004).

Conclusion

The study area covers a substantial portion of Karachi (as commercial, residential, industrial and background areas). The characterisation of trace metal sources in the study area is quite challenging due to a large number of vehicles, industries and commercial activities. Trace metals (Pb and Cd) associated with PM_{10} were characterised at one hundred eight locations in different areas of Karachi to identify and quantify their major sources. The findings of this study may provide a comprehensive database for framing an appropriate strategy for necessary mitigative/preventive measures for the sake of human health.

References

Benoff, S., Jacob, A., Hurley, L.R. 2000. Male infertility and environmental exposure to lead and cadmium. *Human Reproduction Update*, **6:** 107-121.

Callen, M.S., de la Cruz, M.T., Lopez, J.M., Navarro, M.V., Mastral, A.M. 2009. Comparison of receptor models for source apportionment of the PM_{10} in Zaragoza (Spain). *Chemosphere*, **76:** 1120-1129.

Contini, D., Genga, A., Cesari, D., Siciliano, M., Donateo, A., Bove, M.C., Guascito, M.R. 2010. Characterisation and source apportionment of PM_{10} in an urban background site in Lecce. *Atmospheric Research*, **95:** 40-54.

de Kok, T.M., Driece, H.A., Hogervorst, J.G., Briede, J.J. 2006. Toxicological assessment of ambient and traffic-related particulate matter: A review of recent studies. *Mutation Research*, **613:** 103-122.

Freitas, M.C., Pacheco, A.M.G., Verburg, T.G., Wolterbeek, H.T. 2010. Effect of particulate matter, atmospheric gases, temperature, humidity on respiratory and circulatory diseases' trends in Lisbon, Portugal. *Journal of Environmental Monitoring and Assessment*, **162:** 113-121.

Hashmi, D. R., Siddiqui, I., Shaikh, G. H. 2006. Accumulation of heavy metals in Tarry deposit on leaves at various locations of Karachi city. *Journal of Chemical Society of Pakistan,* **28:** 125-129.

Heal, M.R., Hibbs, L.R., Agius, R.M., Beverland, L.J. 2005. Total and water soluble trace metal content of urban background PM_{10}, $PM_{2.5}$ and black smoke in Edinburgh, UK. *Atmospheric Environment*, **39:** 1417-1430.

Järup, L., Alfvén, T. 2004. Low level cadmium exposure, renal and bone effects-the OSCAR study. *Biometals*, **17:** 505-509.

Jones, B. J., Symon, C., Tylor, P.J.L., Walsh, J., Johnston, A.E. 1991. Evidence for a decline in rural herbage lead levels in UK. *Atmosphere and Environment*, **25:** 361-369.

Jorquera, H. 2009. Source apportionment of PM_{10} and $PM_{2.5}$ at Tocopilla, Chile (22°05'5, 70012'W). *Environmental Monitoring and Assessment*, **153:** 235-251.

Khan, M.F., Hirano, K., Masunaga. 2010. Quantifying

the sources of hazardous elements of suspended particulate matter aerosol collected in Yokohama, Japan. *Atmospheric Environment*, **44:** 2646-2657.

Kulshrestha, A., Satsangi, P.G., Masih, J., Taneja, A. 2009. Metal concentration of $PM_{2.5}$ and PM_{10} particles and seasonal variations in urban and rural environment of Agra, India. *Science of the Total Environment*, **407:** 6196-6204.

Limbeck, A., Handler, M., Puis, C., Zbiral, J., Bauer, H., Puxbaum, H. 2009. Impact of mineral components and selected trace metals on ambient PM_{10} concentrations. *Atmospheric Environment*, **43:** 530-538.

Meresova, J., Florek, M., Holy, K., Jeskovsky, M., Sykora, I., Frontasyeva, M.V., Pavlov, S.S., Bujdos, M. 2008. Evaluation of elemental content in air-borne particulate matter in low-level atmosphere of Bratislava. *Atmospheric Environment*, **42:** 8079-8085.

Namdeo, A., Bell, M.C. 2005. Characteristics and health implications of fine and coarse particulates at roadside, urban background and rural sites in UK. *Environment International*, **31:** 565-573.

Onder, S., Dursun, S. 2006. Air borne heavy metal pollution of *Cedrus libani* (A Rich.) in the city centre of Konya (Turkey). *Atmospheric Environment*, **40:** 1122-1133.

Pandit, S., Khillare, S.S. 2012. Airborne inhalable metals in residential areas of Delhi, India: distribution, source apportionment and health risks. *Atmospheric Pollution Research*, **3:** 46-54.

Park, S.S., Kim, Y.J. 2005. Source contributions to fine particulate matter in an urban atmosphere. *Chemosphere*, **59:** 217-226.

Sajjad, S.H., Blond, N., Clappier, A., Raza, A., Shirazi, S.A., Shakrullah, K. 2010. The Preliminary study of urbanization, fossil fuels consumptions and CO_2 emission in Karachi. *African Journal of Bio-technology,* **9:** 1941-1948.

Sanchez de la Campa, A.M., De la Rosa, J., Querol, X., Alastuey, A., Mantilla, E. 2007. Geochemistry and origin of PM_{10} in the Huelva region, Southwestern Spain. *Environmental Research*, **103:** 305-316.

Sharma, M., Maloo, S. 2005. Assessment of ambient air PM_{10} and $PM_{2.5}$ and characterization of PM_{10} in the city of Kanpur, India. *Atmospheric Environment*, **39:** 6015-6026.

Shridhar, V., Khillare, P.S., Agarwal, T., Ray, S. 2010. Metallic species in ambient particulate matter at rural and urban location of Delhi. *Journal of Hazardous Materials*, **175:** 600-607.

Singh, M., Jaques, P.A., Sioutas, C. 2002. Size distribution and diurnal characteristics of particle-bound metals in source and receptor sites of the Los Angeles basin. *Atmospheric Environment,* **36:** 1675-1689.

Theodosi, C., Im, U., Bougiatioti, A., Zarmpas, P., Yenigun, O., Mihalopoulos, N. 2010. Aerosol chemical composition over Istanbul. *Science of the Total Environment*, **408:** 2482-2491.

Tsai, Y.I., Cheng, M.T. 2004. Characterization of chemical species in atmospheric aerosols in a metropolitan basin. *Chemosphere*, **54:** 1171-1181.

Van Der Zee S.C., Hoek, G., Harssema, H., Brunekreef, B. 1998. Characterization of particulate air pollution in urban and nonurban areas in the Netherlands. *Atmospheric Environment*, **32:** 3717-3729.

Vijayanand, C., Rajaguru, R., Kalaiselvi, K., Selvam, K.P., Palanivel, M. 2008. Assessment of heavy metal contents in the ambient air of the Coimbatore City, Tamilnadu, India. *Journal of Hazardous Material*, **160:** 548-553.

Von Schneidemesser, E., Stone, L.A., Quraishi, T.A., Shafer, M.M., Schauer, J.J. 2010. Toxic metals in the atmosphere in Lahore, Pakistan. *Science of the Total Environment*, **408:** 1640-1648.